Universität Potsdam, Institut für Biochemie und Biologie

Arbeitsgruppe Prof. Dr. Bernd Müller-Röber

Functional analysis of MYB112 transcription factor in the model plant *Arabidopsis thaliana*

Dissertation

zur Erlangung des akademischen Grades

"doctor rerum naturalium"

(Dr. rer. nat.)

in der Wissenschaftdisziplin "Molekularbiologie"

eingereicht an der

Mathematisch-Naturwissenschaftlichen Fakultät

der Universität Potsdam

von

Magda Ewa Lotkowska

Potsdam, den 15.05.2013

Erklärung

I hereby declare that this Ph.D. thesis is the result of my own work carried out between the winter semester of 2008 and the winter semester of 2012 in the group of Prof. Dr. Bernd Mueller-Roeber at the University of Potsdam in Golm, Germany. It has not been submitted for any degree or Ph.D. at any other university.

Magda Ewa Lotkowska   Potsdam, 15.05.2013

Acknowledgements

Table of Contents

List of Figures

List of Tables

Abbreviations

ACTs	acyltransferases
AGTs	glycosyltransferases
bp	base pair(s)
BS	binding site
CaMV	Cauliflower Mosaic Virus
cDNA	complementary DNA
CELD	cellulase D from *Neocallimastix patricairum*
ChIP	chromatin immuno preciptitation
DAS	days after sawing
DBD	DNA binding domain
DMSO	dimethyl sulfoxide
DNA	deoxyribonucleic acid
EMSA	electrophoretic mobility shift assay
EST	estradiol
EV	empty vector
GFP	green fluorescent protein
GST	gluthatione S-transferase
GTF	general transcription factor
GUS	β-glucuronidase
HIS	histidine
Imap	infrared mediated mapping of TF binding sites
IRD	infrared dye
kb	kilobase pairs
LB	left border primer
LC-MS	liquid chromatography coupled to mass spectrometry
LUC	luciferase
MBW	MYB-bHLH-WD40 complex
mRNA	messenger RNA
MS (medium)	Murashige-Skoog medium
NPA	1-naphthylphthalamic acid
PCR	polymerase chain reaction
qRT-PCR	quantitative real-time PCR
RB	right border primer
RNA	ribonucleic acid
SAG	senescence associated gene
SDS-PAGE	sodium dodecyl sulfate polyacrylamide gel electrophoresis
T-DNA	transfer DNA
TF	transcription factor
UTR	untranslated region
Wt	wild type

1. Summary

Transcription factors (TFs) are ubiquitous gene expression regulators and play essential roles in almost all biological processes. This Ph.D. project is primarily focused on the functional characterisation of *MYB112* - a member of the R2R3-MYB TF family from the model plant *Arabidopsis thaliana*. This gene was selected due to its increased expression during senescence based on previous qRT-PCR expression profiling experiments of 1880 TFs in *Arabidopsis* leaves at three developmental stages (15 mm leaf, 30 mm leaf and 20% yellowing leaf). *MYB112* promoter GUS fusion lines were generated to further investigate the expression pattern of *MYB112.* Employing transgenic approaches in combination with metabolomics and transcriptomics we demonstrate that *MYB112* exerts a major role in regulation of plant flavonoid metabolism. We report enhanced and impaired anthocyanin accumulation in *MYB112* overexpressors and *MYB112*-deficient mutants, respectively. Expression profiling reveals that MYB112 acts as a positive regulator of the transcription factor *PAP1* leading to increased anthocyanin biosynthesis, and as a negative regulator of *MYB12* and *MYB111*, which both control flavonol biosynthesis. We also identify MYB112 early responsive genes using a combination of several approaches. These include gene expression profiling (Affymetrix ATH1 micro-arrays and qRT-PCR) and transactivation assays in leaf mesophyll cell protoplasts. We show that MYB112 binds to an 8-bp DNA fragment containing the core sequence (A/T/G)(A/C)CC(A/T)(A/G/T)(A/C)(T/C). By electrophoretic mobility shift assay (EMSA) and chromatin immunoprecipitation coupled to qPCR (ChIP-qPCR) we demonstrate that MYB112 binds *in vitro* and *in vivo* to *MYB7* and *MYB32* promoters revealing them as direct downstream target genes. MYB TFs were previously reported to play an important role in controlling flavonoid biosynthesis in plants. Many factors acting upstream of the anthocyanin biosynthesis pathway show enhanced expression levels during nitrogen limitation, or elevated sucrose content. In addition to the mentioned conditions, other environmental parameters including salinity or high light stress may trigger anthocyanin accumulation. In contrast to several other MYB TFs affecting anthocyanin biosynthesis pathway genes, *MYB112* expression is not controlled by nitrogen limitation, or carbon excess, but rather is stimulated by salinity and high light stress. Thus, MYB112 constitutes a previously uncharacterised regulatory factor that modifies anthocyanin accumulation under conditions of abiotic stress.

2. General Introduction

2.1. Transcription Factors

Transcription is the first step leading to gene expression. It is the process of synthesising a complementary RNA strand from a DNA template. In eukaryotes, transcription is mediated by multi-protein complexes. These include the basal transcriptional apparatus composed of general transcription factors (GTFs) and the RNA polymerase complex, multi-subunit cofactors, as well as chromatin remodelling and DNA unwinding factors (Sekine *et al.*, 2012; Levine and Tjian, 2003; Riechmann, 2002; **Figure 1**). Selectivity of transcription is provided by the action of sequence-specific transcription factors (TFs). TFs are typically composed of a DNA binding domain (DBD) and an effector/regulatory domain responsible for activator or repressor activity. These factors recognise specific DNA motifs, usually located in the promoters of target genes, and regulate the frequency of transcription initiation.
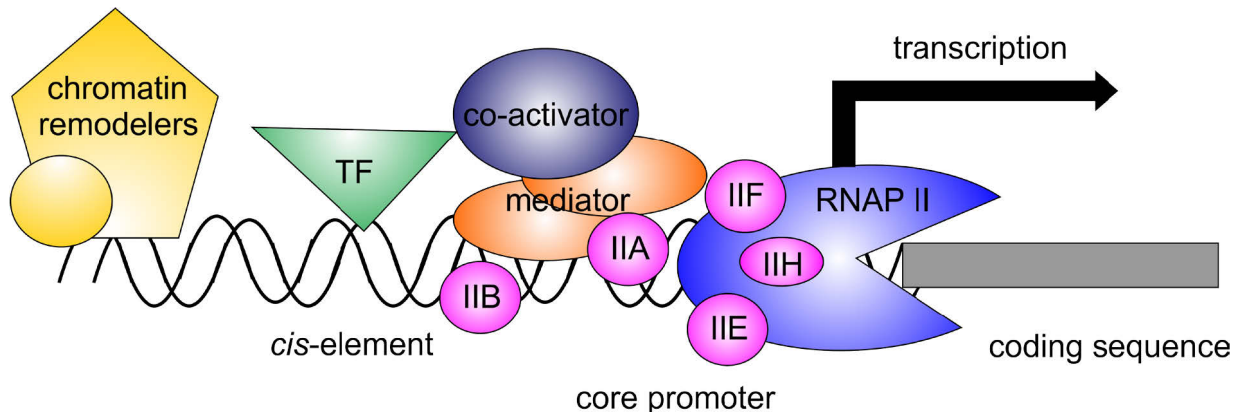
Figure 1. The multi-subunit general transcription apparatus.

The eukaryotic transcriptional apparatus can be subdivided into three broad classes of multi-subunit ensembles that include the RNA polymerase II (RNAPII) core complex and associated general transcription factors (GTFs: IIA, -B, -D, -E, -F and -H), multi-subunit co-activator and mediator proteins and various chromatin modifying or remodelling complexes.

This is achieved through direct or indirect (through transcriptional regulators) interaction between the effector domain of a TF and the basal transcriptional apparatus. The DNA motifs, or *cis*-regulatory elements bound by TFs usually compose of 5 - 10 nucleotides and can often be recognised by a set of different TFs, acting synergistically or as competitors. Properties of TFs open the possibility for precise control over temporal and spatial patterns of gene transcription despite a limited number of factors and binding sites. On the basis of similarities in the DBD sequence, TFs were classified into different families, some widespread among eukaryotes, other exclusive for a particular kingdom (Riechmann *et al.*, 2000).

2.1.1. Transcription Factors in Plants

The genome of the model plant *Arabidopsis thaliana* is estimated to encode over 2400 TF and transcriptional regulator genes, which accounts for around 7.5% of the predicted total number of genes (Pérez-Rodríguez *et al.*, 2009). In *Populus trichocarpa*, TFs account for 6.3% and in *Vitis vinifera* - 5.7% of all genes, whereas in *Drosophila melanogaster*, *Caenorhabditis elegans* and *Saccharomyces cerevisiae* the proportions are 4.6%, 3.5% and 3.5%, respectively (Riechmann *et al.,* 2000; PlnTFDB; Pérez-Rodríguez *et al.*, 2010). The higher number of TFs in plants can be attributed to the complex secondary metabolism (Szathmáry *et al.*, 2001), interactions with environment necessitated by the sessile lifestyle of plants and due to extensive genome duplications (Riechman, 2001). The *Arabidopsis thaliana* TF genes have been classified into 60 families and 22 gene families encoding for other transcriptional regulators (Pérez-Rodríguez *et al.*, 2010). The two largest TF families are the MYB superfamily (197 members in *Arabidopsis*; Katiyar *et al.*, 2012) and the APETALA2/ethylene responsive element binding protein (AP2/EREBP) (147 members;Pérez-Rodríguez *et al.*, 2010; Zhang *et al.*, 2012).

2.1.2. MYB Superfamily of Transcription Factors

MYB domain TFs are present in all eukaryotic organisms and are thought to be over one billion years old (Lipsick, 1996). The *MYB* acronym is derived from

"*myeloblastosis*", a type of leukaemia (cancer of blood cells) and the first *MYB* gene identified was the oncogene *v-Myb* derived from the avian myeloblastosis virus (AMV). This retrovirus causes monoblastic leukemia in chickens and possibly may have originated by the insertion of a retrovirus into a proto-oncogene (c-*Myb*), which mutated and became a part of the virus (Klempnauer and Bishop, 1983). The MYB domain generally consists of up to three imperfect repeats (R1, R2 and R3) composed of 50-53 amino acids each, but four-repeat exceptions exist (Wong *et al*., 1998; **Figure 2**). There is greater conservation between the same repeat from different proteins than between R2 and R3 repeats from the same protein suggesting that each repeat has a specialized function in binding DNA. R2 and R3 domains in c-MYB are required for binding to the DNA although it has been proposed that R3 is involved in more specific interactions with the nucleotides of the binding motif than R2 (Ogata *et al*., 1992). In animals, the MYB superfamily is relatively small, generally comprising only four or five proteins, usually containing three MYB repeats (R1, R2 and R3). Animal MYB factors are responsible for the regulation of cell proliferation, differentiation and apoptosis. In plants, R1R2R3-MYB factors are rare (five members in *Arabidopsis*). The plant DBD usually consists of two imperfect repeats (R2, R3) and out of 1976 MYB proteins, there are 126 members of the R2-R3 group in *Arabidopsis*. There are also several single repeat (MYB-related) factors found in *Arabidopsis* e.g. MYBL2, CPC and TRY (Matsui *et al*., 2008; Simon *et al*., 2007; Tominaga *et al*., 2007). Structural studies showed that imperfect repeats of the MYB domain fold into helix-loop-helix motifs separated by highly conserved tryptophan residues, that stabilise the hydrophobic core of the MYB domain (Kanei-Ishii *et al*., 1990). The MYB domain is generally found in the N-terminus of the protein, however can be also present in the C-termini. Usually however, the regulatory domain is located in the C-terminal part of the protein. Within their regulatory domains, members of the MYB family contain serine and threonine residues, indicating possible post-translational regulation of MYB activity by phosphorylation. For instance, the MYB-related TF *MYB340* from *Antirrhinum* when synthesized in *E. coli* or in yeast, shows little DNA binding affinity and recovers after treatment of extracts with alkaline phosphatase. This indicates that the DNA binding activity of this TF is inhibited by phosphorylation Moyano *et al*., 1996). MYB proteins can also interact with other TFs. Such interactions are common for c-MYB. Also plant

MYB factors interact with partner proteins, such as those from the bHLH TF family. In *Zea mays*, the transcriptional activation of anthocyanin biosynthesis genes by the R2R3 MYB proteins C1 and PI requires the involvement of bHLH proteins from the R/B gene family (Goff *et al*., 1992). Analysis of protein-protein interactions of the MYB family in the model plant *Arabidopsis thaliana* revealed a conserved amino acid sequence ([DE]Lx2[RK]x3Lx6Lx3R) as the structural basis for interaction between MYB and R/B-like bHLH proteins (Zimmerman *et al*., 2010).
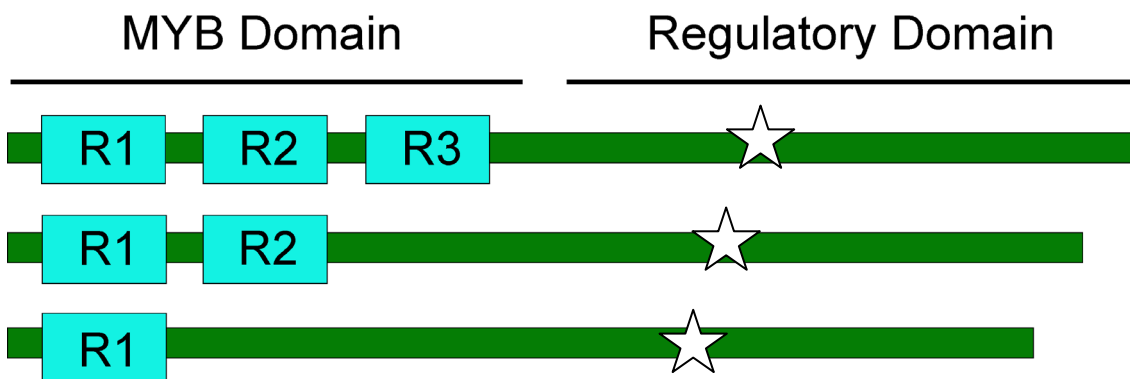
Figure 2. General structure of MYB proteins.

The MYB DNA-binding domain generally consists of up to three imperfect repeats (R1, R2 and R3) composed of 50-53 amino acids and is located in the N-terminus of the protein. The regulatory domain is present in the C-terminus of the protein and contains interaction sites for partner proteins (stars), i.e. a conserved amino acid sequence ([DE]Lx2[RK]x3Lx6Lx3R) as the structural basis for interaction between MYB and R/B-like bHLH proteins.

2.1.2.1. R2R3-MYB Factors

MYB factors were substantially amplified in plants, as compared to animals and yeast, and they comprise one of the largest TF families with at least 197 members in *Arabidopsis* and 155 in rice (Katiyar *et al*., 2012). The majority of MYB TFs in plants contain two imperfect repeats of the MYB domain and there are 126 R2R3-MYBs in *Arabidopsis* and 109 R2R3-MYBs in rice. Contrary to genes encoding R1R2R3-MYB proteins, *R2R3-MYB* genes are not the equivalents of c-MYB from animals and are unique to plants. While plant R1R2R3-MYB proteins play similar functions to their animal counterparts, *R2R3-MYB* genes mainly regulate plant-specific processes. A systematic analysis of knockouts has revealed that R2R3-MYB factors play roles

mainly in the regulation of secondary metabolism, plant cell shape and plant organ development (Stracke *et al*., 2001; Jin and Martin, 1999; Meissner *et al*., 1999, Martin and Paz-Ares, 1997). On the basis of similarities in the C-terminal amino acid sequence, R2R3 factors were classified to 22 subgroups in *Arabidopsis* (Kranz *et al*., 1998). The conserved motifs may facilitate protein functionality outside of the DNA-binding domain and closely related members of the same subgroup often exhibit similar functions. **Figure 3** shows the integrated evolutionary relationships of the 126 *Arabidopsis* R2R3-MYB proteins with their depicted functions.
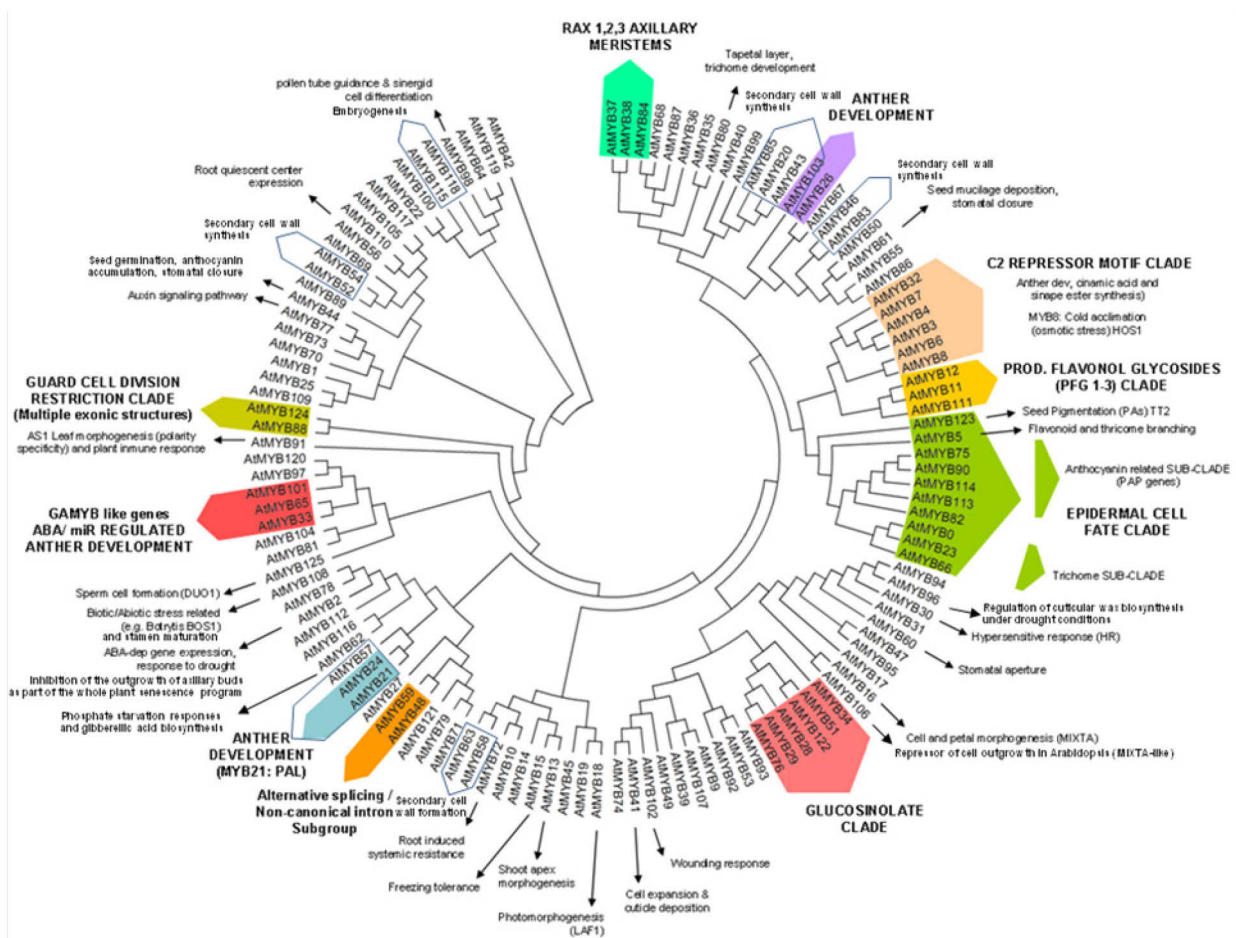
Figure 3. Integrated evolutionary relationships of the 126 *Arabidopsis* R2R3-MYB proteins with indicated functions (Matus *et al*., 2008, modified).

It has been shown for example that factors from subgroup 7 (i.e., MYB11/PFG2, MYB12/PFG1 and MYB111/PFG3) control the flavonol biosynthesis pathway and factors from subgroup 6 (i.e., MYB75/PAP1, MYB90/PAP2, MYB113 and MYB114)

regulate expression of anthocyanin biosynthesis genes. Interestingly, the *MYB114* gene from the Columbia (Col) accession encodes a putative protein that lacks a transcriptional activation domain due to a stop codon just after the MYB domains (at amino acid 140). The Landsberg erecta (L*er*) *MYB114* allele encodes a full-length gene and its function in anthocyanin accumulation was confirmed (Gonzalez *et al*., 2008). Another prominent example represents the three factors which build subgroup 15, i.e. Glabrous 1 (GL1/MYB0), Werewolf (WER/MYB66) and MYB23 (Kranz *et al*., 1998; Stracke *et al*., 2001). WER/MYB66 and GL1/MYB0 are functionally equivalent proteins (Lee and Schiefelbein, 2001) and display their different biological functions in root hair and trichome formation, respectively, only because of their different spatial expression patterns (reviewed in Schiefelbein, 2003). Moreover, MYB23 is redundant to GL1/MYB0 in controlling the initiation of trichome development (Kirik *et al*., 2001). Regulators of Axillary Meristems RAX1/MYB37, RAX2/MYB38, and RAX3/MYB84 belong to subgroup 14 (Muller *et al.*, 2006) and are homologous to the tomato (*Solanum lycopersicum*) *BLIND* gene (Schmitz *et al.*, 2002) controlling the formation of lateral meristems in different, but overlapping zones along the shoot axis.

2.1.3. MYB112 is an R2R3-MYB from Subgroup 20

Phylogenetic analysis of MYB factors in *Arabidopsis* places MYB112 in subgroup 20 of the R2R3-MYB group (Stracke *et al*., 2001). Apart from MYB112, there are five other MYB proteins found in this subgroup: MYB2, MYB62, MYB78, MYB108 and MYB116 (**Figure 4**). The functions of MYB2, MYB62 and MYB108 were previously described. MYB108 contributes to the regulation of stamen maturation and male fertility in response to jasmonate signaling (Mandaokar and Browse, 2009). MYB62 regulates phosphate starvation responses and gibberellic acid biosynthesis (Devaiah *et al.,* 2009). The MYB2 protein has been shown to be a transcriptional activator of the *DEHYDRATION RESPONSIVE GENE* (*rd*22) (Abe *et al*., 2003) and to act in abscisic acid signaling. Guo and Gan (2011) reported that MYB2 regulates whole-plant senescence by inhibiting cytokinin-mediated branching at late stages of development in *Arabidopsis*.
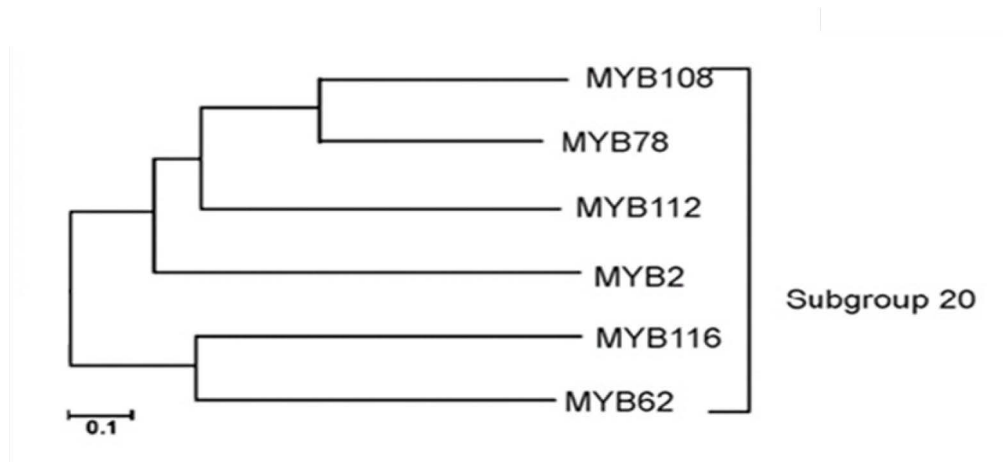
Figure 4. Phylogenetic relationship of transcription factors in subgroup 20 of the R2R3-MYB group (Stracke *et al*., 2001).

The function of MYB112 has not yet been described. A literature search revealed, however, that expression of *MYB112* increases during leaf aging. According to the eFP browser (Winter *et al.*, 2007), when considering the array data from developmental series, *MYB112* expression reaches its maximum value during leaf senescence **(Figure 5A**), which is in accordance with data extracted from Genevestigator (http://www.genevestigator.com, Zimmermann *et al*., 2004a). This also stays in agreement with the results published by Balazadeh *et al.* (2008), when screening for genes showing altered expression in leaves during late stages of development, comprising 50% of leaf full expansion (15 mm), fully expanded leaf (30 mm) and 20% senescent leaf (determined as yellowing of 20% of the leaf blade) with the use of quantitative reverse transcription-polymerase chain reaction (qRT-PCR). The final stage (20% yellowing) is a leaf in which photoassimilates and nutrients are intensively remobilized and transported to other organs of the plant. In this study, a significant increase of *MYB112* expression level was observed in the yellowing leaf (Balazadeh *et al.,* 2008) (**Figure 5B**). Breeze *et al*. (2011) performed microarray-based high-resolution gene expression profiling using samples collected over 11 time points during a 3-week period leading to leaf senescence. They observed that the major switch in gene expression, both in genes up- and down-regulated, occurred

between 29 and 33 days after sawing (DAS). Expression of *MYB112* increased rapidly after at 31 DAS and reached its maximum at 33 DAS **(Figure 5C)**.

A

B

C
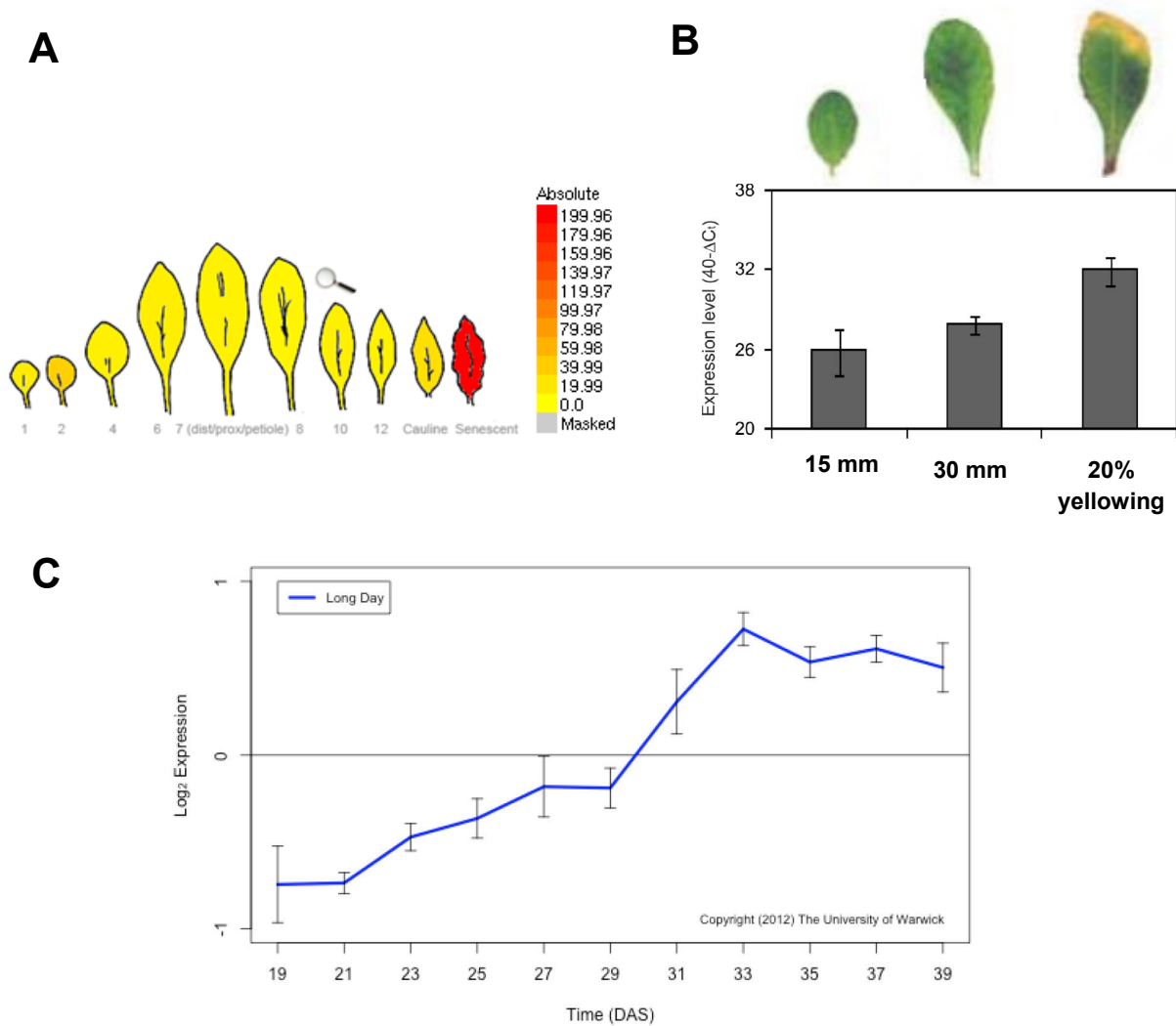
Figure 5. *MYB112* expression profiling during leaf development.

(A) Representation of microarray-based *MYB112* expression profiling during leaf development according to eFP browser (Winter *et al.*, 2007). **(B)** Expression of *MYB112* in leaves at three developmental stages as measured by qRT-PCR (based on Balazadeh *et al.*, 2008). **(C)** Expression of *MYB112* measured using microarrays at 11 stages of 3-week time to leaf senescence as described by Breeze *et al*. (2011). Note the increase of *MYB112* expression during senescence.

The functional analysis of genes up-regulated after 31 DAS illustrates the degradation and mobilization of nutrients, with 44% of these genes involved in catalytic activity, with lipid catabolism highly represented, and 10% having a role in transport (Breeze *et al.*, 2011). According to microarray data (Genevestigator) expression of *MYB112* increases also upon a range of stresses, such as pathogen attack, drought, osmotic stress and salt stress. Interestingly, salt stress can cause premature senescence and expression of many TFs involved in the regulation of senescence processes (senescence-associated TFs, SAGs) increases also during salt stress (reported by Balazadeh *et al.*, 2010).

2.2. Flavonoids

2.2.1. Flavonoid Biosynthesis

Flavonoids are a major class of plant secondary metabolites, composed of a fifteen-carbon skeleton, which consists of two phenyl rings (A- and B-rings) connected by a three-carbon bridge (C-ring) (**Figure 6**). The skeleton can be modified by numerous additional hydroxyl, methoxyl, methyl and/or glycosyl substitutions, giving rise to various compounds. Additionally, aromatic and aliphatic acids, sulfate, prenyl or methylenedioxyl groups also attach to the flavonoid skeleton (Harborne and Baxter, 1999). Depending on their chemical structure, flavonoids are divided into several groups, i.e., anthocyanins, flavonols, flavones, flavanones, dihydroflavonols, isoflavonoids, chalcones, aurones, condensed tannins (or proanthocyanidins), and others (Iwashina, 2000). Flavonoids are synthesised by the phenylpropanoid pathway. Studies in *Arabidopsis thaliana* largely contributed to our understanding of the phenylpropanoid pathway, its enzymes and intermediates. The molecular basis of the flavonoid biosynthesis pathway is well known in plants (for reviews see Koes *et al.*, 2005; Falcone Ferreyra *et al.*, 2012), and metabolic engineering of flavonoid biosynthesis is actively pursued (Butelli *et al.*, 2008; Tanaka *et al.*, 2010; Wang *et al.*, 2011). In this pathway the amino acid phenylalanine is used to produce 4-coumaryol-CoA, which reacts with malonyl-CoA leading to production of the fifteen-carbon chalcones. The first reaction, in which phenylalanine undergoes deamination to

yield *trans*-cinnamic acid and ammonia is catalysed by Phenylalanine Ammonia-Lyase (PAL) (**Figure 7**). In *Arabidopsis*, there are four genes encoding PAL isoforms: *PAL1-PAL4* (Raes *et al*., 2003). Kinetic analysis of PAL activity *in vitro* as well as studies using reverse genetics revealed that *PAL1* and *PAL2* encode the major functional PAL enzymes in *Arabidopsis*, while PAL4 partially compensates for the loss of PAL1 and PAL2. (Cochrane *et al*., 2004; Rohde *et al*., 2004; Huang *et al*., 2010). The fallowing hydroxylation of cinnamate to yield 4-coumarate (also known as *p*-coumaric acid) is catalysed by Cinnamate-4-Hydroxylase (C4H). C4H is a cytochrome P450-dependent monooxygenase and mutation its gene causes reduced epidermal fluorescence and a decreased accumulation of sinapoylmalate and condensed tannins (Ruegger and Chapple, 2001; Schilmiller *et al*., 2009). The metabolic changes are accompanied by developmental, structural, and reproductive phenotypes, i.e., dwarfism, reduced apical dominance, collapsed xylem, male sterility. 4-Coumarate:CoA Ligase (4CL) catalyzes the ATP-dependent formation of the CoA thioester 4-coumaroyl CoA (also known as *p*-coumaroyl CoA; **Figure 7**).
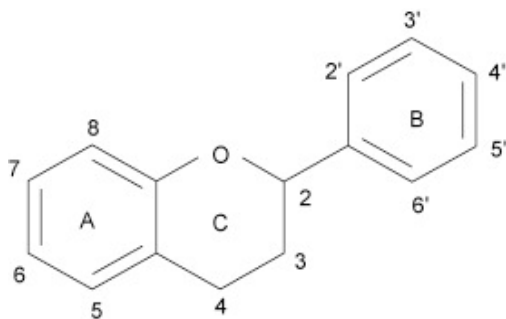
Figure 6. Structure of the flavonoid backbone.

Fifteen-carbon flavonoid skeleton consists of two phenyl rings (A- and B-rings) connected by a three-carbon bridge (C-ring)

The *Arabidopsis* genome encodes at least four such proteins: 4CL1-4CL4 (Ehlting *et al.*, 1999; Hamberger and Hahlbrock, 2004; Costa *et al.*, 2005). Based on their expression patterns and their similarity to 4CL homologues found in other plants, 4CL1 and 4CL2 are proposed to be involved in lignin biosynthesis, while 4CL3 may have a role in flavonoid biosynthesis (Ehlting *et al.*, 1999; Cukovic el al., 2001). 4CL4 exhibits preferential activity not towards *p*-coumarate but towards ferulate and sinapate, suggesting a metabolic function different from the other three isozymes (Hamberger and Hahlbrock, 2004). The first step in flavonoid biosynthesis is catalysed by Chalcone Synthase (CHS). The resulting chalcone scaffold is

11

subsequently modified by the action of Chalcone Isomerase (CHI) and Flavanone-3-Hydroxylase (F3H) to yield dihydroflavonols (**Figure 7**). Dihydroxyflavonols give rise to either flavonols, i. e., quercetin and kaempferol, or anthocyanins. Flavonol Synthase (FLS) catalyses the production of flavonols, whereas Dihydroflavonol-4-Reductase (DFR) is the first enzyme of the anthocyanin branch of the flavonoid pathway. Anthocyanin aglycones are synthesised by Anthocyanidin Synthase (ANS, LDOX) and undergo extensive modifications by glycosyltransferases (AGTs), acyltransferases (ACTs) and glutathione-S-transferases (GSTs) before transport to the vacuole. Similarly, quercetin and kaempferol undergo modifications to glycosylated varieties.

2.2.2. Regulation of Flavonoid Biosynthesis by R2R3-MYB Factors

Understanding the role of flavonoids in plant development and stress response is intimately linked to understand how the expression of the biosynthetic pathway genes is controlled. The precise regulation of flavonoid production is achieved by the combinatorial action of transcription factors (TFs), expressed in a spatially and temporally controlled manner (reviewed in Koes *et al*., 2005; Lepiniec *et al*., 2006). TFs regulating the expression of flavonoid biosynthesis genes have been characterized quite extensively in *Arabidopsis* and other plant species including petunia (*Petunia hybrid*), maize (*Zea mays*) and snapdragon (*Antirrhinum majus*) (Broun, 2005; Ramsay and Glover, 2005; Allan *et al*., 2008; Hichri *et al*., 2011; Petroni and Tonelli, 2011). Regulators belonging to different TF families, including WD40, WRKY, BZIP, MADS-box, bHLH and MYB proteins, have been proven to control expression of flavonoid biosynthesis genes (reviewed in Ramsay and Glover, 2005). The first plant TF reported to be involved in the regulation of the flavonoid pathway was the MYB factor Colorless1 (C1) isolated from *Zea mays* in 1987 (Paz-Ares *et al*., 1987). C1 interacts with bHLH factors B and R to activate the promoter of *DIHYDROFLAVONOL-4-REDUCTASE* (*DFR*) (Chandler *et al.,* 1989; Ludwig *et al.*, 1989; Goff *et al.*, 1992, Mol *et al.*, 1996). The specificity of this interaction was confirmed by comparing C1 with a closely related P protein - a MYB TF which controls a set of flavonoid biosynthesis genes independent of bHLH TFs (Grotewold *et al*., 1994). The regulation of the flavonoid pathway dependent on MYB and bHLH

partnership is conserved throughout the plant kingdom, i. e., the *Petunia hybrida* MYB protein Anthocyanin2 (AN2) interacts with the bHLH proteins JAF13 and AN1, the *Antirrhinum* MYBs Ros1, Ros2 and VeMut interact with Del bHLHs, and MYB1 from strawberry is able to interact with the maize bHLH protein R (Quattrocchio *et al.*, 1999; Aharoni *et al.*, 2001). In *Arabidopsis*, four anthocyanin-regulating MYBs have been identified, including Production of Anthocyanin Pigment 1 (PAP1/MYB75), including Production of Anthocyanin Pigment 2 (PAP2/MYB90), MYB113 and MYB114. These TFs belong to subgroup 6 of the R2R3-MYB family and interact with bHLH factors, including Glabra 3 (GL3/bHLH001), Enhancer of Glabra 3 (EGL3/bHLH002) and TT8/bHLH042 (Zhang *et al.*, 2003; Baudry *et al.*, 2006; Gonzalez *et al.*, 2008). The regulatory complex also includes the WD40 protein Transparent Testa Glabra 1 (TTG1), a homolog of AN11 from *Petunia hybrida*, which also controls anthocyanin production (de Vetten *et al.*, 1997; Walker *et al.*, 1999). The resulting MYB/bHLH/WD40 (MBW) complex binds to the *DFR* promoter and induces its expression. The seed-specific R2R3-MYB factor Transparent Testa 2 (TT2/MYB123) also requires interaction with a bHLH factor, i.e., TT8, to activate the target genes *DFR*, *BANYULS* (*BAN*) and the *MULTIDRAG AND TOXIC COMPOUND EXTRUSION (MATE)-type transporter TT12*. Seeds of *transparent testa* mutants are yellow or pale-brown in colour because they fail to produce proanthocyanidins in the testa (seed coat) (Koornneef, 1990; Shirley *et al.*, 1995; Nesi *et al.*, 2001). The *Arabidopsis* Production of Flavonol Glycoside factors from the R2R3-MYB subgroup 7, namely PFG1/MYB12, PFG2/MYB11 and PFG3/MYB111, have been found to control the flavonol branch of the flavonoid biosynthesis pathway by activating *CHALCONE SYNTHASE* (*CHS*), *CHALCONE ISOMERASE* (*CHI*), *FLAVANONE-3-HYDROXYLASE* (*F3H*) and *FLAVONOL SYNTHASE* (*FLS*) in a bHLH-independent manner (Mehrtens *et al.*, 2005; Stracke *et al.*, 2007, Stracke *et al.*, 2010). Analysis of protein-protein interactions of the MYB family in the model plant *Arabidopsis thaliana* revealed a conserved amino acid sequence ([DE]Lx2[RK]x3Lx6Lx3R) as the structural basis for the interaction between MYB and bHLH proteins (Zimmerman *et al.*, 2010). A number of RR3-MYBs were reported to act as negative regulators. For example, MYB4 from *Arabidopsis* was reported to act as a negative regulator of *CHS*, *4CL1* and *4CL3* genes (Zimmerman *et al.*, 2004),

13

and the *myb4* knockout mutant showed an increase in sinapate ester accumulation, which resulted in enhanced UV-B irradiation tolerance (Jin *et al.*, 2000)..

phenyloalanine
PAL
cinnamic acid
C4H
p-coumaric acid
4CL
p-coumaryol CoA
CHS
naringenine chalcone
CHI
naringenin
F3H

FLAVONOL
MYB11, MYB12, MYB111

FLS
dihydroxykaempferol ⟶ kaempferol
F3'H
FGT
FLS
quercetin ← dihydroxyquercetin
kaempferol glycosides
FGT
quercetin glycosides
DFR

LAR
leucocyanidin
ANS
ANTHOCYANIN
PAP1, PAP2, MYB113, MYB114
catechin
BAN
cyanidin
AGT
AAT
(-)-epicatechin
cyanidin derivatives
GST
cyanidin derivatives

transporter
transporter
CYTOPLASM
proanthocyanidin
cyanidin derivatives
VACUOLE

Figure 7. Flavonoid biosynthesis pathway.

Flavonoids are synthesised from phenylalanine in the phenylpropanoid pahway. The first step in flavonoid biosynthesis is catalysed by chalcone synthase (CHS). Flavonol biosynthesis branch of the pathway is indicated with a blue box. Expression of genes encoding flavonol biosynthesis enzymes is directly regulated by MYB11, MYB12 and

MYB111. PAP1, PAP2, MYB113, and MYB114 control the expression of anthocyanin biosynthesis genes (red box).

Overexpression of *MYB1* from strawberry in tobacco resulted in suppression of anthocyanin and flavonol accumulation (Aharoni *et al.*, 2001). Recently, transient suppression of *MYB1* gene was shown to cause increased accumulation of anthocyanins in strawberry fruits (Salvatierra et al., 2013). Jin *et al.* (2000) identified a conserved repression motif (pdLNLD/ELxiG/S) in the C-terminal regions of these MYB proteins.

To summarise, branches of flavonoid metabolism are regulated by interplay between branch-specific activating and repressing MYB TFs, some of which depend on specific bHLH or WD40 protein partners. However, it remains unclear how the TF activity itself is regulated by internal or external signals to pursue controlled responses and what regulates these regulators.

2.2.3. Anthocyanins – the Colourful Flavonoids

Flavonoids are a diverse class of secondary metabolites, proven to play a remarkable role in the interaction between plants and their environment, often critical for plant survival. These compounds are crucial for the symbiotic plant-microbe interactions and in plant sexual reproduction by promoting the pollen tube development (Koes *et al.*, 1994). They also have apparent roles in plant stress defence, such as in protection against damage caused by wounding, pathogen attack, osmotic stress, salinity, extreme temperatures and excessive light (Dixon and Paiva, 1995; Winkel-Shirley, 2002). Anthocyanins are a small group of flavonoid pigments. In plant reproductive organs, anthocyanins act as pollinator attractants. The production of anthocyanins in plant foliage has long been the subject of study and speculation (early references reviewed by Wheldale, 1916; Dooner *et al.*, 1991; Mol *et al.*, 1996). Over the years numerous hypotheses have been proposed to account for the presence of anthocyanins in leaves of a wide range of species. In the late 19th century several authors suggested the light screen hypothesis, which states that foliar anthocyanins protect the photosynthetic apparatus from excess light (reviewed

by Wheldale, 1916). When leaves receive more light energy than can be used in photochemistry, they show a decline in the quantum efficiency of photosynthesis, termed photoinhibition (Long *et al*., 1994). Under severe conditions chloroplasts generate reactive oxygen species (ROS), which have the potential to destroy thylakoid membranes and denature proteins associated with photosynthetic electron transport. Therefore, the development of mechanisms that protect the photosynthetic apparatus under challenging conditions has been an essential component of higher plant evolution. *In vivo*, anthocyanins absorb the green and yellow wavelengths of light, commonly between 500 and 600 nm (Neill and Gould, 1999; Gitelson *et al*., 2001) and therefore serve as a useful optical filter, diverting excess high-energy quanta away from the photosynthetic apparatus. Chloroplasts irradiated with light that has first passed through a red filter have been shown to generate fewer superoxide radicals, resulting in reduced structural damage to the photosystems (Neill and Gould, 2003). In addition, anthocyanins have been shown to be excellent scavengers of free radicals, suggesting dual photoprotective role of these compounds (Rice-Evans *et al*., 1997; Wang *et al*., 1997; Gould *et al*., 2002; Nagata *et al*., 2003). It has been shown that under stress conditions, e.g., high light, drought, salt stress and nutrient deficiencies (Heldt 1997; Dauborn and Brueggemann, 1998) as well as during senescence (Kar *et al*. 1993; Hoch *et al*.; 2003; Wingler *et al*. 2004), the probability of photoinhibition increases and even moderate irradiances can induce photoinhibitory damage. The close relationship between the appearance of anthocyanins in senescing leaves of wild-type plants and the development of photoinhibition in anthocyanin-deficient mutants of three woody species investigated by Hoch *et al*. (2003) suggests the need for the additional photoprotection provided by anthocyanins. The light screen hypothesis was later extended to formulate the resorption protection hypothesis, proposing that shielding photosynthetic tissues from excess light by anthocyanins allows the resorption of critical foliar nutrients during foliar senescence (Hoch *et al*., 2001). Anthocyanins protect the degrading chlorophyll from damaging light levels, thereby restricting the formation of ROS that could jeopardize the resorptive process. Consistent with this hypothesis, nitrogen resorption has been shown to be more efficient in wild-type than in anthocyanin-deficient mutants of woody species (Feild *et al*., 2001, Hoch *et al*., 2001 and 2003, Lee, 2003).

2.3. Aim of the Thesis

Plant genome research is a major focus in our group and we study molecular and physiological processes that control plant development and responses to abiotic stress. We are particularly interested in the functional analysis of transcription factors and the regulatory networks they control. We explore such networks in *Arabidopsis thaliana* and other model plants. The aim of this thesis was to unravel the function of a previously uncharacterised gene encoding an R2R3-MYB factor - *MYB112*, as well as the MYB112-controlled gene expression network, including the identification of the early responsive and direct target genes. Systematic analysis of mutant plants with impaired expression of R2R3-MYB proteins in *Arabidopsis* as well as in other species resulted in rapid increase in our understanding of their function in plants. R2R3-MYB factors were reported to play roles mainly in the regulation of secondary metabolism, plant cell shape and plant organ development. *MYB112* was selected due to its elevated expression during senescence based on previous qRT-PCR expression profiling of 1880 TFs in *Arabidopsis* leaves at three developmental stages (15 mm leaf, 30 mm leaf and 20% yellow leaf). The main goal of this work was to investigate the function of the MYB112 transcription factor through the integration of metabolomics and transcriptomics, and to unravel MYB112 gene expression network using available *in vitro* and *in vivo* approaches.

3. Results

3.1. Molecular Characterisation of *MYB112* Transgenic Plants

The *MYB112* gene consists of three exons and encodes a protein of 243 amino acids. In order to investigate the function of *MYB112 in planta* we analysed two *myb112* mutants with the T-DNA insertion localised to the 5'-UTR (*myb112-1*; GK093E05) or 3'-UTR (*myb112-2*; Salk098029) of the gene (**Figure 8A**). Decreased level of functional, full-length *MYB112* transcript in homozygous mutants was confirmed using PCR (**Figure 8B**). This measurement revealed that down-regulation of *MYB112* expression was more pronounced in case of line *myb112-1* than in the *myb112-2* line. *MYB112* RNAi lines were obtained from AGRIKOLA (http://www.agrikola.org) and *MYB112* transcript level was analysed in seven selected lines (**Figure 8C**). The strongest decrease in *MYB112* expression, around 32-fold compared to wild type, was observed for lines RNAi#2 and RNAi#10. These lines were used for further analysis of growth phenotypes.

Transgenic plants expressing *MYB112* under the control of both, a synthetic estradiol (EST)-inducible promoter (*MYB112-IOE*) and the constitutive Cauliflower Mosaic Virus (CaMV) *35S* promoter (*35S:MYB112* and *MYB112-GFP*) were generated in the *Arabidopsis* Col-0 background. *MYB112-IOE* plants were obtained by cloning of the *MYB112* coding sequence into the pER8 vector (Zuo *et al*., 2000). After selection on antibiotic containing MS media, two-week old *MYB112-IOE* seedlings were transferred to liquid MS media and expression of *MYB112* was induced by addition of 10 µM estradiol. After two hours of induction plants were harvested and the *MYB112* transcript level was measured using qRT-PCR. We could detect around 5-fold increase of *MYB112* expression in the estradiol-treated plants in comparison to DMSO-treated control plants (**Figure 9A**). We have also tested the expression level of *MYB112* in selection-surviving *35S:MYB112* and *MYB112-GFP* lines. Measurements were performed using two-week-old seedlings grown *in vitro* on MS media (**Figure 9B** and **9C**). We could observe an up to 5- and 15-fold increase in *MYB112* expression in *35S:MYB112-GFP#4* and *35S:MYB112#3* lines, respectively. These lines were selected for further studies.
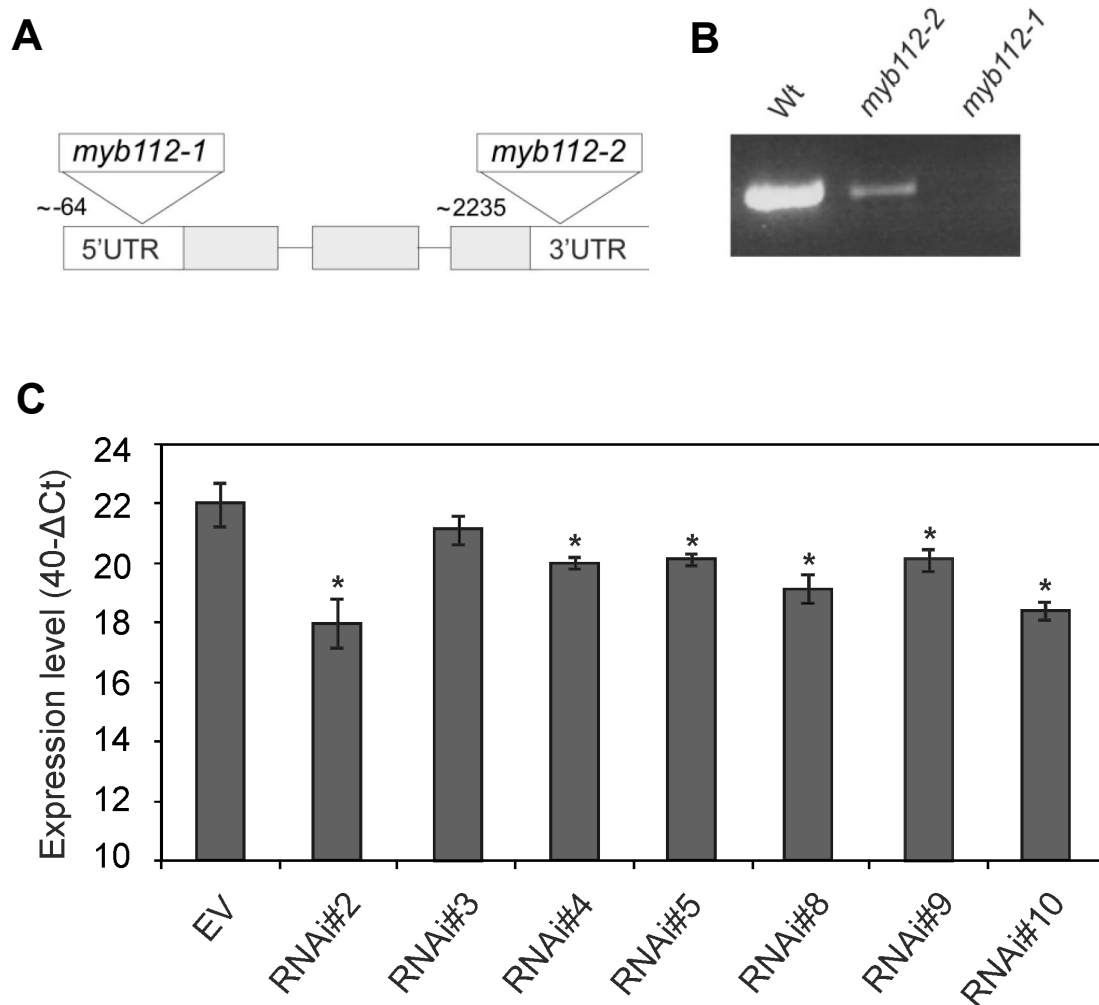
Figure 8. Molecular characterisation of *myb112* T-DNA insertion mutants and *MYB112* RNAi lines.

(A) Location of T-DNA insertion in the two *myb112* T-DNA insertion mutants. **(B)** Decreased level of *MYB112* transcript in *myb112-1* and *myb112-2* mutant plants, shown by semi-quantitative RT-PCR (26 cycles) with primers annealing to the start and stop regions of the coding segment. **(C)** *MYB112* expression level in empty vector (EV) and RNAi plants determined using qRT-PCR. The data is represented as $40 - \Delta C_t$, where ΔC_t is equal to C_t gene of interest $- C_t$ reference gene *UBQ10*. Data are means of three independent experiments $\pm$ SD.
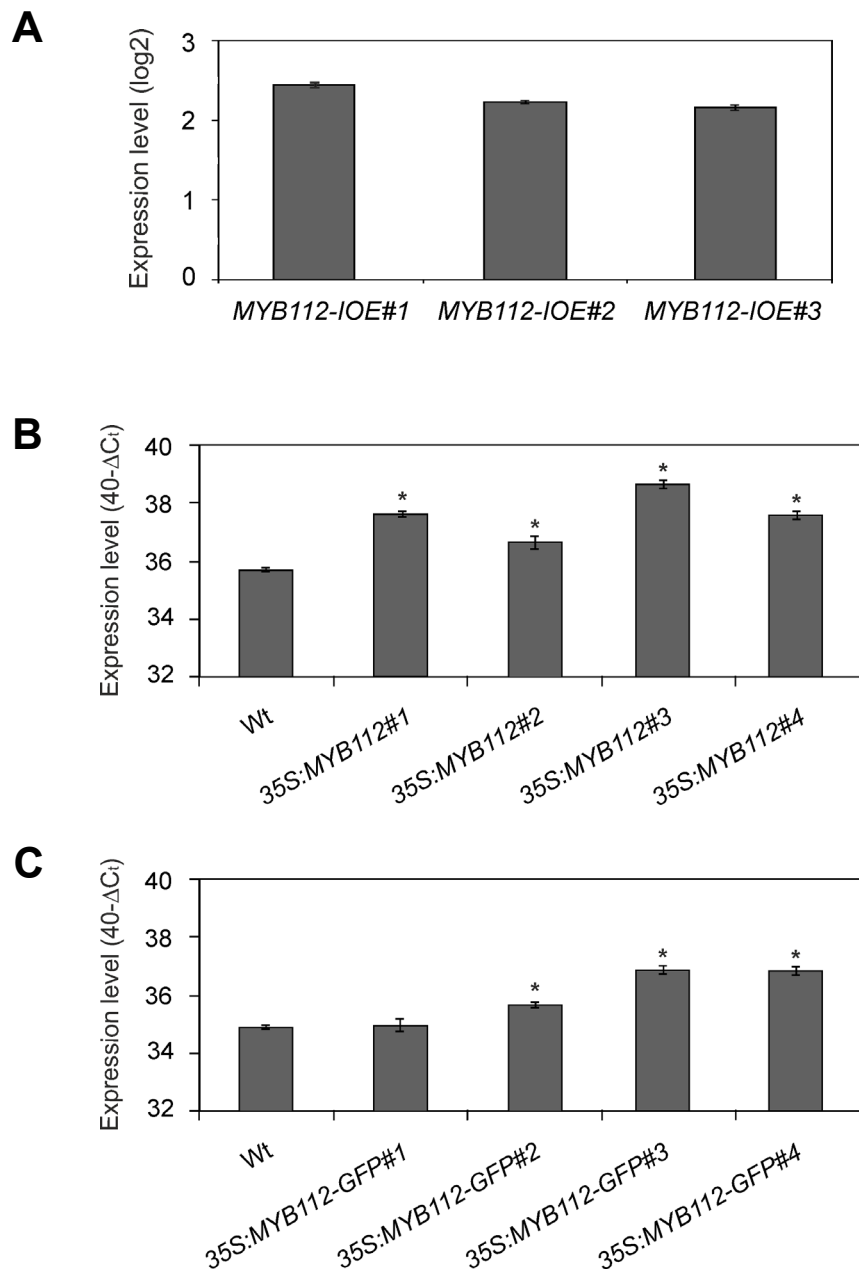
Figure 9. Molecular characterisation of *MYB112* overexpression plants.

Comparison of *MYB112* expression in selected lines of *MYB112* overexpression plants measured in two-week-old *Arabidopsis* seedlings using qRT-PCR. **(A)** *MYB112-IOE* seedlings treated for 2 h with 10 µM estradiol in liquid MS medium, supplemented with 1% sucrose. As controls, DMSO-treated *MYB112-IOE* plants were used. Average log2 values ± SD measured by qRT-PCR are shown. **(B)** *35S:MYB112* and wild-type seedlings. **(C)** *35S:MYB112-GFP* and wild-type seedlings. The data are represented as $40-\Delta C_t$, where ΔC_t is equal to $C_{t\ \text{gene\_of\_interest}} - C_{t\ \text{reference\_gene\_Actin}}$. Data are means of three independent experiments ± SD. Asterisks indicate statistically significant differences to wild type as determined by Student's *t*-test, p<0.05 **(B-C).**

20

3.2. Subcellular Localisation and Spatio-temporal Expression Pattern of MYB112

a.   Subcellular Localisation of MYB112

To test the subcellular localisation of MYB112 protein we expressed it as a fusion to the N-terminus of green fluorescent protein (GFP) using the Cauliflower Mosaic Virus *35S* (CaMV) promoter. The *35S:MYB112-GFP* construct was transformed into *Arabidopsis* plants and transgenic lines were selected on antibiotic-containing MS medium. Increased expression of *MYB112* was confirmed for three out of four *35S:MYB112-GFP* transgenic lines using qRT-PCR (see **Figure 9C**). The localisation of MYB112-GFP fusion protein in roots of ten-day old *35S:MYB112-GFP3* and *35S:MYB112-GFP4* transgenic seedlings was analysed under the fluorescence microscope. GFP fluorescence was exclusively present in nuclei (**Figure 10A**), consistent with the role of MYB112 as a TF.

Conclusion: MYB112 is a Nuclear Protein

b.   Tissue-specific Expression of *MYB112*

To investigate *MYB112* expression at the tissue level, a ~1.3-kb long 5´ upstream regulatory region, including the 5'-UTR, was transcriptionally fused to the β-glucuronidase (*GUS*) reporter gene and the resulting construct, *Pro$_{MYB112}$:GUS* in the pCAMBIA1305 vector, was transformed into *Arabidopsis thaliana* by *Agrobacterium*-mediated transformation.
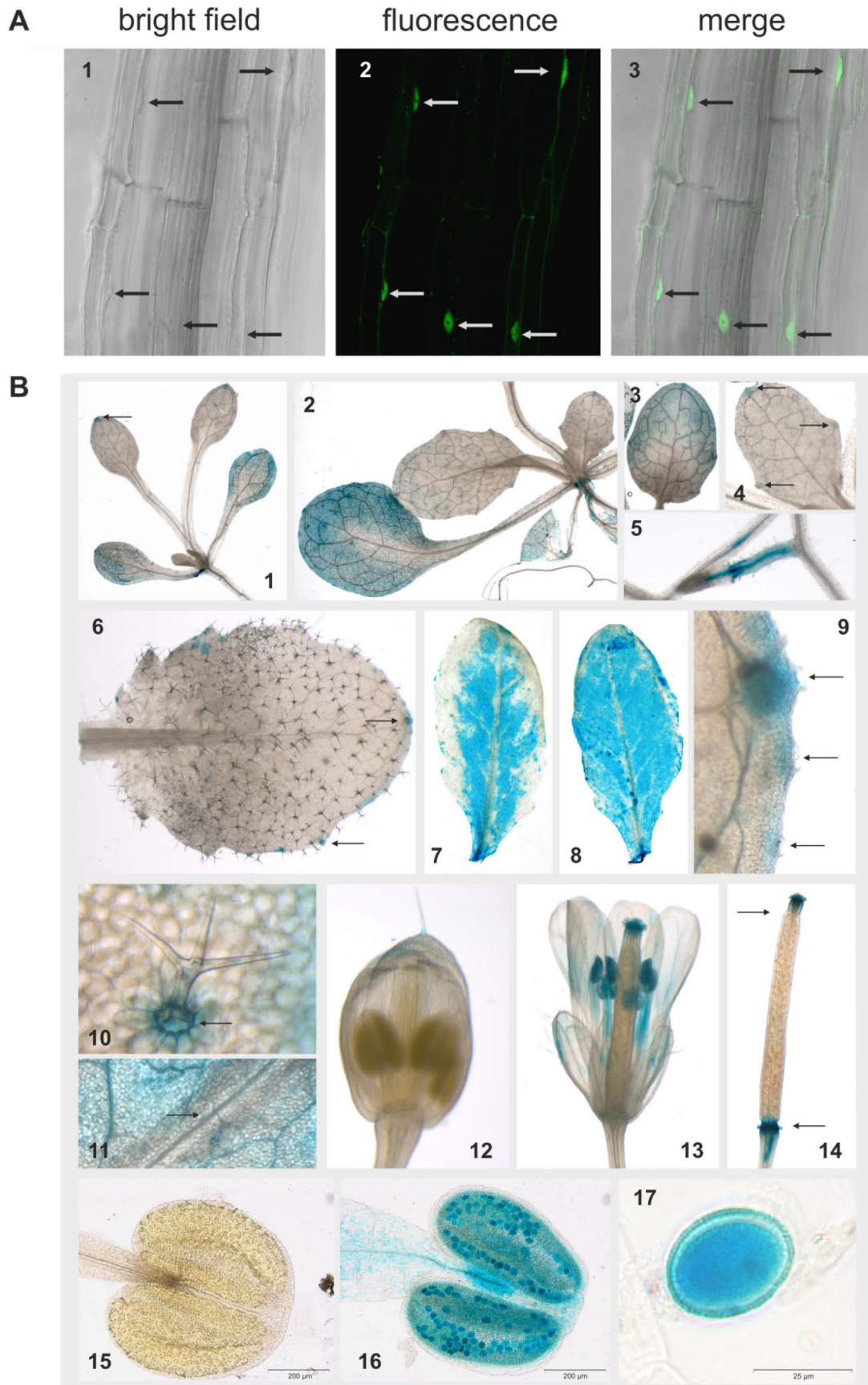
Figure 10. Localisation of *MYB112* expression.

(A) Subcellular localization of MYB112-GFP fusion protein in roots of transgenic *Arabidopsis*. 1, Bright field. 2, GFP fluorescence. 3, Merged. Arrows indicate the presence of MYB112-GFP protein in the nuclei. **(B)** GUS activity in *Arabidopsis thaliana* Pro$_{MYB112}$:*GUS* seedlings. 1, Ten-day-old seedling. GUS staining is mainly localized to cotyledons. Staining is also visible in the tip and margin regions of leaves number one and two (arrow). 2 - 5, 14-day-old seedlings. 2 and 3, GUS activity in leaves one and two. 4, GUS staining in hydathodes of leaf six (arrows). 5, Lateral root. 6 - 14, three- to six-week-old plants. 6, GUS activity in a young rosette leaf is restricted to hydathodes (arrows). 7, GUS activity in mature rosette leaves is often absent from the leaf edges, with the exception of hydathodes (zoom in 9) and the trichome base (zoom in 10); also the mid vein remains unstained (zoom in 11). 8, Strong GUS staining in a senescent leaf. 12, No detectable *GUS* expression in a flower bud. 13, GUS activity in a mature flower. 14, GUS staining in stigma and the internode of gynoecium (abscission zone) (arrows). 15, No staining in a young anther. 16, Intense GUS staining in a mature anther and pollen grains (zoom in 17). Staining was performed for ~1-2 h.

GUS activity driven by the *MYB112* promoter was tested in five independent transgenic lines of T2 and T3 generations. Representative expression patterns are shown in **Figure 10B**. Expression of the *MYB112* gene was observed in most tissues both, in young seedlings and throughout plant development. At approximately ten days after sowing (DAS), GUS activity was detected in cotyledons and in the margins of the first leaves, where hydathodes are localised (**Figure 10B.1**). Hydathodes enable water conduction (Candela *et al.*, 1999). By two weeks, the following rosette leaves were fully expanded and displayed relatively strong GUS activity, while GUS staining was restricted to hydathodes in recently emerged leaves (**Figure 10B.2-4**). *GUS* expression was also detected in lateral roots of young seedlings (**Figure 10B.5**). In older plants, GUS activity was observed in both leaves and flowers. Young rosette leaves, like young seedling leaves, exhibited gene expression exclusively in hydathodes (**Figure 10B.6** and **10B.9**). In mature rosette leaves GUS staining was also detected at the base of trichomes and around the mid vein (**Figure 10B.7** and **10B.10**), however no GUS activity was observed in the mid vein itself (**Figure 10B.7** and **10B.11**). The strongest GUS signal was observed in old rosette leaves, demonstrating that *MYB112* is a senescence-associated gene (SAG; **Figure 10B.8**); this finding is in accordance with previous reports that found elevated *MYB112* transcript abundance in senescing leaves compared to non-senescent leaves, as determined by microarray hybridizations and quantitative real-time PCR (qRT-PCR) (Balazadeh *et al.*, 2008; Breeze *et al.*, 2011). Staining in the floral parts was mainly localised to anthers and pollen (**Figure 10B.13** and **10B.16** and **17)**. Immature floral

tissue showed no GUS activity (**Figure 10B.12** and **10B.15**), consistent with virtually undetectable *MYB112* expression on microarrays (see eFP browser; http://bar.utoronto.ca/efp). *GUS* expression was also noted at the stigma and bottom end (later fruit abscission zone) of the gynoecium (**Figure 10B.14**).

3.3. Identification of MYB112 Early Responsive Genes

a.   Expression Profiling after Short-term Induction of *MYB112* Expression in *MYB112-IOE* Plants

To identify downstream target genes of the MYB112 TF and thus define its regulatory network, we used two-week-old *MYB112-IOE* plants and tested EST-dependent *MYB112* expression 1 h, 3 h and 5 h after EST treatment. As controls we either used DMSO-treated *MYB112-IOE* lines or EST-treated empty-vector plants. *MYB112* expression increased strongly (by up to ~115-fold) already within 1 h of EST treatment, further increased after 3 h (to ~294-fold), and reached its maximum (~765-fold) 5 h after EST application (**Figure 11**). To find genes responsive to MYB112, two-week-old *MYB112-IOE* seedlings were transferred to liquid MS medium containing either 10 µM EST or DMSO as control. Seedlings were harvested 3 h and 5 h after EST induction and after removal of the roots were subjected to expression profiling using Affymetrix ATH1 arrays. By including the wild-type control line in our analyses we could distinguish between genes responding solely to the EST treatment from those responding to elevated *MYB112* expression. Two independent experiments were performed and analysed from the 5 h time point (*MYB112-IOE*-5 h), and one experiment from the 3 h time point (*MYB112-IOE*-3 h). Statistical tests using the Limma Bioconductor package (Gentleman *et al.*, 2004) allowed us to identify 56 genes that were significantly differentially expressed (>2-fold) upon 5 h induction of *MYB112*, of which 28 were up- (**Figure 12**, **Table 2**) and 28 were down-regulated (**Figure 12**, **Table 1**), excluding the EST-responsive genes in wild-type plants (see Gene Expression Omnibus, http://www.ncbi.nlm.nih.gov/geo/, accession no. GSE36721).
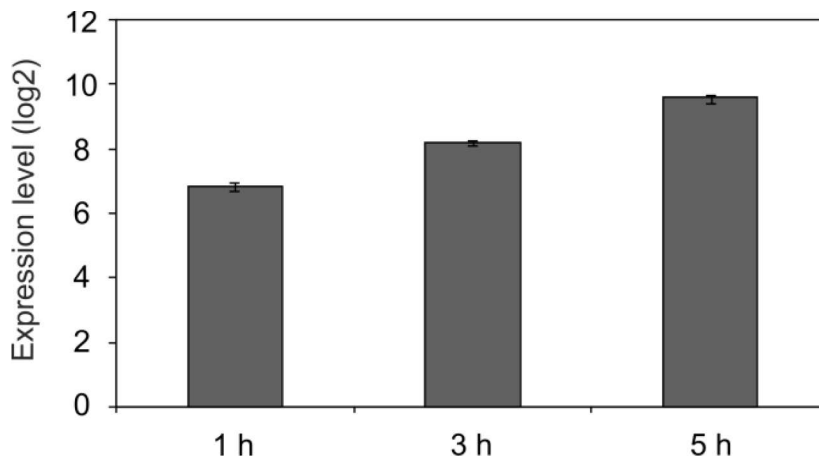
Figure 11. Expression level of *MYB112* in estradiol-treated *IOE* plants.

Two-week-old *Arabidopsis MYB112-IOE* seedlings were treated for 1 h, 3 h and 5 h with estradiol in liquid MS medium supplemented with 1% sucrose. As controls, DMSO-treated *MYB112-IOE* plants were used. Average log2 values ± SD measured by qRT-PCR are shown (n = 3).

Among the up-regulated genes three encoded TFs, namely *MYB32*, *MYB7* and *MYB6*. Interestingly, all three TFs belong to the same subgroup 4 of the R2R3-MYB family. MYB factors of this subgroup were shown to be involved in the regulation of flavonoid and lignin biosynthesis in *Arabidopsis* (Preston *et al*., 2004; Zhong and Ye, 2012). *UGT84A2* is another gene with a function in phenylpropanoid biosynthesis and modification, and was up-regulated after 5 h of *MYB112* induction. UGT84A2 is a sinapic acid-*O*-glucosyltransferase (Sinlapadech *et al*., 2007) that plays a major role in providing sinapoyl-glucose for anthocyanin sinapoylation (therefore being highly important in the production of the anthocyanin derivative A11; Yonekura-Sakakibara *et al*., 2012). Moreover *MYB32*, *MYB7* and *UGT84A2* were previously shown to be up-regulated during age-dependent senescence in wild-type *Arabidopsis* (Buchanan-Wollaston *et al*., 2005; Balazadeh *et al*., 2008; GENEVESTIGATOR). Besides *MYB32*, *MYB7* and *UGT84A2*, eleven other upregulated transcripts (representing half of the MYB112 up-regulated genes, see **Table 2**) were previously reported to be senescence-associated (eFP brawser; Winter *et al.* 2007, Balazadeh *et al.,* 2008;

Breeze *et al.*, 2011; http://www2.warwick.ac.uk/fac/sci/lifesci/research/prestadata/ senescence). This result supports the model that MYB112 is a senescence-regulatory TF and that expression of several known senescence-associated genes (including TFs) is regulated by this MYB TF. In the single 3 h Affymetrix experiment we identified (>4-fold) 15 differentially expressed genes (one up-, and 14 down-regulated; see Gene Expression Omnibus, accession no. GSE36721). There was an overlap of one up-regulated gene (*MYB7*) and seven down-regulated genes at both 3 h and 5 h after *MYB112* induction (**Figure 12**). We next tested the expression of 28 genes up-regulated after 5 h of EST treatment, using qRT-PCR and could confirm expression changes for 22 of the 28 up-regulated genes in RNA samples from a third, independent biological experiment (**Table 2**).
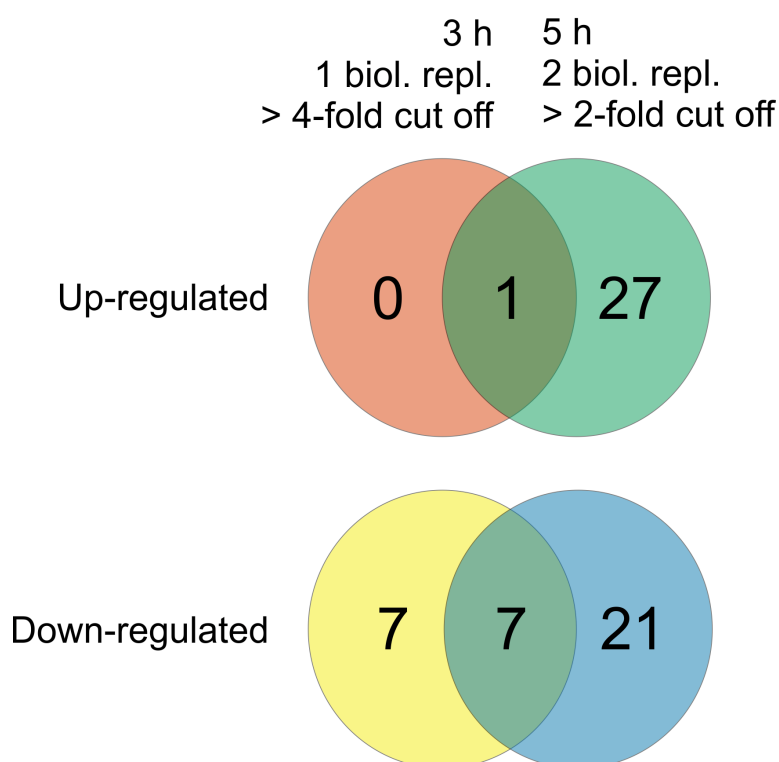
Figure 12. Identification of MYB112 early responsive genes.

The number of up- and down-regulated gens in *MYB112-IOE* two-week-old seedlings treated with estradiol for 3 h (one biological replicate) or 5 h (two biological replicates) as measured using Affymetrix ATH1 microarray. Cut off 4-fold and 2-fold was used for the 3 h and 5 h experiment, respectively.

Table 1. MYB112-dependent down-regulated genes.

| AGI | Annotation | MYB112-IOE; log2 (EST-Mock) | | | | |
| | | ATH1 | | | qRT-PCR | |
		3 h_1	5 h_1	5 h_2	5 h	SD
AT3G02550	LBD41	-2,40	-2,31	-2,20	-2,39	0,20
AT5G62520	SRO5	-1,79	-2,05	-3,18	-1,60	0,03
AT4G33070	Pyruvate decarboxylase	-2,20	-1,76	-3,45	-1,55	0,06
AT4G10270	Wound-responsive family protein	-1,69	-2,01	-1,42	-1,65	0,47
AT5G42200	RING/U-box superfamily protein	-2,21	-2,07	-1,19	-0,82	0,11
AT3G10040	Transcription factor	-2,64	-1,73	-2,69	-1,42	0,38
AT4G24110	Unknown protein	-1,64	-1,84	-2,86	-1,56	0,24
AT5G39890	Unknown protein	-2,95	-1,51	-2,68	-1,53	0,23
AT1G33055	Unknown protein	-2,74	-2,03	-1,70	-1,28	0,43
AT5G66985	Unknown protein	-2,42	-1,31	-1,39	-1,31	0,38
AT1G24260	SEP3	0,24	-1,32	-1,85	n.t.	n.t.
AT1G13300	HRS1	-0,85	-1,24	-2,44	n.t.	n.t.
AT4G17460	HAT1	-0,45	-1,26	-1,00	n.t.	n.t.
AT5G47370	HAT2	-0,64	-1,23	-1,27	n.t.	n.t.
AT2G43060	IBH1__ILI1 binding bHLH 1	-0,62	-1,26	-1,98	n.t.	n.t.
AT3G27170	CLC-B	0,16	-1,03	-1,17	n.t.	n.t.
AT1G15960	NRAMP6	-0,40	-1,20	-1,17	n.t.	n.t.
AT3G19470	F-box family protein	-0,07	-1,35	-1,04	n.t.	n.t.
AT4G37770	ACS8	-0,51	-1,10	-1,76	n.t.	n.t.
AT5G61160	AACT1	0,40	-1,10	-1,24	n.t.	n.t.
AT1G78050	PGM	-0,42	-1,14	-1,32	n.t.	n.t.
AT1G75960	AMP-binding protein, putative	-0,03	-1,04	-1,16	n.t.	n.t.
AT2G26020	PDF1.2b	0,46	-1,88	-3,53	n.t.	n.t.
AT2G43590	Chitinase, putative	-0,28	-1,24	-3,43	n.t.	n.t.
AT3G07350	DUF506	-0,18	-1,02	-1,85	n.t.	n.t.
AT1G21050	DUF617	-0,76	-1,16	-1,80	n.t.	n.t.
AT5G12050	Unknown protein	-0,44	-1,16	-1,04	n.t.	n.t.
AT4G28085	Unknown protein	0.00	-1,30	-1,55	n.t.	n.t.

Change in expression of genes after 3 h (one replicate) and 5 h (two replicates) of *MYB112* induction in EST-treated *MYB112-IOE* seedlings as measured by microarray expression profiling (Affymetrix ATH1) and qRT-PCR. Data are shown as log2 values normalised to mock treated control plants. SD, standard deviation; n.t., not tested. Hypoxia-responsive genes are shown in red (Liu *et al*., 2005; Licausi F., personal communication).

Interestingly, we noted that ten of the MYB112 down-regulated genes, were previously described as hypoxia-responsive (Liu *et al,* 2005; Licausi F., personal communication). These include seven genes common for the 3 h and 5 h induction and three genes responding after 5 h EST treatment (see **Table 2**), According to the available gene expression data (i. e. Genevestigator, publications), expression of *MYB112* does not change upon hypoxia or anoxia, or after reoxygenation. However, transcript level is only one part of the regulatory process; factors such as RNA stability, translation rates, protein processing and stability and many others are likely to have essential roles in the moderation of MYB112 cellular activity. We therefore designed qRT-PCR primers for 50 genes previously described as hypoxia-responsive (Liu *et al*., 2005) and measured their expression in *MYB112-IOE* seedlings treated with EST for 5 h. We could confirm the decreased transcript level of nine genes shown in **Table 1**, using RNA from an independent biological experiment. Moreover, we found that expression of additional four hypoxia-responsive genes was decreased in transgenic plants in comparison to DMSO-treated plants (see **Supplementary Table 1**). The relation between MYB112 and decreased expression of hypoxia-responsive gens is currently unclear and requires further investigation.

Conclusion: MYB112 Acts as Both Positive and Negative Regulator of Gene Expression

b.   Transactivation Assay in *Arabidopsis* Mesophyll Protoplasts

To confirm that MYB112 regulates the expression of genes identified by expression profiling, we assayed the trans-activation capacity of MYB112 on the promoters of *MYB32*, *MYB7* and *MYB6*. These putative downstream target genes were selected from the dataset considering their function as TFs. Interestingly enough, all three TFs belong to subgroup 4 of the R2R3-MYB family.
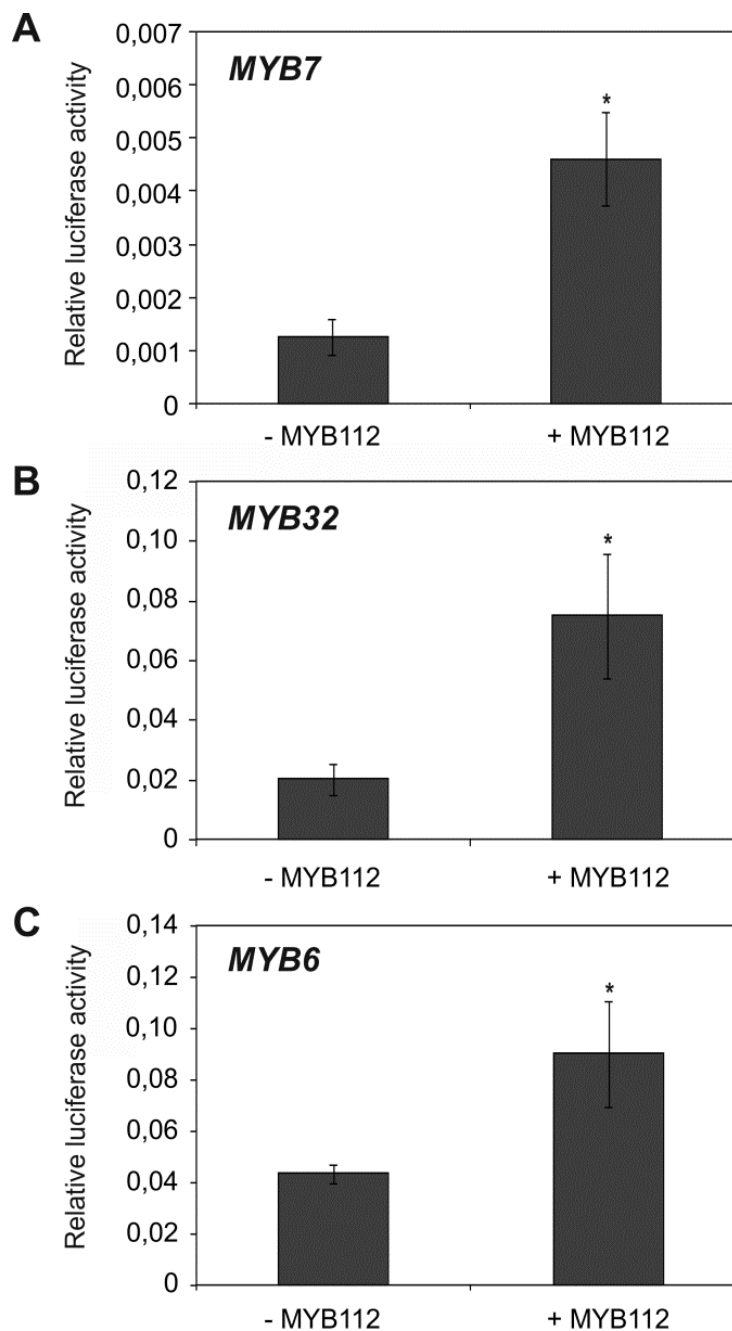
Figure 13. Transactivation assay in *Arabidopsis* mesophyll protoplasts.

Transactivation of **(A)** *MYB7*, **(B)** *MYB32* and **(C)** *MYB6* expression by MYB112 in *Arabidopsis* mesophyll cell protoplasts. The *Pro$_{MYB7}$:fLUC*, *Pro$_{MY32}$:fLUC*, or *Prom$_{MYB6}$:fLUC* constructs harbouring the respective promoters (~1.7 kb) upstream of the firefly (*Photinus pyralis*) luciferase (fLUC) open reading frame were co-transformed with the *35S:MYB112* plasmid (omitted in control experiments). The *35S:rLUC* vector was used for transformation-efficiency normalization. Given are means ± SD of five independent transformations. Asterisks indicate significant differences to control as determined by Student's *t*-test, *p* < 0.05.

MYB factors of this subgroup were shown to be involved in the regulation of flavonoid and lignin biosynthesis in *Arabidopsis* (Preston *et al*., 2004; Zhong and Ye, 2012). Mesophyll cell protoplasts were prepared from wild-type (Col-0) *Arabidopsis* leaves and transiently transformed with constructs expressing *MYB112* under the control of the Cauliflower Mosaic Virus (CaMV) *35S* promoter. Simultaneously, protoplasts were transfected with vectors carrying the firefly (*Photinus pyralis*) luciferase open reading frame fused to the upstream sequences of the selected MYB112 target genes. For normalization, protoplasts were additionally transformed with a third construct expressing the *Renilla* luciferase from the *35S* promoter. Protoplasts lacking the *35S*:*MYB112* effector construct served as controls. *MYB7* and *MYB32* promoters displayed over 3-fold and *MYB6* ~2-fold induction of the reporter gene when *MYB112* was overexpressed in the protoplasts (**Figure 13**).

c.   Expression in *myb112* T-DNA Insertion Mutants
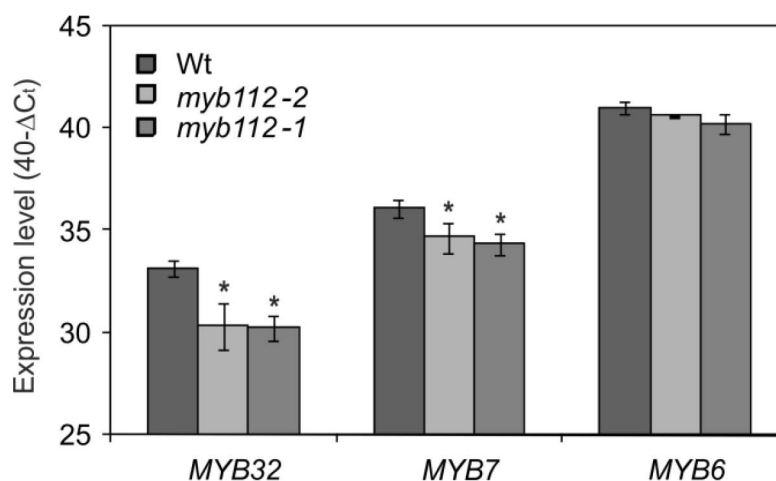
Figure 14. Expression of *MYB32*, *MYB7* and *MYB6* in *myb112* T-DNA insertion lines.

Transcript levels of *MYB32*, *MYB7* and *MYB6* in wild-type, *myb112-1* and *myb112-2* mutant two-week-old seedlings as measured by qRT-PCR. Data are represented as $40-\Delta C_t$, where ΔC_t is equal to $C_{t\ gene\_of\_interest} - C_{t\ reference\_gene\_ACTIN}$. Data are means of three replicates ± SD. Asterisks indicate statistically significant differences to wild type (Wt) as determined by Student's *t*-test, $p < 0.05$.

In addition, we measured transcript abundance of *MYB32*, *MYB7* and *MYB6* in *MYB112* mutants grown for two weeks on MS medium supplemented with 1% sucrose. Expression of both, *MYB32* and *MYB7* was decreased in the *myb112-1* and *myb112-2* lines by ~9- and ~3-fold, respectively. Expression of *MYB6* remained unchanged (**Figure 14**), possibly due to functional redundancy of upstream regulatory TFs. However, taken together the microarray and transactivation assay data confirm a regulatory function of MYB112 towards *MYB32*, *MYB7* and *MYB6.*

Conclusion: MYB112 Triggers the Expression of *MYB32, MYB7* and *MYB6*; R2R3-MYB Transcription Factors of Subgroup 4

3.4. Identification of MYB112 Direct Target Genes

a.   Identification of the MYB112 DNA Binding Site

In order to estimate the location of a putative MYB112 binding site within the *MYB32* promoter we used Imap (Infrared mediated mapping of TF binding sites) - a method recently established in our group. The *MYB32* promoter was divided into three 300 bp long DNA fragments and each fragment was labeled with an infrared dye (IRD). Obtained labeled DNA fragments (I-IRD: to around 300 bp upstream the ATG start codon, II-IRD: from - 300 bp to - 600 bp, and III-IRD from - 600 bp to - 900 bp, see **Figure 15**) were next incubated with *in vitro* expressed MYB112-GST fusion protein. After subsequent washing steps, the amount of DNA bound to the protein was assessed by measuring the IRD signal intensity (**Figure 15**). Control experiments were performed using GST instead of the MYB112-GST fusion protein. Strong IRD signal was detected in case of the I-IRD fragment which was compromised in the presence of its non-labeled version (1:1 ratio, competition experiment). This result indicates that MYB112 recognises a specific sequence within the - 600 to - 900 bp promoter region upstream of the translation initiation site.
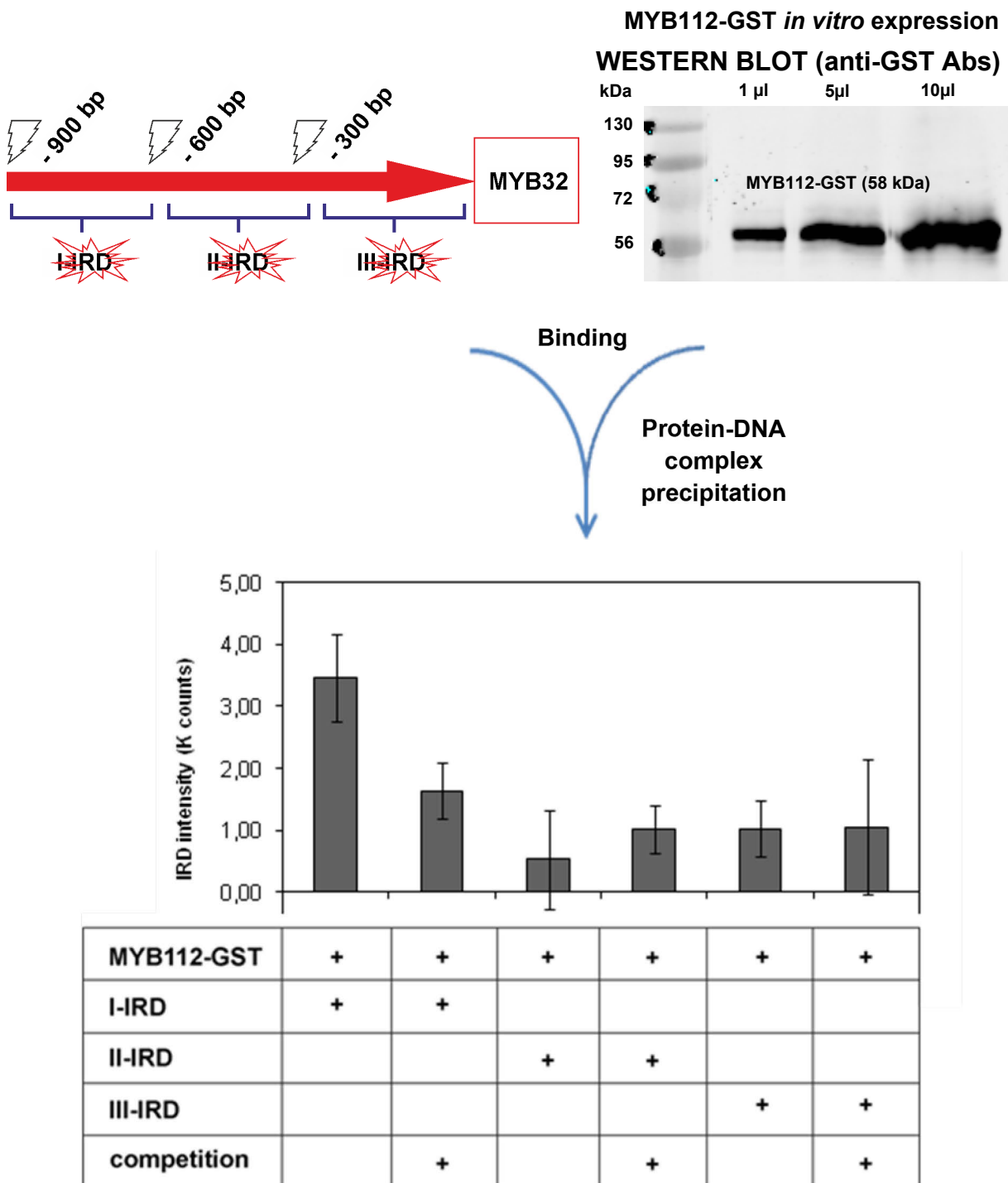
Figure 15. Infrared mediated mapping of TF binding sites (Imap).

MYB112-GST fusion protein was expressed *in vitro* using *E. coli* lysate and incubated with three infrared labeled fragments of the *MYB32* promoter (each ~300 bp long). After washing and protein-DNA complex precipitation, IRD signal intensity was measured. For competition experiments, non-labeled DNA fragments were used (1:1 ratio). As control, GST was used instead of the MYB112-GST fusion protein. Average values ± SD are shown for two independent experiments.

Simultaneously, in collaboration with Gang-Ping Xue (CSIRO Plant Industry, Brisbane, Australia), we performed an *in vitro* binding site (BS) selection experiment to identify sequence motifs recognized by MYB112 using the CELD-transcription factor fusion method (Xue, 2002; Xue, 2005). MYB112 was translationally fused to the catalytic domain of a 6xHIS-tagged cellulase D (CELD) from *Neocallimastix patricairum*. CELD is a highly reactive cellulase enzyme. The MYB112-CELD-HIS fusion under the control of a *tac* promoter (P*tac*) was transformed to XL1-Blue strain of *E. coli*. Positive clones, containing the in-frame fusion, were identified using carboxymethyl (CM)-cellulose as a substrate. This substrate was added to the *E. coli* Luria Broth (LB) medium and was hydrolised only by positive clones. The hydrolysis of cellulose was visualized by Congo Red staining (**Figure 16A**). The MYB-CELD-HIS fusion protein was next purified from the positive clones using a 1-mL Ni^{2+} column (GE Healthcare, Munich, Germany) coupled to an Äkta-Purifier FPLC system (GE Healthcare). Aliquots of the flow-through fractions were analysed by electrophoresis on 12% polyacrylamide gel (SDS-PAGE) and Coomassie staining (**Figure 16B**).
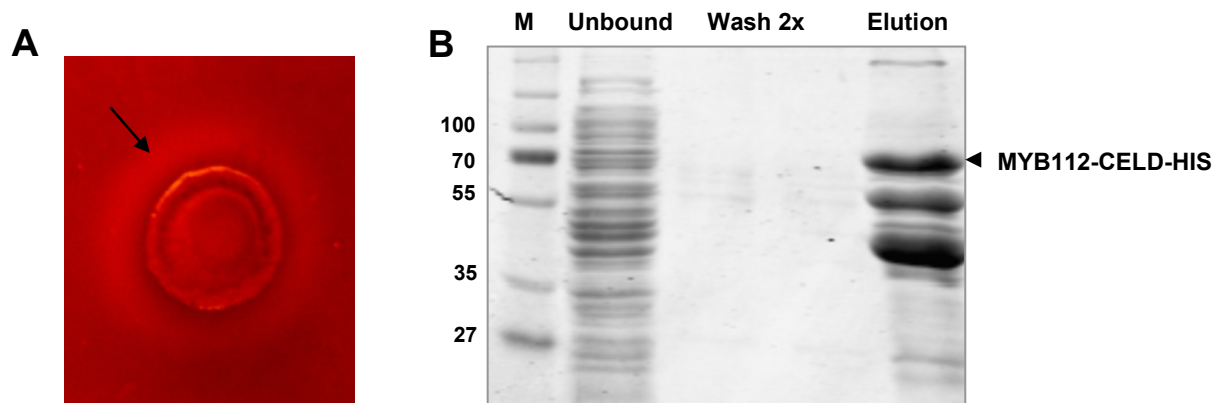
Figure 16. Screening for cellulase-positive MYB112-CELD-HIS clones.

(A) MYB112-CELD-HIS expressing *E. coli* colony grown on carboxymethyl (CM)-cellulose-containing medium after Congo Red staining. Due to the CELD activity CM-cellulose present in the medium is hydrolysed and this effect is visualised by Congo Red staining (note the light hallow indicated by an arrow). **(B)** MYB112-CELD-HIS protein (~70 kDa) was purified from *E. coli* lysates of cellulose-positive clones using a 1-mL Ni^{2+} column (GE Healthcare, Munich, Germany) coupled to an Äkta-Purifier FPLC system (GE Healthcare). Aliquots of the flow-through fractions were analysed by electrophoresis on 12% polyacrylamide gel (SDS-PAGE) and Coomassie staining. The first line on the gel represents separation of the marker

peptides (M). The second line contains proteins that did not bind to the Ni^{2+}-agarose beads (unbound fraction). The two following lines contain proteins washed away during two washing steps. In the fourth line, MYB112-CELD-HIS protein is separated.

Expressed and purified recombinant MYB112-CELD-HIS protein was incubated with biotin-labeled random-sequence oligonucleotide probes (performed by Gang-Ping Xue). Oligonucleotides bound by the MYB112-CELD-HIS fusion protein were recovered by means of affinity purification of the DNA-MYB112-CELD-HIS complex and amplified using PCR (Xue, 2002; Xue, 2005). Next, the amplified DNA fragments were cloned into bacteria and sequenced (**Figure 17A**). Twenty nine sequences were obtained and analysed for binding activity. An alignment of the target sequences is shown in **Figure 17B**. MYB112 binds to an 8-bp DNA fragment containing the consensus sequence (A/T/G)(A/C)CC(A/T)(A/G/T)(A/C)(T/C). The identified MYB112 recognition site is present in promoters of genes up-regulated by MYB112 in estradiol-inducible overexpression lines (**Table 2, Supplementary Data 1**), including *UGT84A2* (one BS at ~-1.6 kb counted from the translation initiation codon) and the three MYB genes (within the 1-kb upstream regions): *MYB32* (two BSs), *MYB7* (one) and *MYB6* (three). One of the two MYB112 recognition sites identified within the *MYB32* promoter is localised at position -777 bp, i.e. within the region previously selected using Imap (**Figure 15**). The second BS is located at the position -986 bp, so beyond the analysed region of -900 bp. The MYB112 BS identified here is similar to the MYB consensus motif: (A/C)ACC(A/T)A(A/C)C (Sablowski *et al.*, 1994) identified as *cis* element responsible for the binding of MYB proteins in the anthocyanin pathways in *Antirrhinum* (Sablowski *et al.,* 1994; Tamagnone *et al.*, 1998) and maize (Grotewold *et al.*, 1994).

In addition, the MYB112 BS is not present within the 1-kb promoter regions of MYB112-dependent down-regulated hypoxia-responsive genes. This indicates an indirect effect of MYB112 on the expression of these genes through activation of other TFs.

A

Ptac   MYB112   CELD   6HIS

MYB112-CELD-6HIS   oligonucleotides

4-7x

binding

complex precipitation

PCR

clonning & sequencing

B

```
ATGTTAGGTAGTTTGGTTGATACCTAACAC
     TGCAGTTAGGTAGTATACCTAACTAAACGG
                AAACCTAACAATGCCTTGTTAGGTACCAGC
    GTGGGTATGGTCTTGACCAAACCATAACCT
  ACTGTAGTTAGGTACTACCTAACCCGCCAC
  ACTGTAGTTAGGTACTACCTAACCCGCCAC
  GTGGCGGGTTAGGTAGTACCTAACTACAGT
  GTGGCGGGTTAGGTAGTACCTAACTACAGT
 GGTGTAGTTAGGTACCCAACCTAACATGAT
  GTGTAGTTAGGTACCCAACCTAACATGATA
CAAAGGCGTTAGGTCTTCCAACCTAACGTC
                AACCTAACTTAACAGTATAGTTAGGTACTC
            GAGTACCTAACTATACTGTTAAGTTAGGTT
     AACGTTGGGGTGGTTACCTGACATGTCTAC
            GAGTACCTACCTATACTGTTAAGTTAGGTT
GTTGGGGAATAATGCGATGTTTACCTAACG
        ACGTGTTAGGTTAGGACCTAACATATACCC
    GGGATTAGGTCCCACCTAACCTAATCGGGAA
     GATTAGGTCATTACTACCTAATCTCCCCCA
CGCGTTGTTAGGTTCCTGCCTACCTAACTT
       GGAGTTAGGTCAGAACCTAACCCCTGTTTC
          GGCGGTTTTACCTAACTGGCGAGATCCCCC
               TAACCTAACTACGGCGGGGAAAGCGGTTGG
  CCAAGGTTAGGTAAAAACCTAACTTCGTGG
  CCAAGGTTAGGTAAAAACCTAACTTCGTGG
             GTATCCCTAATGTCGTGAACGAGCTGGCAT
  TCGGTTAGGTCTCACAACCTAACTGACGGT
CAAGGTACAGTTAGGTTACAGACCTAACTA
             CGCACTAACCTTACGGTTGGGCAGGACTGG
```

C

Figure 17. Identification of MYB112 DNA binding site.

(A) Schematic representation of the *in vitro* binding site selection experiment. **(B)** Alignment of 29 sequences derived from oligonucleotides bound to MYB112-CELD-HIS fusion protein after *in vitro* binding site selection. **(C)** A motif common for 29 positive clones identified using MEME. The selected motif is present in the promoters of putative direct target genes.

Conclusion: **MYB112 BS is Present within the Promoters of Genes Encoding R2R3-MYB Factors of Subgroup 4 and *UGT84A2***

Table 2. MYB112-dependent up-regulated genes with indicated number of MYB112 binding sites (BS).

| AGI | Annotation | MYB112-IOE; log2 (Est-Mock) | | | | | BS |
| | | ATH1 | | | qRT-PCR | | |
		3 h_1	5 h_1	5 h_2	5 h	SD	
AT1G48000	MYB112	8,20	10,17	10,03	9,58	0,12	
AT2G16720	MYB7	2,17	2,84	1,10	1,88	0,02	1
AT4G34990	MYB32	0,76	2,34	3,24	2,52	0,63	2
AT4G09460	MYB6	0,26	1,10	1,55	1,54	0,16	3
AT3G21560	UGT84A2	0,91	1,30	1,45	1,61	0,17	0
AT1G22360	UGT85A2	0,47	1,87	1,87	1,49	0,15	0
AT4G19460	UDP-Glycosyltransferase protein	0,07	1,48	1,23	2,15	0,33	2
AT2G35060	KUP11	0,68	1,54	1,33	1,37	0,25	0
AT1G66090	Disease resistance protein	-0,39	2,25	1,06	1,19	0,15	1
AT1G29230	CIPK18	0,00	2,04	2,18	4,19	0,31	3
AT1G54890	LEA protein-related	0,50	1,91	2,73	4,91	1,30	2
AT3G51300	ARAC11	-0,04	1,69	1,40	2,21	0,05	3
AT2G25530	AFG1-like ATPase family protein	0,00	1,37	2,11	1,16	0,13	2
AT4G24380	Serine hydrolase	0,05	1,57	1,38	1,94	0,31	1
AT5G44910	Toll-Interleukin-Resistance protein	0,28	1,03	1,91	2,77	0,44	1
AT2G29340	NAD-dependent epimerase/dehydratase	0,27	1,20	1,06	1,45	0,35	2
AT4G20460	NAD-dependent epimerase/dehydratase	0,50	1,77	2,02	1,98	0,38	0
AT5G52810	NAD(P)-binding Rossmann-fold protein	0,51	1,45	2,00	2,07	0,26	0
AT3G18250	Putative membrane lipoprotein	0,51	2,77	3,86	2,08	0,67	1
AT4G38950	Kinesin motor family protein	0.00	4.14	3.48	2.55	0.47	0
AT5G19875	Unknown protein	0,28	2,00	2,50	2,20	0,18	1
AT5G38320	Unknown protein	0,00	3,12	4,88	1,88	0,13	0
AT3G14060	Unknown protein	0,02	1,50	2,00	1,19	0,15	0
AT1G71830	SERK1	0,03	1,01	1,05	0,48	0,66	0
AT1G69870	NRT1.7	0,25	1,43	1,48	0,47	0,03	1
AT1G12010	2-oxoglutarate Fe(II)-dependent oxygenase	0,00	1,00	1,08	0,40	0,26	1
AT4G27657	Unknown protein	0,00	1,61	1,16	0,49	0,81	0
AT3G18560	Unknown protein	-0,02	1,48	1,09	0,53	0,52	3
AT5G58790	Unknown protein	0,42	1,14	1,33	0,60	0,01	0

Change in expression of genes after 3 h (one replicate) and 5 h (two replicates) of *MYB112* induction in EST-treated *MYB112-IOE* seedlings as measured by microarray expression profiling (ATH1) and qRT-PCR. Data are shown as log2 values normalised to mock-treated control plants. Right column (BS) shows the number of MYB112 binding sites within 1-kb promoter region. SD, standard deviation. Senescence-associated genes (SAGs) are shown in red (eFP browser; Winter *et al.* 2007; Balazadeh *et al.,* 2008; Breeze *et al*., 2011; http://www2.warwick.ac.uk/fac/sci/lifesci/research/prestadata/ senescence).

b.   EMSA and ChIP Assay

We next employed an electrophoretic mobility shift assay (EMSA) to test *in vitro* the physical interaction between MYB112 protein and promoter fragments of *MYB6*, *MYB7* and *MYB32*. Expressed and purified MYB112-CELD-HIS protein was incubated with infrared dye (IRD)-labeled 40-bp long promoter fragments of the selected putative target genes containing the identified MYB112 binding site (BS). The probes included the single MYB112 BS of the *MYB7* promoter (fragment *MYB7_1*), either of the twoBSs of the *MYB32* promoter (*MYB32_1* or *MYB32_2*), or two neighboring sites of the three present in the *MYB6* promoter (both included in *MYB6_1/2* fragment). Locations of the BSs within the promoters of target genes are shown in the **Supplementary Data 1**. After incubation of the fusion protein with respective IRD-labeled promoter fragments, DNA-protein complexes were separated on 6% retardation gel and the IRD signal was detected using the Odyssey Infrared Imaging System from LI-COR Biosciences (Bad Hamburg, Germany). Retardation of DNA movement through the gel (the shift) indicates interaction between the DNA fragment and the DNA-binding protein. This effect is abolished in the presence of an unlabeled version of the DNA fragment (competitor). In the presence of MYB112-CELD-HIS, the IRD-labeled promoter fragments of *MYB6*, *MYB7* and *MYB32* were shifted on the gel (**Figure 18A**, line 2) as compared to the fragments migrating in the absence of the fusion protein (**Figure 18A**, line 1). Binding between the protein and IRD-labeled probes is compromised in the presence of unlabeled versions of the promoter fragments (200-fold molar excess), indicating that MYB112 binding activity is specific. These results indicate a physical interaction of MYB112 with the *MYB6*, *MYB7* and *MYB32* promoters.

Finally, to verify MYB112 binding to the respective promoters *in vivo*, we performed chromatin immunoprecipitation coupled to quantitative polymerase chain reaction (ChIP-qPCR) using plants bearing a *35S:MYB112-GFP* construct (accumulating MYB112-GFP fusion protein in the nucleus, see **Figure 5A**). We designed primers flanking the MYB112 binding sites of the different promoters and measured their abundance using qPCR. As shown in **Figure 18B**, the *MYB32* (binding site 2) and *MYB7* promoter fragments containing the selected *cis* element were enriched relative to control, proving direct binding of MYB112. In contrast, we did not detect significant

binding of MYB112 to the *MYB6* and *UGT84A2* promoters. It may, however, be that these two genes are targets of MYB112 in other physiological conditions that we did not test in our experiments. Taken together, our data firmly prove that MYB112 acts as a direct transcriptional regulator of *MYB32* and *MYB7*.
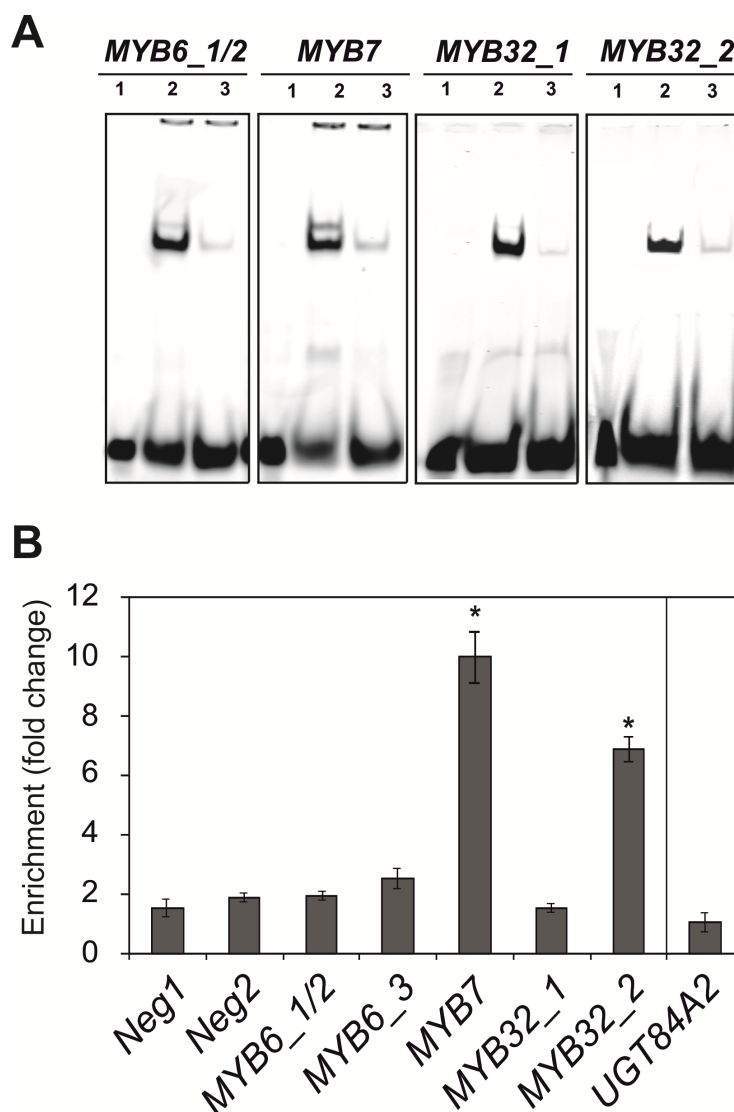
Figure 18. Electrophoretic mobility shift assay (EMSA) and chromatin immunoprecipitation (ChIP) assay.

(A) Electrophoretic mobility shift assay (EMSA). Purified MYB112-CELD-His protein binds specifically to the MYB112 binding sites present in the *MYB6*, *MYB7* and *MYB32* promoters. *In vitro* DNA binding reactions were performed with 40-bp double-stranded oligonucleotides including the MYB112 binding sites of the respective target gene promoters. The DNA fragments were labeled with infrared dye (IRD). The fragments contained two (*MYB6_1/2*) or one (*MYB7*, *MYB32_1* and *MYB32_2*) MYB112 binding motif. 1, IRD-labeled DNA fragment. 2, MYB112 protein with labeled DNA fragment. Note distinct shift indicating binding. 3,

MYB112 protein, labeled DNA fragment and 200 x excess competitor. Note the shift disappearance. **(B)** ChIP-qPCR. Whole shoots of two-week-old *Arabidopisis* seedlings expressing GFP-tagged MYB112 under the control of *35S* CaMV promoter (*35S:MYB112-GFP*) and wild-type plants were harvested for the ChIP experiment. Enrichment of the respective promoter fragments was quantified by qPCR. Primers annealing to promoter regions of two *Arabidopsis* genes lacking MYB112 binding sites, i.e. *At2g22180* (Neg1) and *At3g1840* (Neg2), were used as negative controls. Data represent means ± SD of three independent experiments. Asterisks indicate statistically significant differences to controls as determined by Student's *t*-test, *p* < 0.05. Enrichment of *MYB7* and *MYB32* promoter fragments is detected.

<p style="color:red"><i>Conclusion:</i> MYB112 Binds to the <i>MYB7</i> and <i>MYB32</i> Promoters <i>in vitro</i> and <i>in vivo</i></p>

3.5. Flavonoid Accumulation in *MYB112* Transgenic Plants

The two identified direct MYB112 target genes, i.e. *MYB32* and *MYB7*, like *MYB112* itself, are both senescence-associated. The two candidates were previously proposed to play a role in the regulation of the flavonoid biosynthesis pathway, i.e. anthocyanin and lignin production (Preston *et al*., 2004; Zhong and Ye, 2012). In order to analyse the possible role of *MYB112* in controlling flavonoid accumulation in plants, we generated estradiol (EST)-inducible overexpression (*MYB112-IOE*) lines using the pER8 vector developed by Zuo *et al*. (2000) and induced its expression with 10 µM EST in seedlings grown in liquid MS medium supplemented with 1% sucrose. As controls we used DMSO-treated *MYB112-IOE* lines or EST-treated empty-vector plants. After 5 days of EST treatment, leaves of *MYB112-IOE* seedlings accumulated anthocyanins, whereas mock-treated plants (DMSO) (**Figure 19A**) as well as EST-treated empty-vector plants (not shown) did not. At shorter induction times (i.e., 5 h) no anthocyanin accumulation was observed in *MYB112-IOE* lines (not shown), indicating that MYB112 is not immediately upstream of anthocyanin pathway genes. We extracted and measured the anthocyanin level in *MYB112-IOE* seedlings of two lines (IOE#1 and IOE#2). Interestingly, the two *MYB112-IOE* lines accumulated 23- and 29-fold more anthocyanins than mock-treated plants (**Figure 19B**). We next analysed the flavonoid metabolite profiles of *MYB112-IOE* seedlings using liquid chromatography coupled to mass spectrometry (LC-MS). Compared with

DMSO-treated plants, EST-induced seedlings showed a significant increase in the content of two cyanidin derivatives, namely cyanidin-3-*O*-[2-*O*-(2-*O*-(sinapoyl)-xylosyl)-6-*O*-(*p*-*O*-coumaroyl)-glucoside]-5-*O*-[6-*O*-(malonyl)-glucoside] (A11; **Figure 19C**) and cyanidin-3-*O*-[2″-*O*-(xylosyl)-6″-*O*-(*p*-*O*-(glucosyl)-*p*-coumaroyl) glucoside]-5-*O*-[6‴-*O*-(malonyl)-glucoside] (A8; Tohge *et al*., 2005, **Figure 19D**). Other cyanidin derivatives were not reliably detected in the samples. Flavonol glycosides derived from kaempferol (named F1 to F3, according to Tohge *et al*., 2005) were reduced (**Figure 19E**), whereas the levels of flavonoid glycosides derived from quercetin (named F5 and F6) accumulated in EST-treated plants (**Figure 19F**) in comparison to control plants.

We next measured the expression of genes encoding enzymes involved in flavonoid biosynthesis as well as regulatory genes in *MYB112-IOE* seedlings treated with EST for 5 days (**Figure 19G**, **Figure 20** and **Supplementary Table 2**). Transcript levels of *PHENYLALANINE AMMONIA LYASE* (*PAL)* and *CINNAMATE-4-HYDROXYLASE* (*C4H*), genes associated with the pathway of phenylpropanoid biosynthesis,, remained unchanged in the EST-treated seedlings. *CHALCONE SYNTHASE* (*CHS*) and *CHALCONE ISOMERASE* (*CHI*) were slightly down-regulated (~2-fold). Transcript levels of the genes *DIHYDROXYFLAVONOL-4-REDUCTASE* (*DFR*) and *ANTHOCYANIDIN SYNTHASE* (*ANS*, *LDOX*) were substantially increased in seedlings overexpressing *MYB112*. DFR catalyses the conversion of dihydroquercetin to leucocyanidin, and *ANS* encodes a dioxygenase that operates downstream of DFR and catalyses the conversion of leucocyanthocyanidins to anthocyanidins. In addition to the anthocyanin biosynthesis genes indicated above, several genes proposed to be involved in the production of specific anthocyanin derivatives were up-regulated. These include three glycosyltransferase family genes, namely *UGT79B1* (*A3G2″XT*, anthocyanin-3-O-glusocide-2″-O-xylosyltransferase; Yonekura-Sakakibara *et al*., 2012), *UGT84A2* (*SGT*, sinapic acid 1-O-glucosyltransferase) and *UGT75C1* (*A5GT*, anthocyanin-5-*O*-glucosyltransferase; Tohge *et al*., 2005), and the acyltransferase family gene *A5GMaT* (At3g29590, anthocyanin-5-*O*-glucoside-6″-*O*-malonyltransferase; D'Auria *et al*., 2007) and the glutathione-*S*-transferase family gene *TT19*.
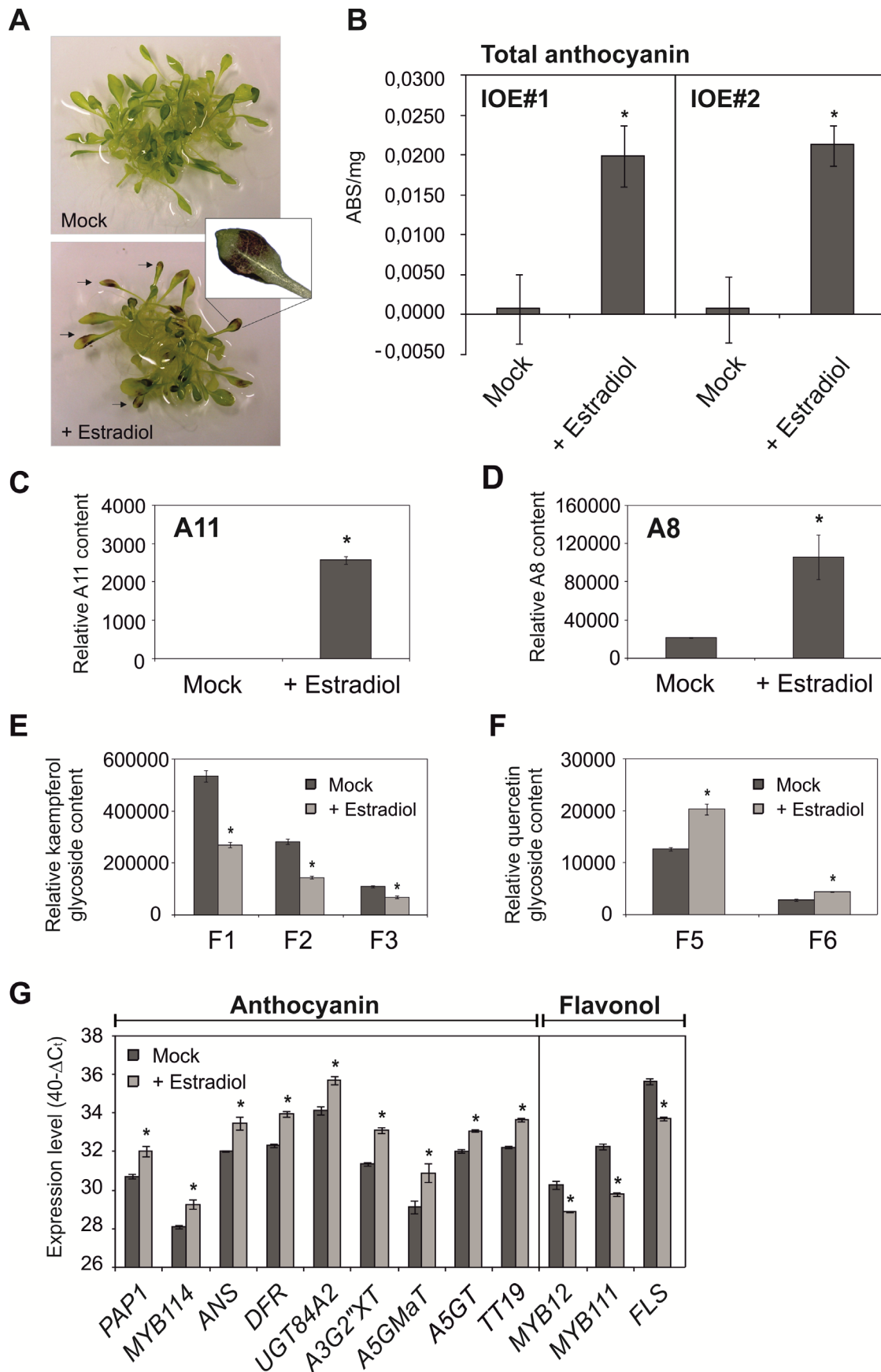
Figure 19. Overexpression of *MYB112* causes changes in flavonoid content.

(A) *MYB112-IOE* seedlings treated with 10 µM estradiol for 5 days accumulate red pigment in the middle of the leaves spreading to the edges (arrows and magnified image). **(B)** Total anthocyanin content was measured spectrophotometrically after extraction with HCl solution ($ABS_{535-(650*2.2)}$ / mg frozen weight). Mean value ± SD of five replicates is shown. **(C)** LC-MS analysis of A11 and (D) A8 content (Tohge *et al*., 2005) in mock- and estradiol-treated *MYB112-IOE*. **(E)** LC-MS analysis of flavonol content (F1 - kaempferol 3-*O*-rhamnoside 7-*O*-rhamnoside, F2 - kaempferol 3-*O*-glucoside 7-*O*-rhamnoside, F3 - kaempferol 3-*O*-[2″-*O*-(rhamnosyl) glucoside] 7-*O*-rhamnoside and **(F)** F5 - quercetin 3-*O*-glucoside 7-*O*-rhamnoside and F6 - quercetin 3-*O*-[2″-*O*-(rhamnosyl) glucoside] 7-*O*-rhamnoside. For **(C - F)** mean values ± SD are shown for three replicates. Asterisks indicate statistically significant differences as compared to DMSO-treated plants determined by Student's *t*-test, $p < 0.05$. **(G)** Transcript levels of selected enzymatic (*ANS, DFR, TT19, A3G2″XT, UGT84A2, A5GMaT, A5GT* and *FLS*) and regulatory (*PAP1, MYB114, MYB111* and *MYB12*) genes involved in anthocyanin and flavonol biosynthesis in *MYB112-IOE* seedlings. Data are represented as $40-\Delta C_t$, where ΔC_t is equal to $C_{t\ gene\_of\_interest} - C_{t\ reference\_gene\_Actin}$. Mean values ± SD are shown for three replicates**.**

The genes encoding glycosyltransferases and acyltransferases catalyze modification reactions for the formation of the most extensively modified A11 anthocyanin (Tohge *et al*., 2005; D'Auria *et al*., 2007; Yonekura-Sakakibara *et al*., 2012). TT19 is required for vacuolar sequestration of anthocyanins (Kitamura *et al*., 2004). The transcript level of *FLAVONOL SYNTHASE* (*FLS*), which catalyses the synthesis of the flavonols quercetin and kaempferol from dihydroquercetin and dihydrokaempferol, respectively, was down-regulated in the EST-treated *MYB112-IOE* seedlings.

Apart from flavonoid biosynthesis genes, a set of regulatory genes also displayed altered expression in *MYB112* overexpressing plants. Expression of *PAP1* as well as *MYB114* was increased in EST-treated *MYB112-IOE* plants. It should be mentioned however that the *MYB114* gene from the Columbia (Col) accession encodes a putative protein that lacks a transcriptional activation domain due to a stop codon just after the Myb domains (at amino acid 140). The Landsberg *erecta* (L*er*) *MYB114* allele encodes a full-length gene and its function in anthocyanin accumulation was confirmed (Gonzalez *et al*., 2008). *MYB12* and *MYB111*, previously shown to control the expression of genes involved in flavonol biosynthesis, were down-regulated (**Figure 19**, **Figure 21**, **Supplementary Table 2**). This suggests that *MYB112* acts through the expression of these regulatory genes.

Conclusion: **Estradiol-inducible Overexpression of *MYB112* Induces Anthocyanin Formation**

We next analysed the relative anthocyanin content in the two *myb112* T-DNA insertion mutants using spectrophotometric measurements **(Figure 20A)**. Compared to wild-type seedlings, anthocyanin content was reduced by over 27% in the *myb112-1* mutant grown for two weeks on Murashige-Skoog (MS) medium containing 4% sucrose.
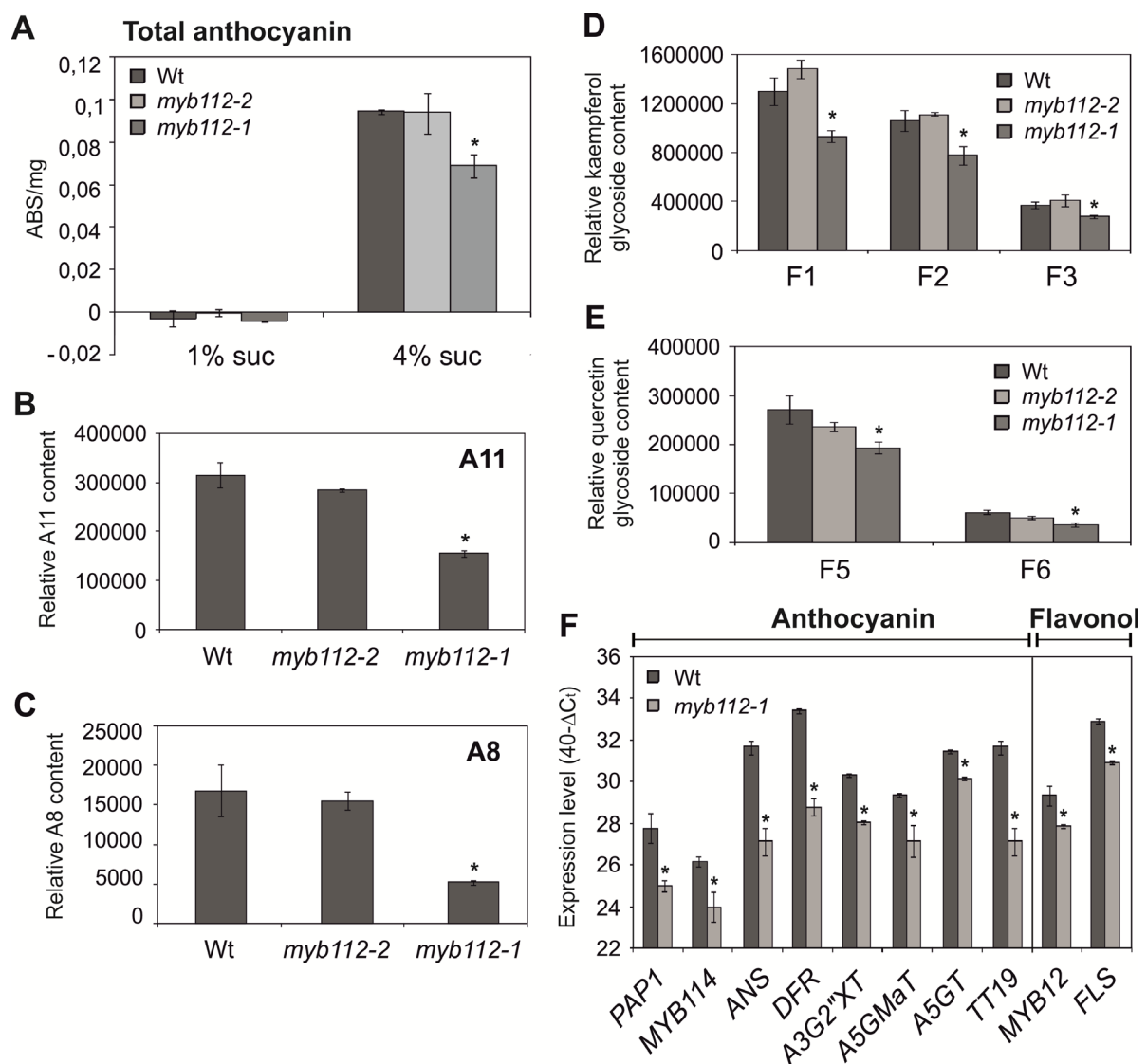
Figure 20. Reduced flavonoid content in *myb112* T-DNA mutants.

(A) Total anthocyanin content ($ABS_{535-(650*2.2)}$ / mg frozen weight) and **(B)** LC-MS analysis of A11 and **(C)** A8 content (Tohge *et al*., 2005) in *myb112* mutants in comparison to wild-type seedlings grown on 4% sucrose. **(D)** LC-MS analysis of flavonols content (F1 - kaempferol 3-*O*-rhamnoside 7-*O*-rhamnoside, F2 - kaempferol 3-*O*-glucoside 7-*O*-rhamnoside, F3 - kaempferol 3-*O*-[2″-*O*-(rhamnosyl) glucoside] 7-*O*-rhamnoside and **(E)** F5 - quercetin 3-*O*-glucoside 7-*O*-rhamnoside and F6 - quercetin 3-*O*-[2″-*O*-(rhamnosyl) glucoside] 7-*O*-rhamnoside in *myb112* mutants in comparison to wild-type plants. Mean values ± SD are shown for five replicates **(A)** and three replicates **(B - E).** Asterisks indicate statistically significant differences as compared to wild-type (Wt) plants determined by Student's *t*-test, *p* < 0.05. **(F)** Transcript levels of selected biosynthetic (*ANS, DFR, A3G2″XT, A5GMaT, A5GT, TT19* and *FLS*) and regulatory (*PAP1, MYB114* and *MYB12*) genes involved in anthocyanin and flavonol biosynthesis in two-week-old *myb112-1* seedlings grown on MS medium + 1% sucrose. Data are represented as 40-ΔC_t, where ΔC_t is equal to $C_{t\ gene\_of\_interest} - C_{t\ reference\_gene\_Actin}$. Mean values ± SD are shown for three replicates.

No difference in total anthocyanin content was observed between wild-type and *myb112-2* plants indicating, that the level of *MYB112* transcript present in this knock-down mutant (**Figure 20A**) is sufficient to sustain normal anthocyanin levels. LC-MS analysis revealed that the changes in the total anthocyanin content in the *myb112-1* mutant are caused by decreased accumulation of A11 (**Figure 20B**) and A8 (**Figure 20C**) derivatives in these plants. We also detected a slight decrease of flavonol accumulation in *myb112-1* seedlings compared to wild-type seedlings (**Figure 20D** and **E**). Expression profiling revealed decreased transcript levels of genes coding for key enzymes of flavonoid biosynthesis (*ANS, DFR, A3G2″XT, A5GMaT, A5GT, TT19*, and *FLS*) as well as regulatory genes (*PAP1, MYB114, MYB12*) in the *myb112-1* mutant (**Figure 20F**, **Figure 21** and **Supplementary Table 2**).

Conclusion: Silencing of *MYB112* Results in Decreased Anthocyanin and Flavonol Content

An integrated schematic view of the transcriptomic and metabolomic shifts occurring in *MYB112*-modified plants compared to wild type or DMSO-treated *MYB112-IOE* plants is given in **Figure 21**.
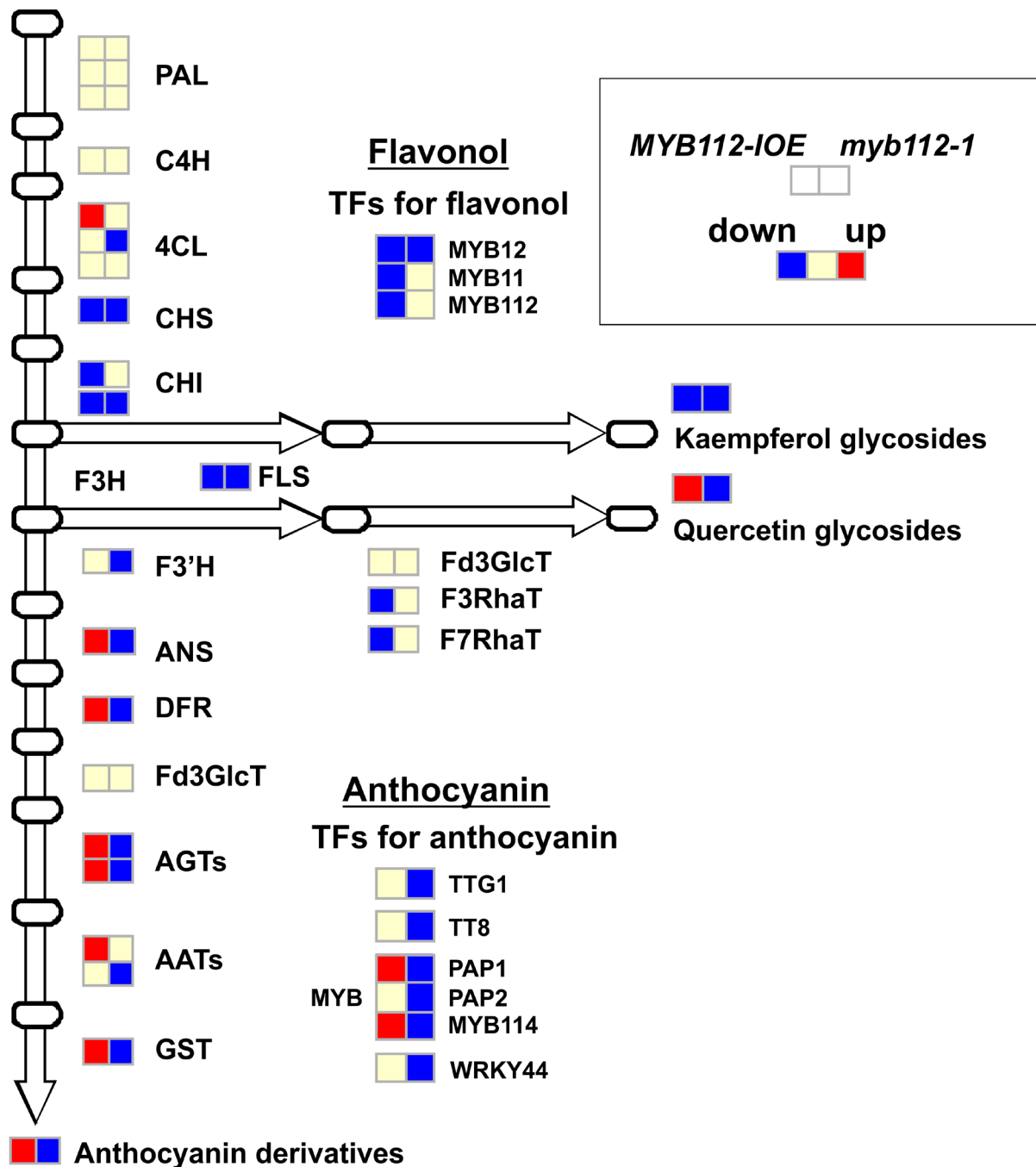
Figure 21. Integrated transcriptomics and metabolomics data.

Expression of 23 flavonoid biosynthesis genes and nine TFs as measured by qRT-PCR and metabolite content analysed by LC-MS in *MYB112-IOE* seedlings treated with estradiol for 5 days (left box) and in *myb112-1* mutant (right box). Gene expression level and metabolite content changes against DMSO-treated and wild-type plants, respectively, is indicated by colour (cut off: 2-fold).

3.5.1. Salt-dependent Flavonoid Accumulation in *MYB112* Transgenics

It has been previously demonstrated that sucrose is an effective inducer of anthocyanin biosynthesis in *Arabidopsis* seedlings and that the expression of *PAP1* strongly increases upon sucrose treatment (Teng *et al*., 2005; Sofanelli *et al*., 2006). In order to investigate the effect of sucrose concentration on *MYB112* expression, we measured its transcript levels in two-week-old seedlings grown on MS medium supplemented with either 1% or 4% sucrose. As shown in **Figure 22A**, no significant change in *MYB112* expression was detected, while the transcript level of *PAP1* increased significantly in plants grown on high-sucrose medium.
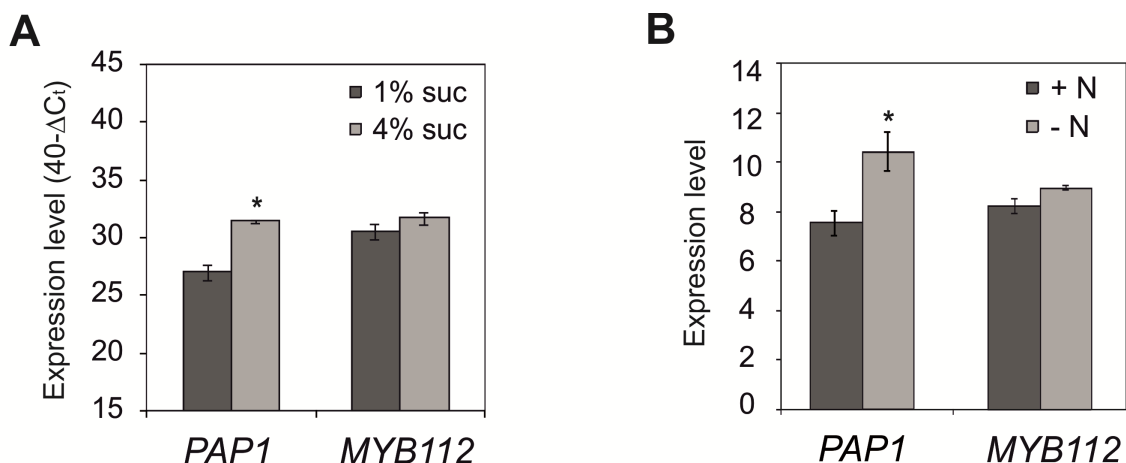
Figure 22. *MYB112* expression is neither affected by sucrose nor nitrogen.

(A) Transcript levels of *PAP1* and *MYB112*, determined by qRT-PCR, in two-week-old seedlings grown on MS medium with 1% or 4% sucrose. Note the absence of an effect of elevated sucrose concentration on *MYB112* expression. The data are represented as 40-ΔC_t, where ΔC_t is equal to $C_{t\ gene\_of\_interest} - C_{t\ reference\_gene\_ACTIN}$. Means of three independent replicates ± SD are shown. The asterisk indicates a statistically significant difference compared to control plants as determined by Student's *t*-test, $p < 0.01$. **(B)** Expression level of *PAP1* and *MYB112* in plants grown on media with or without nitrogen. Plants were grown in a hydroponic system and after 19 days were transferred to medium without nitrogen source. Gene expression was measured 6 days after the transfer. *MYB112* expression is not affected by nitrogen availability while *PAP1* expression increases by ~8-fold. Data were extracted from Affymetrix ATH1 hybridisations (unpublished) and represent the means ± SD of three biological replicates. Numbers indicate log2 values.

Our result is in agreement with previously published global transcriptome data on of sucrose-responsive genes (Sofanelli *et al*., 2006; Osuna *et al*., 2007). Nitrogen deficiency also enhances expression of specific MYB and bHLH transcription factors and accumulation of end products of the flavonoid pathway (Lea *et al*., 2007; Rubin *et al*., 2009). Klaus Humbeck (Martin-Luther Universität Halle-Wittenberg, Germany) performed an experiment in which 19-day-old *Arabidopsis* plants grown on full media supplemented with nitrate were transferred to media without nitrogen for six days. Lack of nitrate resulted in leaf yellowing and anthocyanin accumulation. Expression profiling proved, however, that *MYB112* transcript abundance in plants grown for six days on medium with no nitrogen source was comparable to the transcript level in control plants grown on full (nitrogen-sufficient) MS medium (**Figure 22B**, K. Humbeck, personal communication). In the same experiment, as anticipated, *PAP1* expression increased ~8-fold (**Figure 22B**).

Conclusion: Neither Increased Sucrose nor Decreased Nitrogen Level Affect *MYB112* Expression

According to microarray data obtained from the Genevestigator and eFP databases, expression of *MYB112* increases upon abiotic stress, namely salt stress. To verify salt-induced expression of *MYB112* we employed the *MYB112* promoter-reporter (*GUS*) gene fusion lines; we transferred two-week-old *Pro$_{MYB112}$:GUS* seedlings to MS medium containing NaCl (150 mM, 24 h). Histochemical staining revealed enhanced GUS activity in salt-treated seedlings compared with untreated controls (**Figure 23A**). Salt-responsive *MYB112* expression was further confirmed by qRT-PCR in seedlings treated with salt (150 mM NaCl) for 4, 8 and 24 h in liquid medium (**Figure 23B**, treatment performed by Amin Omidbakhshfard). In addition, we grew *Arabidopsis* Col-0 plants in a hydroponic culture system and subjected them to short- and long-term salt stress (150 mM NaCl), as described previously (Balazadeh *et al*., 2010a; Balazadeh *et al* 2010b). In short-term experiments, leaves of 28-day-old plants were sampled 6 hours after stress treatment. In long-term stress experiments, leaves were sampled after 4 days of salt treatment at approximately 20% chlorophyll

loss, indicating senescence. Expression of the senescence-specific marker gene *SAG12* (Noh and Amasino, 1999) was not detected in control plants and plants subjected to short-term salt stress, whereas it was induced under long-term salt stress which induces senescence (Balazadeh *et al.*, 2010b). Microarray gene expression profiling revealed no change in *MYB112* transcript level after short-term stress, however, after 4 days of salt treatment, transcript level increased by over 3-fold (**Figure 23C**, experiment performed by Annapurna Devi Allu). Similar salinity stress-triggered expression changes have previously been observed for many SAGs (Balazadeh *et al.*, 2010a; Balazadeh *et al.*, 2010b).
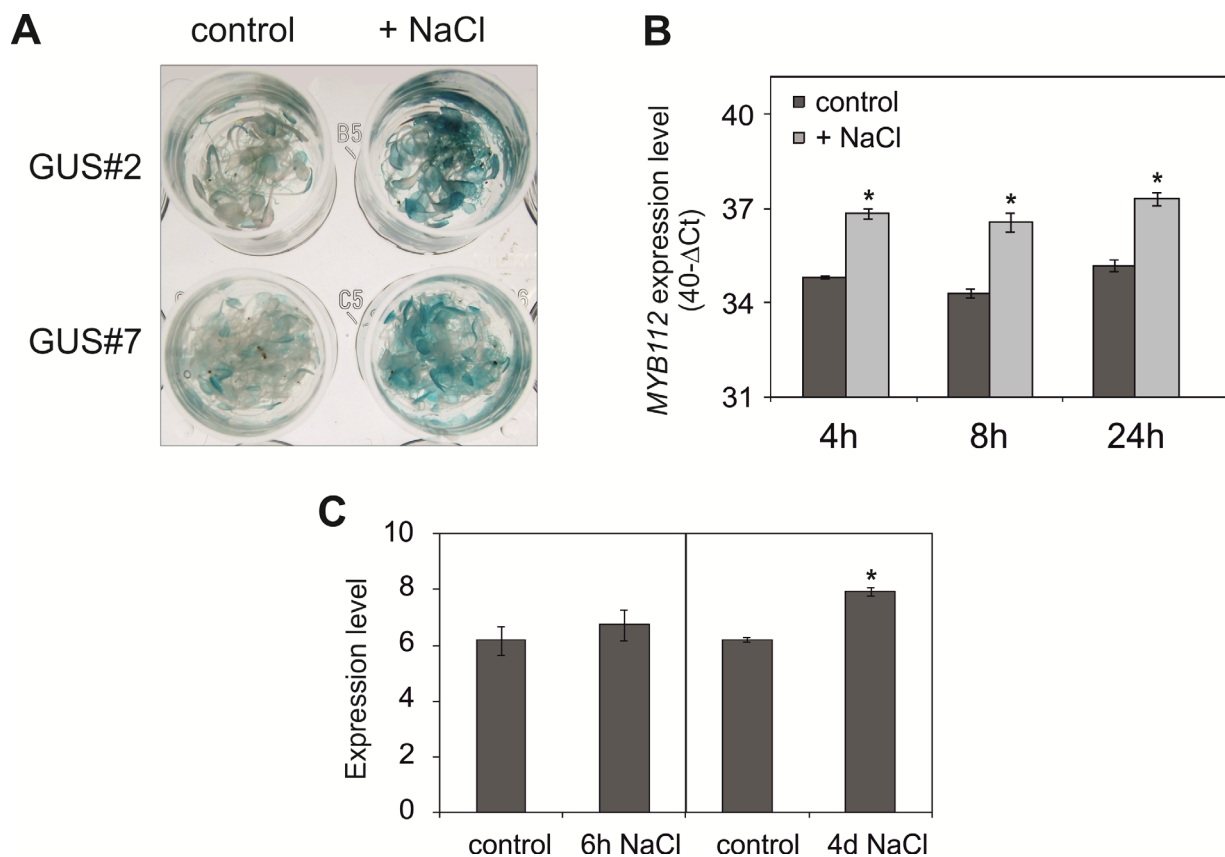
Figure 23. Salt-induced expression of *MYB112*.

(A) Ten-day-old *Arabidopsis* Pro$_{MYB112}$:*GUS* seedlings #2 and #7 were treated for 72 h with 0 mM NaCl (control) or 150 mM NaCl (+ NaCl) in liquid MS medium. Enhanced GUS staining is visible in salt-treated seedlings (right panel). **(B)** Transcript level of *MYB112* in wild-type seedlings treated with 150 mM NaCl in liquid culture. Incubation times were 4, 8 and 24 h. The data are represented as 40-ΔC_t, where ΔC_t is equal to $C_{t\ gene\_of\_interest} - C_{t\ reference\_gene\_ACTIN}$. Mean values of three independent replicates ± SD are shown. Asterisks indicate statistically significant differences in comparison to the controls, as determined by Student's *t*-test, *p* <

0.01. **(C)** Expression profiling using Affymetrix ATH1 arrays shows elevated *MYB112* transcript abundance in plants grown hydroponically with 150 mM NaCl in comparison to control plants. Plants were harvested after 6 h and 4 days of treatment. The experiment was performed in three independent replications. Numbers on the y axis indicate average log2 values ± SD.

Conclusion: **Expression of *MYB112* is Stimulated by Increased Salt Content**
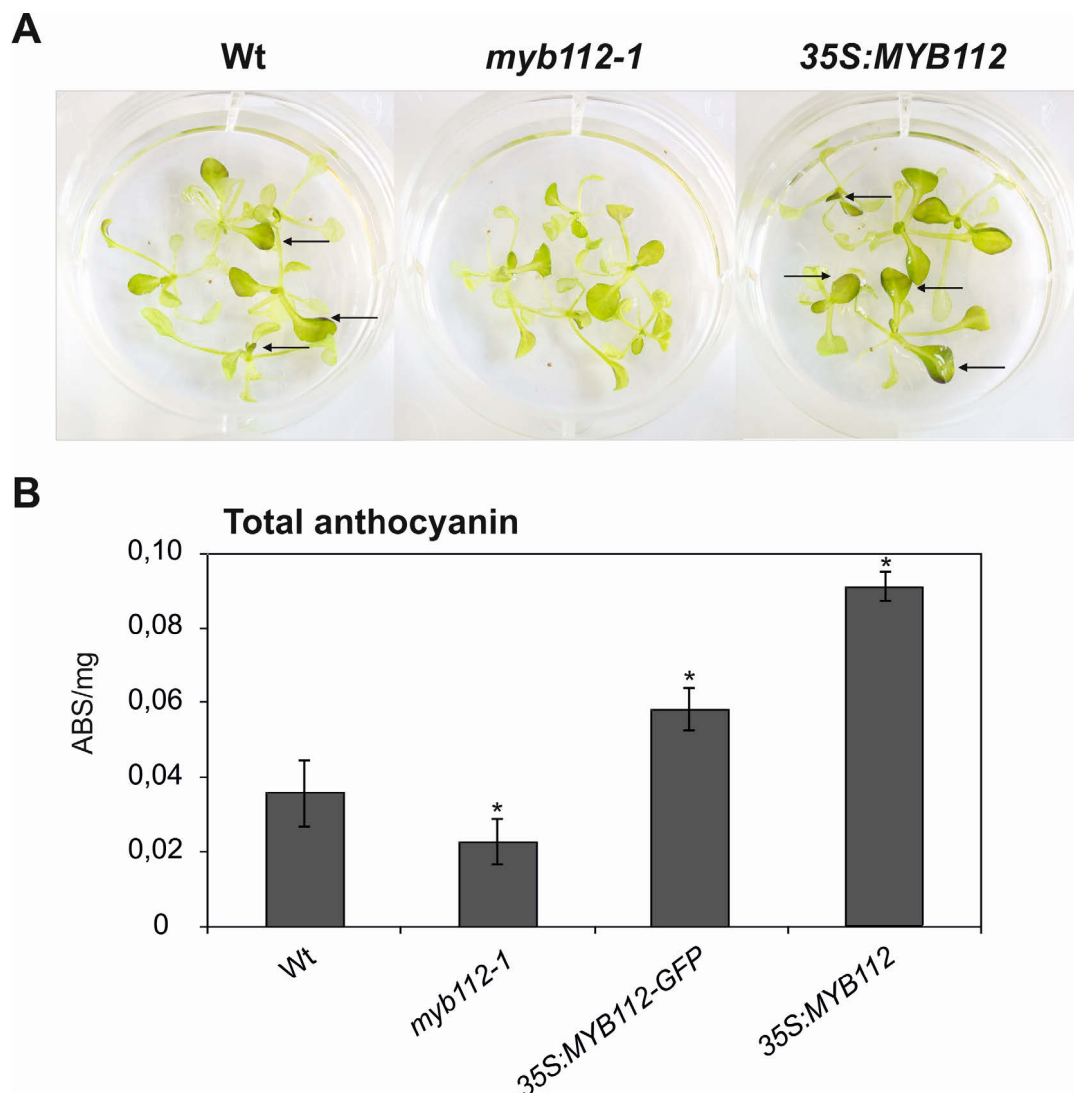
Figure 24. *MYB112* regulates anthocyanin accumulation during salt stress.

(A) Appearance of seedlings treated with salt for three days. Plants were grown on MS medium supplemented with 1% sucrose and after two weeks were transferred to liquid medium containing 150 mM NaCl. Note the lack of red pigmentation in *myb112-1* seedlings. **(B)** Total anthocyanin content was measured spectrophotometrically ($ABS_{535-(650*2.2)}$ / mg frozen weight) after extraction with HCl solution. Mean values ± SD are shown for three replicates. Asterisks indicate statistically significant differences in comparison to wild-type (Wt) plants as determined by Student's *t*-test, $p<0.05$.

To test whether *MYB112* may be involved in controlling anthocyanin accumulation during salt stress, we transferred ten-day-old seedlings to liquid MS medium containing 150 mM NaCl. After three days, wild-type and *MYB112* overexpression plants (i.e., *35S:MYB112* and 35S*:MYB112-GFP* lines) turned red, whereas *myb112-1* mutant plants accumulated visibly less anthocyanin (**Figure 24A**). Spectrophotometric analysis of anthocyanin content in these plants revealed a decrease in total anthocyanin content by 37% in the *myb112-1* mutant compared to wild type. *35S:MYB112* and *35S:MYB112-GFP* plants accumulated ~2.5-fold and ~65% more anthocyanins, respectively, than wild-type plants (**Figure 24B**). We therefore concluded, that *MYB112* contributes to regulating anthocyanin production in response to salinity stress.

Conclusion: **MYB112 Regulates Anthocyanin Accumulation under Salt Stress**

3.5.2. High light-dependent Flavonoid Accumulation in *MYB112* Transgenics

TSP9 (Thylakoid-soluble Phosphoprotein of 9 kDa) is a mobile thylakoid protein that interacts with light-harvesting complex (LHC) II and the peripheries of both photosystems. It was shown to regulate light harvesting by facilitating the dissociation of light-harvesting proteins from photosystem II. Upon phosphorylation, TSP9 is partially released from the membrane and therefore was proposed to play a role in chloroplast signalling (Hansson *et al*., 2007). Global expression profiling identified 23

genes, including *MYB112*, that were high light-dependent in wild-type plants, but not in a *tsp9* T-DNA insertion mutant (GK_377A12) (**Table 3**; Fristedt *et al*., 2009). (**Table 3**). This finding suggests a function of *MYB112* in TSP9-dependent high light signalling. To investigate further the relation between the two genes, we measured total anthocyanin content in two *tsp9* T-DNA insertion lines under high light stress. However, anthocyanin accumulation was not affected in these mutants, suggesting that the level of *MYB112* expression in these plants was still sufficient to sustain the wild-type phenotype. To verify high light-induced expression of *MYB112*, we employed the *Pro$_{MYB112}$:GUS* reporter lines. Ten-day-old *Arabidopsis Pro$_{MYB112}$:GUS* seedlings as well as three-week-old plants were treated for 6 h and 20 h, respectively, with high light (500 µmol m^{-2} s^{-1}).

Table 3. Genes found to be down-regulated in the *tsp9* mutant after 3 h of high light treatment as compared to wild-type plants.

AGI	Annotation
AT3G47070	TSP9
AT3G10880	Hypothetical protein
AT2G16460	Expressed protein
AT3G18640	Zinc finger protein-related
AT3G52290	Calmodulin-binding family protein
AT2G34570	Expressed protein, contains Pfam profile
AT1G48000	MYB112
AT2G20875	Expressed protein
AT3G24860	Hydroxyproline-rich glycoprotein family protein
AT1G44180	Aminacylase, putative
AT2G25260	Expressed protein
AT4G33890	Expressed protein
AT4G23000	Calcineurin-like phosphoesterese family protein
AT1G26480	14-3-3 protein (GRF12)
AT1G05630	Inositol polyphosphate 5-phosphatase
AT5G05050	Peptidase CIA papain family protein
AT4G19550	Expressed protein
AT4G31250	Leucine-rich repeat transmembrane potein kinase
AT4G15340	Pentacyclic triterpene synthase
AT1G05000	Tyrosine-specific protein phosphatase
AT1G03000	AAA-type ATPase family protein
AT4G23330	Eukaryotic translation initiation factor-related
AT4G28365	plastocyanin-like domain-containing protein

according to Fristedt *et al*., 2009

In both cases, histochemical staining revealed enhanced GUS activity in high light-treated plants compared to controls kept in normal light condition (100 µmol m^{-2} s^{-1}) (**Figure 25A**, **B**). Spectrophotometric analysis of anthocyanin content in three-week-old *myb112* mutants grown under high light condition (500 µmol m^{-2} s^{-1}) for three days showed a ~4-fold decrease in pigment content in *myb112-1* plants (**Figure 26**), suggesting that *MYB112* is involved in high light-induced anthocyanin accumulation.
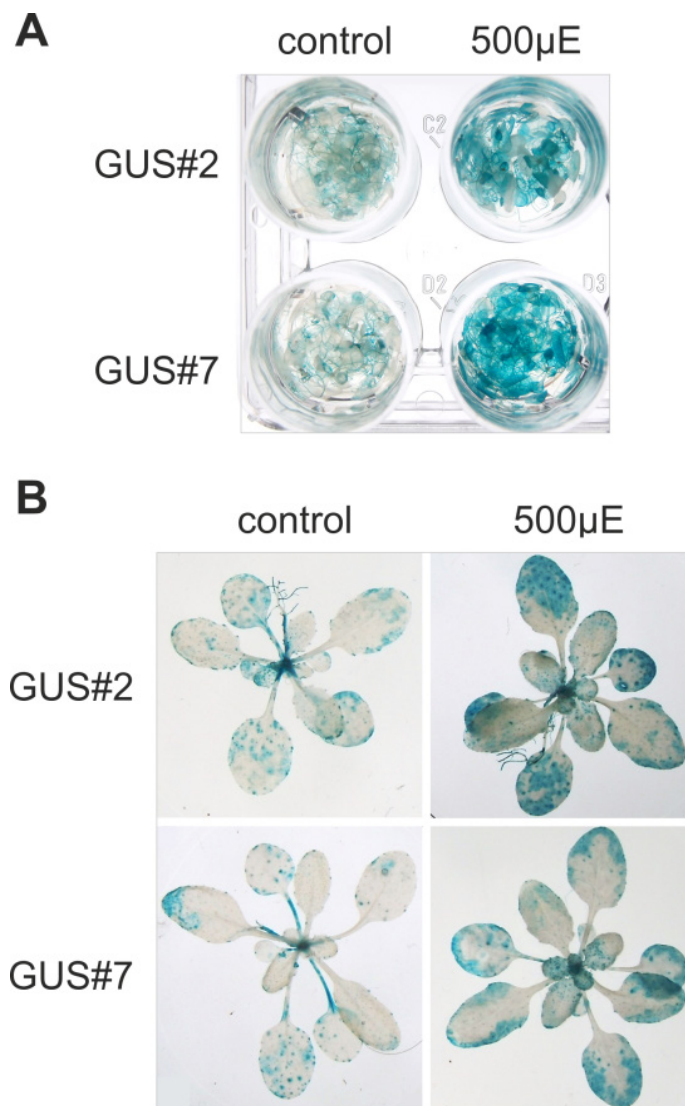
Figure 25. High light-induced expression of *MYB112*.

(A) *MYB112* promoter activity in ten-day-old *Arabidopsis Pro$_{MYB112}$:GUS* seedlings #2 and #7 treated for 6 h with high light (500 µE; right panel) in comparison to control seedlings grown with100 µE (left panel). **(B)** GUS activity in three-week-old *Pro$_{MYB112}$:GUS* plants #2 and #7 treated with high light for 20 h (right panel) in comparison to control plants kept in 100 µE (left panel). Note the enhanced GUS staining of plants treated with high light.
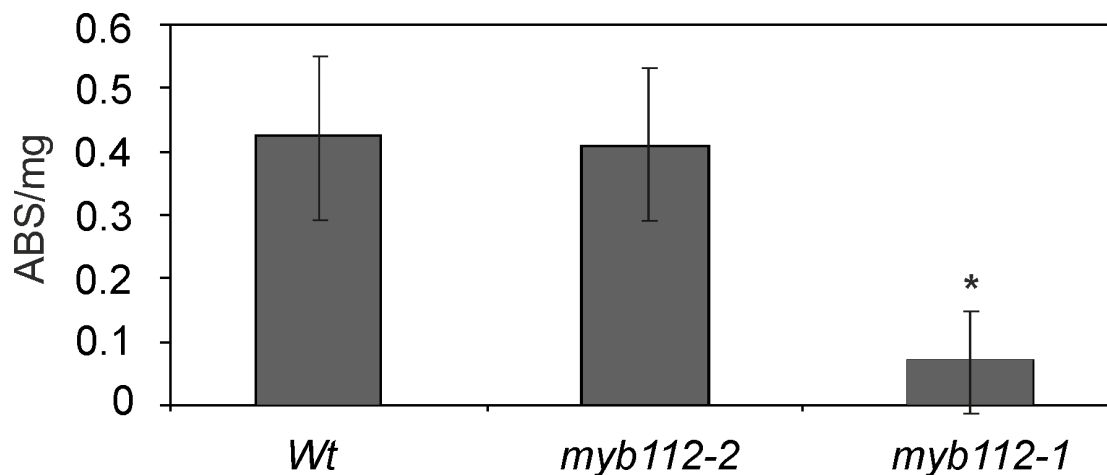
Figure 26. Anthocyanin content in *myb112* T-DNA insertion lines grown under high light condition.

Plants were grown in long-day conditions and after three weeks were transferred to high light (500 µE) for three days. Total anthocyanin content was measured spectrophotometrically ($ABS_{535-(650*2.2)}$ / mg frozen weight) after extraction with HCl solution. Mean values ± SD are shown for five replicates. The asterisk indicates statistically significant difference in comparison to wild-type (Wt) plants as determined by Student's *t*-test, $p<0.05$.

Conclusion: MYB112 **is a High Light-induced Gene**

3.6. Pollen Viability of *MYB112* Transgenics

MYB32, identified here as a direct MYB112 target gene, as well as the closely related *MYB4* have been reported to influence pollen development, leading to structural distortions and a lack of cytoplasm in pollen of two *myb32* T-DNA insertion lines, as well as in *myb4* dSpm insertion and overexpression lines ((Preston *et al*., 2004).

A
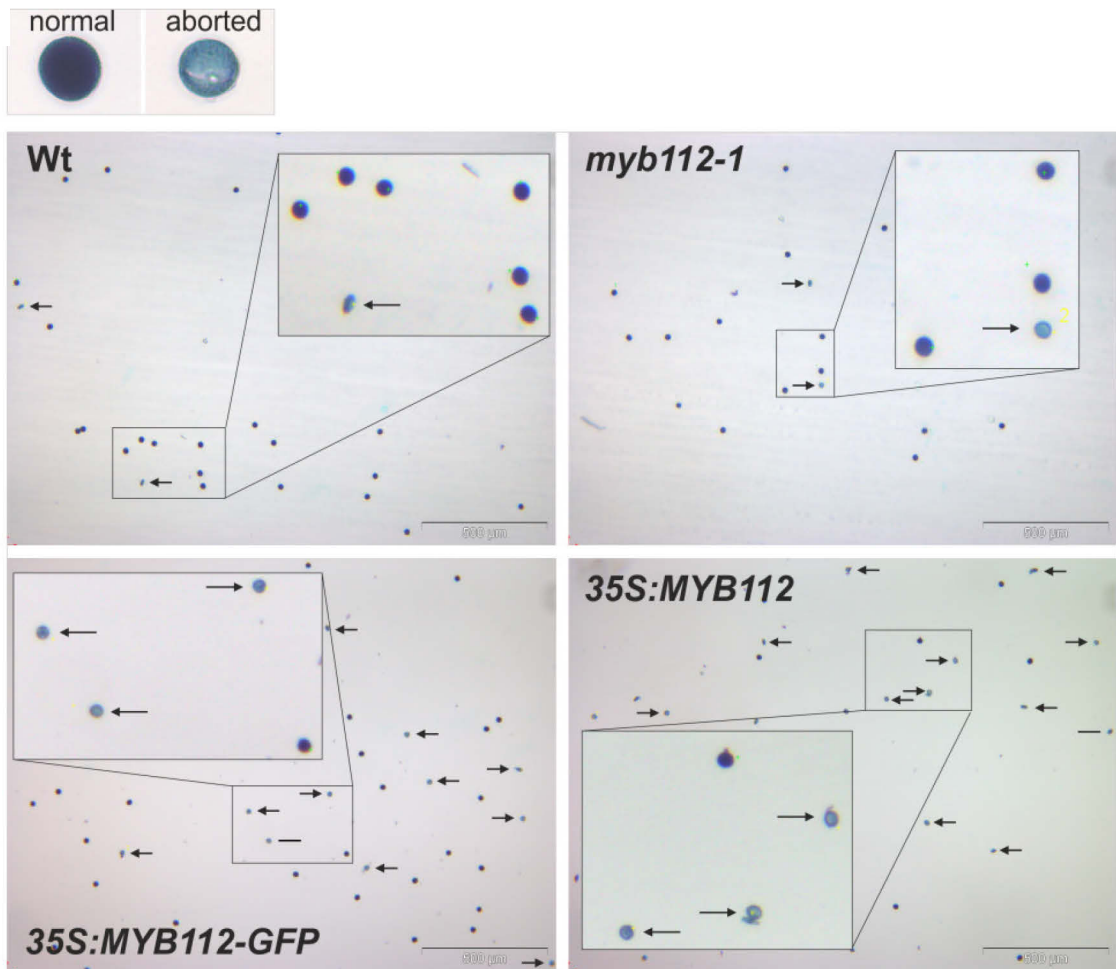
B
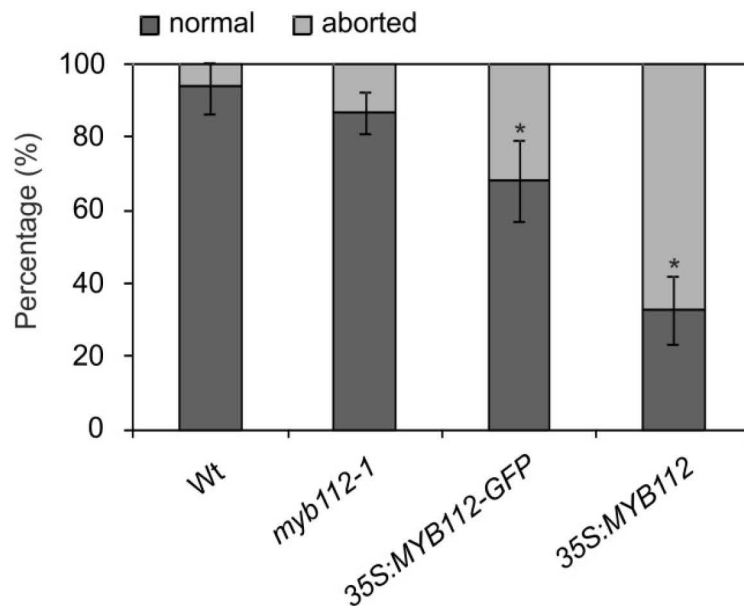
Figure 27. Pollen viability in *MYB112* transgenic plants.

54

(A) Appearance of pollen grains after staining with Alexander dye. Normal pollen grain is purple while sterile pollen stains blue (arrows). Note the increase in the number of aborted pollen in *MYB112* overexpression lines. **(B)** Percentage of viable and aborted pollen in *MYB112* transgenic plants determined after Alexander staining. Pollen was obtained from six plants and six individual microscope images were analysed. Mean values ± SD are shown. Asterisks indicate statistically significant difference to wild type (Wt) as determined by Student's *t*-test, *p*<0.01.

Of note, expression of the anthocyanin biosynthesis genes *DFR* and *ANS* decreases in *myb32* knock-out plants and expression of *CAFFEIC ACID O-METHYLTRANSFERASE* (*COMT*) is increased (Preston *et al*., 2004). MYB4 suppresses *C4H* encoding Cinnamate-4-Hydroxylase which upstream of the flavonoid-specific pathway converts *trans*-cinnamate into 4-hydroxycinnamate (in the general phenylpropanoid pathway). MYB4 also suppresses the anthocyanin pathway gene *CHS*, whilst it stimulates *CCoAOMT*, encoding Caffeoyl CoA *O*-Methyl Transferese which is involved in the biosynthesis of sinapate esters and polymerized phenolic derivatives (Jin *et al*., 2000). Preston *et al*. (2004) speculate, that changes in expression of flavonoid and phenylpropanoid biosynthesis genes in the *myb32* and *myb4* mutants significantly influence the flux along these pathways, interfering with pollen development by altering structural components of the pollen wall. Sporopollenin is the most likely compound to be affected as it consists of polymerized phenols and fatty acid derivatives. By analysing *MYB112* promoter activity in *Pro$_{MYB112}$:GUS* lines we show that *MYB112* is also expressed in pollen (**Figure 8B.16** and **17**). We therefore tested pollen viability in *MYB112* transgenic plants after staining of flowers with Alexander dye (Alexander, 1969). We found that overexpression of *MYB112* leads to partial pollen sterility; 35% and 70% of pollen was aborted in *35S:MYB112-GFP* and *35:MYB112* overexpression plants, respectively (**Figure 28**). The observed decrease in pollen viability in these lines corresponds to the level of *MYB112* overexpression (~5-fold increase in *35S:MYB112-GFP* and ~15-fold in *35S:MYB112*; **Figure 10**).
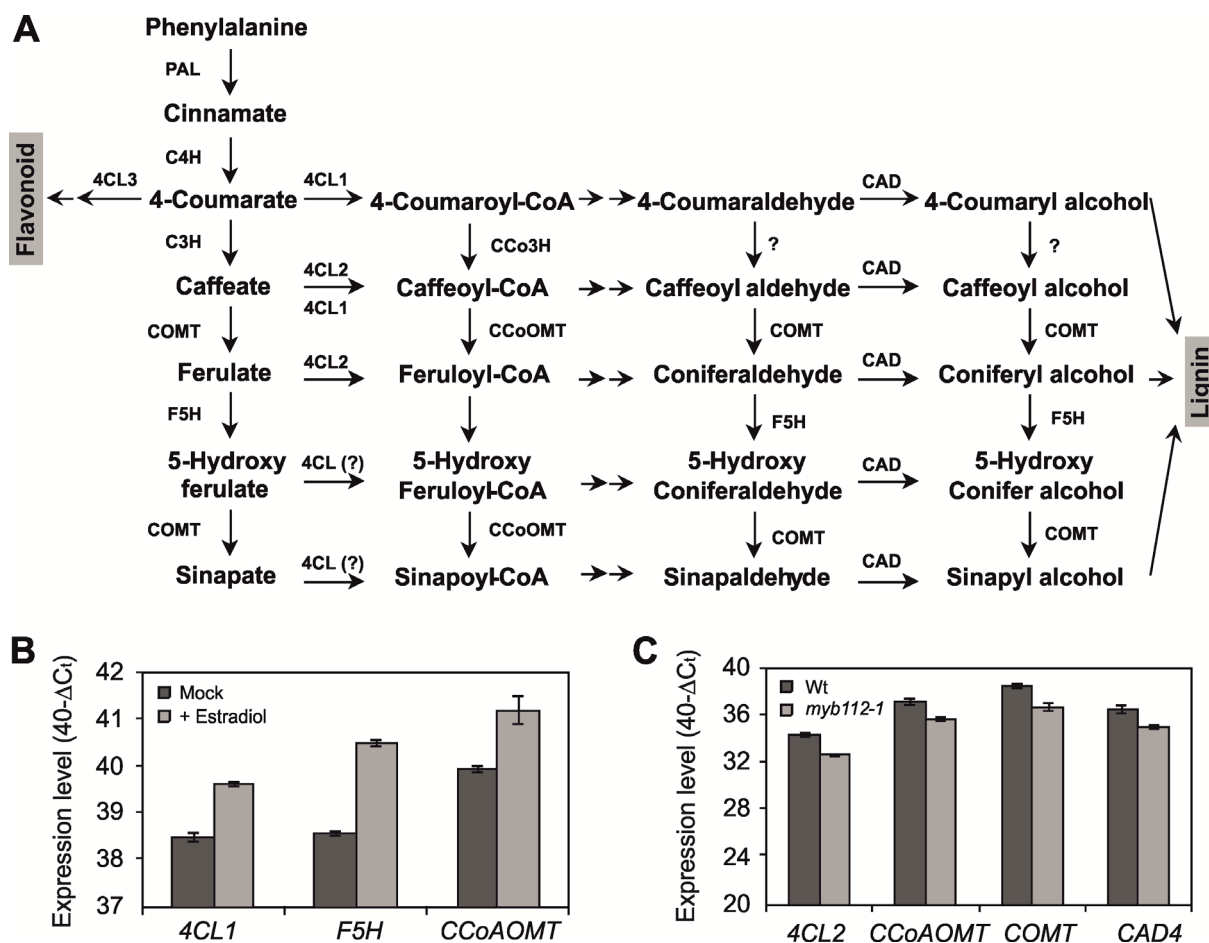
Figure 28. Changes in expression of lignin biosynthesis genes in *MYB112* transgenic plants.

(A) Lignin biosynthesis pathway with indicated biosynthesis enzymes. **(B)** Expression of selected lignin biosynthesis genes in *MYB112-IOE* seedlings treated with estradiol in liquid MS medium supplemented with 1% sucrose for 5 days as compared to mock-treated plants. **(C)** Expression of selected lignin biosynthesis genes in *myb112-1* T-DNA mutant seedlings as compared to wild-type plants. The data are represented as $40-\Delta C_t$, where ΔC_t is equal to $C_{t\ gene\_of\_interest} - C_{t\ reference\_gene\_Actin}$. Data are the means of two biological replicates, measured in two technical replicates each ± SD.

We also analysed transcript levels of genes encoding key phenylpropanoid biosynthesis enzymes in the *myb112-1* mutant and the *MYB112-IOE* plants treated with estradiol for 5 days (**Supplementary Table 2**). **Figure 29** shows significant changes in the expression of a number of phenylpropanoid biosynthesis genes in *MYB112* transgenic plants. For example, expression of *CCoAOMT* is increased in plants overexpressing *MYB112* (**Figure 29B**), similar to *MYB4* overexpression plants (Jin *et al*., 2000). *CCoAOMT* is downregulated in the *myb4* knockout line (Jin *et al*.,

2000) and the *myb112-1* mutant (**Figure 29C**), but is not affected in *MYB32*-modified plants (Preston *et al.*, 2004).

Conclusion: MYB112 Affects Pollen Viability

3.7. Growth Phenotype of *myb112* T-DNA Mutants and RNAi Plants

We have analysed growth phenotypes of *myb112* T-DNA insertion mutant plants. Plants germinated uniformly and in early stages of vegetative growth there was no visible difference between the phenotype of wild-type (Wt) and mutant plants. Bolting time differed between wild-type and *myb112* mutants, as determined when the main florescence stalk had elongated to 1 cm. Wild-type plants bolted 55 days after sowing (DAS), while the two mutants bolted at 58 DAS, when grown in 12 h/12 h day/night regime in soil (**Figure 29A** and **B**). At this time there was a slight difference in the number of leaves between the genotypes (Wt, 33 leaves; *myb112-1*, 34 leaves; **Figure 29C**).
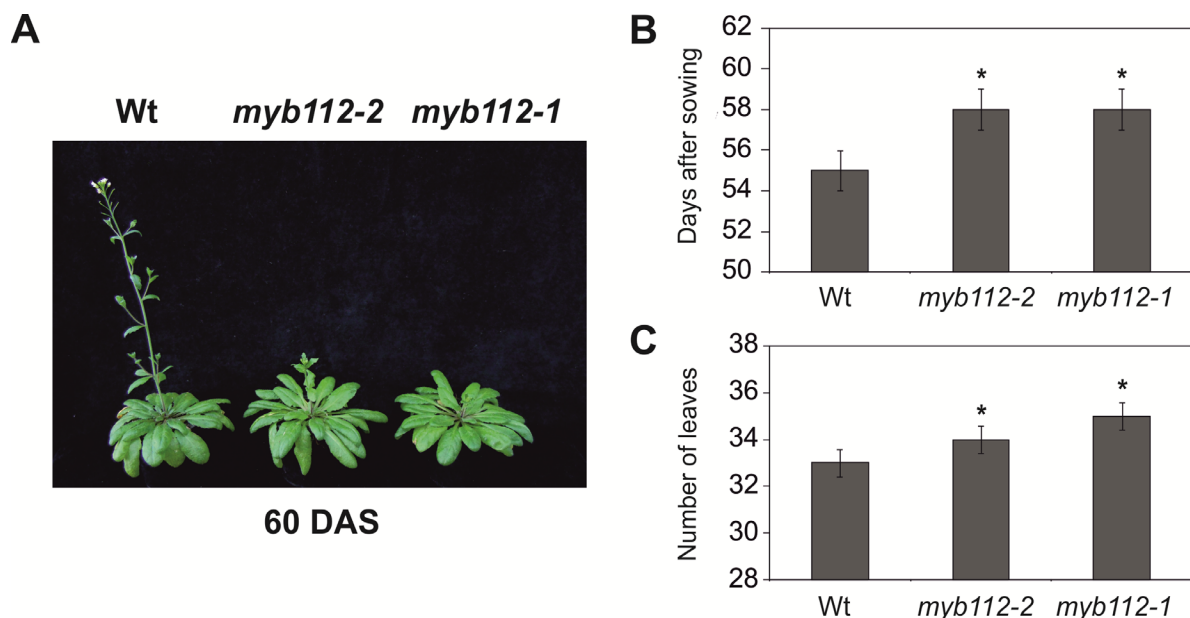
Figure 29. Growth phenotype of *myb112* T-DNA insertion mutants.

(A) Phenotype of *myb112* T-DNA insertion mutants at 60 DAS. Plants were grown in 12 h/12 h day/night conditions. **(B)** Bolting time of *myb112* mutants. The time (DAS), when the main stalk elongated to 1 cm was recorded. **(C)** Number of rosette leaves at the bolting time. For **(B)** and **(C)**, 30 plants were counted to calculate mean values ± SEM. Asterisks indicate statistically significant differences to wild type as determined by Mann-Whitney Rank Sum Test, *p*<0.05.

In addition, we analysed the phenotypes of seven *MYB112* RNAi lines.Plants were initially grown on MS medium supplemented with 1% sucrose. After two weeks, seedlings were transferred to soil and grown in long-day conditions (16 h/8 h, day/night). No visible phenotype was observed between RNAi plants and empty vector (EV)-transformed plants during the early developmental stages. However, RNAi lines #2 and #10 showed a strong delay in bolting in comparison to the empty vector plants. Control plants began to bolt at 21 DAS, whereas RNAi lines #2 and #10 started to bold at 30 and 34 DAS, respectively (**Figure 30A** and **C**).
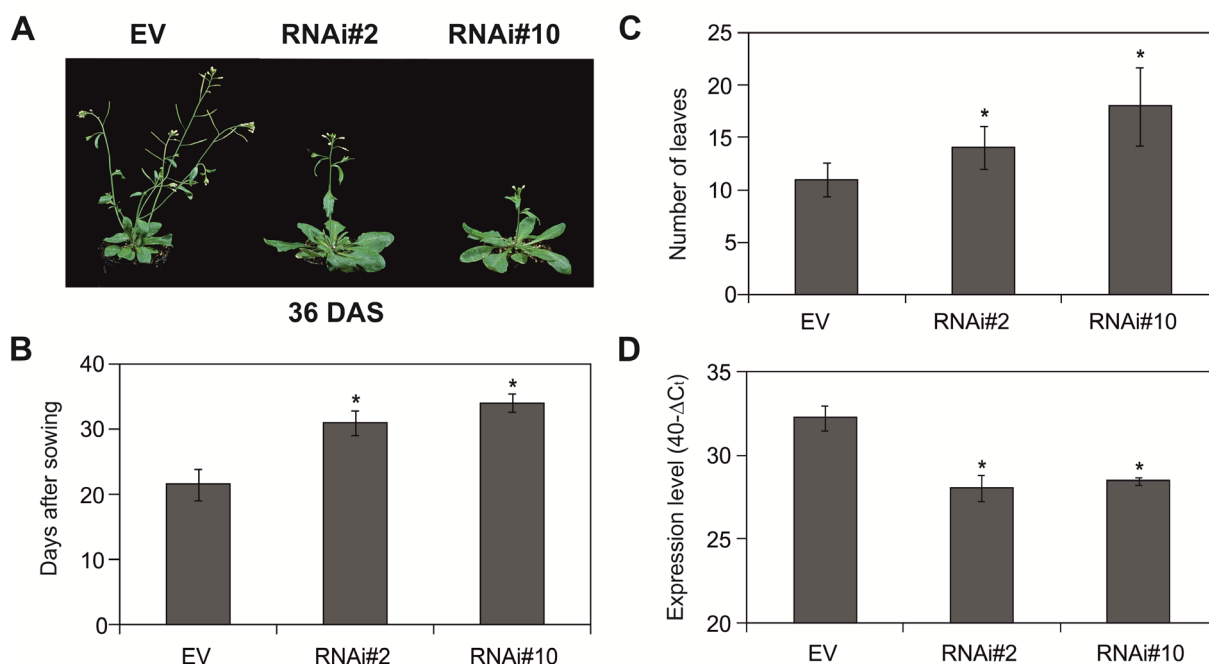
Figure 30. Growth phenotype of *MYB112* RNAi lines.

(A) Appearance of transgenic *MYB112* RNAi lines 36 DAS. Plants germinated on MS medium and after 2 weeks were transferred to soil. **(B)** *MYB112* expression level in EV and RNAi plants determined using qRT-PCR. The data is represented as 40-ΔC_t, where ΔC_t is equal to C_t gene_of_interest $-$ C_t reference_gene_*UBQ10*. Data are means of three independent

experiments ± SD. **(C)** Bolting time of *MYB112* RNAi lines. The time (DAS), when the main stalk elongated to 1 cm was recorded and **(D)** the number of rosetta leaves was measured at the bolting time. For **(C)** and **(D)**, 10 plants were counted to calculate mean values ± SD. Asterisks indicate statistically significant differences to empty vector (EV) lines as determined by Student's *t*-test, $p < 0.05$.

The delay of bolting in the RNAi lines correlated to the level of *MYB112* expression measured by quantitative real-time PCR (qRT-PCR) (**Figure 30B**). We also observed a difference in the number of leaves during bolting between wild-type and transgenic plants. We also observed a difference in the number of leaves at bolting between control plants and transgenics. At this time, empty-vector plants had 8-12 leaves, while RNAi#2 and #10 developed, respectively, 14 and 18 leaves on average per rosette (**Figure 30D**). In this case, the delay of bolting was not caused by the overall delayed growth rate but rather by developmental retardation in the bolting process. The cause of the observed phenotypic changes is unclear, however, it may be related with the decreased level on flavonoid accumulation in *MYB112*-deficient plants (**Figure 20**). It was reported that certain flavonoids modulate auxin signalling in plants (Jacobs and Rubery, 1988; Kuhn *et al*., 2011). The ability of flavonoids to establish auxin gradients translates into phenotypes with strikingly different morpho-anatomical traits (Taylor and Grotewold, 2005; Peer and Murphy, 2007; Besseau *et al*., 2007; Buer and Djordjevic, 2009). Flavonoids at the plasma membrane are effective inhibitors of PIN and MDR-glycoproteins, that are involved in the cell-to-cell movement of auxin. In addition, evidence of a nuclear location of flavonoids (as well as of enzymes involved in flavonoid biosynthesis), is consistent with flavonoids being capable of regulating the activity of proteins responsible for cell growth: flavonoids may therefore act as transcriptional regulators (Saslowsky *et al*., 2005; Naoumkina *et al*., 2008).

Conclusion: MYB112 Affects Bolting Time

3.8. Does MYB44 Act Upstream of *MYB112*?

Published literature indicates that the expression of *MYB112* is negatively regulated under conditions of salt stress, but not in control experiments, by MYB44, a member of subgroup 22 of the R2R3-MYB TF family (Jung *et al*., 2008). Microarray-based expression profiling revealed relatively small differences between wild-type and *35S:MYB44* or *myb44* knock-out plants in the absence of salt stress (Jung *et al*., 2008). However, following 24 h of salinity stress (250 mM NaCl), a clear difference in global transcriptome patterns was observed between wild type plants and *MYB44* overexpressors. Compared to wild-type plants, 816 genes were higher expressed in the *35S:MYB44* line and 496 genes had lower transcript abundance (>2-fold change). Analysis of the data revealed that *MYB112* was among the down-regulated genes; in two independent experiments *MYB112* expression level after salt stress was ~4- and ~20-fold lower in the *35S:MYB44* line than the wild type. Notably, the expression of *MYB32* and *MYB7*, the two direct MYB112 target genes identified here, was also lower in *35S*:*MYB44* than wild-type plants during salt stress (Jung *et al*., 2008; E-ATMX-30; **Table 4**), indicating that MYB44 functions as a direct or indirect negative upstream regulator of *MYB112* expression.

Table 4. Expression of *MYB112* and selected flavonoid biosynthetic and regulatory enes in *35S: MYB44* plants.

- NaCl	Wt1	35S1	Wt2	35S2	35S/Wt1	log2 35S-Wt1	35S/Wt2	log2 35S-Wt2
PAP1	30,3	22,8	2308,8	720,6	0,752475	-0,41028	0,31211	-1,67987
ANS	117	158,2	9528	7752,1	1,352137	0,435241	0,813613	-0,29759
MYB32	205,4	143	496,1	173,7	0,696203	-0,52242	0,350131	-1,51403
MYB7	87,9	69,7	259,9	87	0,792947	-0,3347	0,334744	-1,57887
MYB112	18,4	17,5	243,7	28,9	0,951087	-0,07235	0,118588	-3,07596
DFR	75,1	95,4	10634,5	8712,3	1,270306	0,345176	0,819249	-0,28763
+NaCl	Wt1	35S1	Wt2	35S2	35S/Wt1	log2 35S-Wt1	35S/Wt2	log2 35S-Wt2
PAP1	2590,5	352,7	4159,5	187,3	0,136151	-2,87672	0,045029	-4,47299
ANS	605,8	40,6	9303,8	94,1	0,067019	-3,89929	0,010114	-6,62748
MYB32	691	289,4	488,9	81,5	0,418813	-1,25562	0,166701	-2,58467
MYB7	396,8	119,3	446,4	71,2	0,300655	-1,73382	0,159498	-2,64839
MYB112	672,9	166	1479,9	71,5	0,246693	-2,01921	0,048314	-4,37141
DFR	807,7	117,9	8395,5	93,8	0,14597	-2,77626	0,011173	-6,48388

according to Jung *et al*. (2008)

In addition, expression levels of genes encoding proteins associated with anthocyanin biosynthesis, such as *CHS*, *F3H*, *ANS*, *DFR*, *PAP1* and *PAP2*, were decreased in *35S*:*MYB44* plants upon salt stress (Jung *et al.*, 2008; E-ATMX-30; **Table 4**). It was later reported that 12-day-old *35S*:*MYB44* seedlings grown on MS medium accumulate less anthocyanin than wild-type plants, particularly after jasmonate treatment, whereas *myb44* knockout plants show elevated levels of anthocyanin (Jung *et al.*, 2010). The phenotype of *MYB44* transgenic seedlings is opposite to that of *MYB112* transgenics (see **Figure 19** and **20**). This finding provides further support for the negative regulation of *MYB112* expression. Moreover, bolting time is affected in *35S*:*MYB44* plants. Wild-type plants bolt earlier than *35S*:*MYB44* overexpressors and the number of rosette leaves at bolting time is higher in these plants compared to wild type (Jung *et al.*, 2008). A similar phenotype is evident in *myb112* T-DNA mutant and *MYB112* RNAi plants (see **Figure 29** and **30**), consistent with the model that *MYB112* expression is under negative control of MYB44.
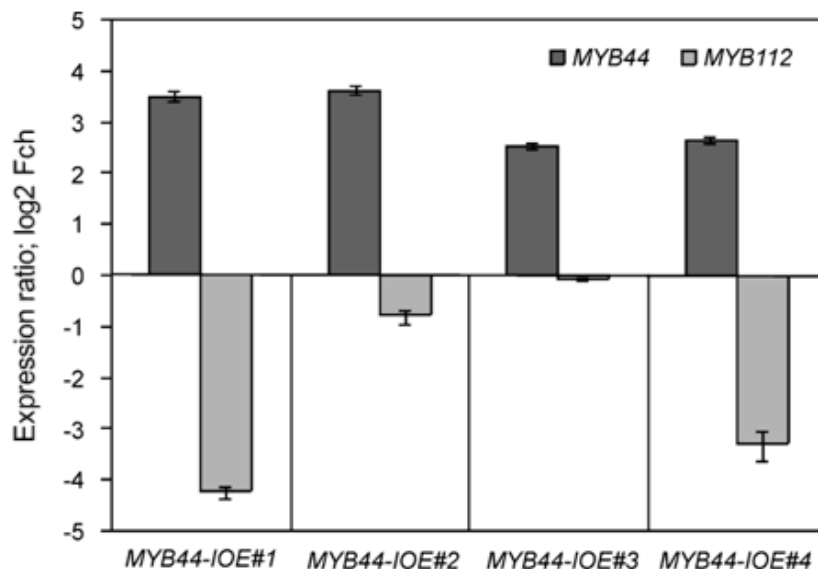
Figure 31. Negative regulation of *MYB112* expression by MYB44.

Two-week-old *Arabidopsis MYB44-IOE* seedlings (lines #1, #2, #3 and #4) were treated with estradiol for 5 h and then for an additional 2 h with 150 mM NaCl in in liquid MS medium supplemented with 1% sucrose. Numbers on the y axis indicate log2 fold-change (FCh) expression ratio compared to control conditions. Data are the means of three biological replicates ± SD, measured by qRT-PCR.

To verify the model, we generated estradiol-inducible *MYB44* overexpression (*MYB44-IOE*) plants and treated transgenic seedlings for 5 h with estradiol in the absence of salt stress, and then induced salt stress (150 mM NaCl) for 2 h (in presence of estradiol). Using qRT-PCR we detected decreased *MYB112* expression in two out of four tested lines (**Figure 31**), indicating that the regulation of *MYB112* expression by MYB44 may be indirect and may require additional factors, modulating this regulation.

4. General Discussion and Outlook

Systematic analysis of mutant plants with impaired expression of R2R3-MYB proteins in *Arabidopsis* as well as in other species resulted in rapid increase in our understanding of their function in plants. R2R3-MYB factors were reported to play roles mainly in regulation of secondary metabolism, plant cell shape and plant organ development (Mandaokar *et al*., 2006; Baumann *et al*., 2007; Dubos *et al*., 2010). A number of R2R3-MYB TFs were described as regulators of flavonoid production. Flavonoid biosynthesis is unique to plants and plays an essential role in their adaptation to sedentary life in a changing environment. These compounds are crucial for the symbiotic plant-microbe interactions and male fertility by promoting the pollen tube development (Koes *et al*. 1994; Hassan and Mathesius, 2012; Ma *et al*., 2012; Weston and Mathesius, 2013). Flavonoids have been shown to modulate auxin transport and seem to modulate the activity of regulatory proteins such as protein phosphatases and kinases (Gamet-Payrastre *et al*., 1999; Peer and Murphy, 2007; Grunewald *et al*., 2012; Weston and Mathesius, 2013). Anthocyanins are a class of water-soluble flavonoid pigments that can provide red to blue colours in flowers, fruits, leaves, and storage organs. Their occurrence in reproductive organs attracts pollinators and aids seed dispersal (Petroni and Tonelli, 2011). The accumulation of anthocyanin pigments in vegetative tissue can be induced by environmental stressors, such as high light, extreme temperatures, osmotic stress, salt stress, sucrose feeding, nutrient deficiency, mechanical damage, pathogen attack, pollution, and herbicides (Chalker-Scott, 1999; Winkel-Shirley, 2002; Gould, 2004, Azuma *et al*., 2012). The presence of anthocyanins in leaves at particular stages of development, and their induction by a variety of environmental stressors is dependent on the highly coordinated transcriptional regulation of anthocyanin biosynthesis genes. This regulation is achieved through a set of specific transcription factors (TFs), including MYB, bHLH and WD-repeat proteins that form MBW complexes (de Vetten *et al*., 1997; Walker *et al*., 1999; Zhang *et al*., 2003; Carey *et al*., 2004; Morita *et al*., 2006; Schwinn *et al*., 2006). According to the current model for the activation of anthocyanin biosynthesis genes, these transcriptional regulators interact with each other and form complexes in conjunction with promoters of anthocyanin biosynthesis genes. For example, the MYB factor encoded by the

COLORLESS1 (*C1*) gene from maize (*Zea mays*) interacts with bHLH factors B and R to activate the promoter of the *DIHYDROFLAVONOL-4-REDUCTASE* (*DFR*) gene (Chandler *et al.*, 1989; Ludwig *et al.*, 1989; Goff *et al.*, 1992). In *Arabidopsis* there are four MYB factors that inercact within MBW complexes, including PAP1/MYB75, PAP2/MYB90, MYB114 and MYB113 (Walker *et al.*, 1999; Zhang *et al.*, 2003; Baudry *et al.*, 2006; Gonzalez *et al.*, 2008). A number of bHLH TFs can participte in this complex: Glabra 3 (GL3/bHLH001), Enhancer of Glabra 3 (EGL3/bHLH002) and TT8/bHLH042 (Zhang *et al.*, 2003; Baudry *et al.*, 2006; Gonzalez *et al.*, 2008). Resulting complexes regulate expression of anthocyanin biosynthesis genes such as *ANTHOCYANIDIN SYNTHASE* (*ANS*) or *DFR.* Intrevterestingly, the *ttg1* mutant, as well as the double *gl3egl3* mutant show a pleiotropic phenotype, including defective anthocyanin production, trichome patterning, seed coat mucilage production, and position-dependent root hair spacing (Payne *et al.*, 2000; Bernhardt *et al.*, 2005; Bouyer *et al*, 2008; Zhao *et al.*, 2008). Multiple experiments revealed that TTG1 and TT8 in complex with a MYB factor Transparent Testa 2 (TT2/MYB123) can form an additional MBW complex to specifically regulate anthocyanidin biosynthesis, providing substrated for epicatechin and proanthocyanidin in seeds and *ban* embryos (Nesi *et al.*, 2001; Baudry *et al.*, 2004, Lepieniec *et al.*, 2006). In addition, *Arabidopsis* Production of Flavonol Glycoside (PFG) factors from subgroup 7 of the R2R3-MYB family, namely MYB11/PFG2, MYB12/PFG1 and MYB111/PFG3 have been reported to control the flavonol branch of the flavonoid biosynthetic pathway by activating *CHS*, *CHI*, *F3H* and *FLAVONOL SYNTHASE* (*FLS*) (Mehrtens *et al.*, 2005; Stracke *et al.*, 2007).

Flavonoids accumulate in plant tissues in response to environmental inputs. Particularly well studied has been the effect of nutrient (mostly nitrogen) limitation on anthocyanin accumulation. Several early (*CHS*, *F3H*, *F3´H*) and late (*DFR*, *ANS*) flavonoid/anthocyanin biosynthesis genes have been reported to be induced by nitrogen and phosphorous depletion in a number of experiments, in *Arabidopsis* and other plant species (e.g. Scheible *et al.*, 2004; Misson *et al.*, 2005; Morcuende *et al.*, 2007; for a comprehensive review see Lillo *et al.*, 2008). Furthermore, many genes encoding enzymes known or predicted to be involved in biosynthesis or modification of flavanoids including various UDP-dependent glycosyl transferases (UGTs) were

found to be (highly) induced by mineral nutrient depletion (Lillo *et al*., 2008). In addition to nutrient limitation, light quantity and quality have been shown to strongly affect anthocyanin biosynthesis (Mancinelli, 1985; Wade *et al*., 2001; Takos *et al*., 2006; Cominelli *et al*., 2008; Albert *et al*., 2009; Stracke *et al*., 2010; Azuma *et al*., 2012). Similarly, several TFs controlling the expression of flavonoid biosynthesis genes in response to other environmental cues have been reported. In *Arabidopsis*, the Phytochrome-Interacting Transcription Factor3 (PIF3), a member of the bHLH protein family, acts as a positive regulator of anthocyanin biosynthesis (Shin *et al*., 2007). The bZIP transcription factor Elonglated Hypocotyl5 (HY5) plays a key role for light-dependent processes in plants and has been shown to positively regulate the expression of several flavonoid biosynthesis genes, including *CHS* and *F3H*, as well as the *MYB12/PFG1* transcription factor (Stracke *et al*., 2010). Of note, *HY5* expression is not much altered by mineral depletion (reported in Lillo *et al*., 2008), indicating the involvement of other TFs in the regulation of nitrogen and phosphorous deficiency-modulated expression of flavonoid biosynthesis genes. Indeed, both, *PAP1* and *PAP2* are induced by nitrogen and phosphorous depletion (Lillo *et al*., 2008). PAP1 has been shown to upregulate the expression of twenty flavonoid biosynthesis genes (Tohge *et al*., 2005), and expression of almost all of these genes was also elevated by nitrogen and/or phosphorous limitation (see meta-analysis by Lillo *et al*., 2008), indicating that PAP transcription factors play an important role in the mineral nutrition response of flavonoid/anthocyanin pathway genes. However, there are notable differences in the expression of *PAP1* and *PAP2* themselves. In several studies, *PAP2* expression was found to be more stimulated than *PAP1* expression under conditions of mineral nutrient deprivation (see for example Misson *et al*., 2005; Lea *et al*., 2007; Morcuende *et al*., 2007), and PAP1 acts in the sucrose-mediated up-regulation of flavonoid biosynthesis genes (Teng *et al*., 2005; Solfanelli *et al*., 2006). Of particular note, *PAP1* and *PAP2* are also upregulated by exposure of plants to light, a condition that also upregulates many flavonoid biosynthesis genes (Cominelli *et al*., 2008). High light induces the expression of *MYB12/PFG1* and *MYB111/PFG3*, key regulators of the flavonol pathway; this induction correlates with the strong influence high light has on flavonol biosynthesis (Mehrtens *et al*., 2005). The Glabra 3 (GL3/bHLH001) transcription factor interacts with PAP1 and PAP2 to activate the expression of the anthocyanin biosynthesis gene *DFR* (Zimmermann *et*

al., 2004b). Notably, expression of *GL3* increases upon nitrogen limitation. Given that the nitrogen depletion-triggered accumulation of anthocyanins, that is normally seen in wild-type plants, was absent in the *gl3* mutant, it was concluded that GL3 is important for the nutrient deprivation response (Feyissa *et al*., 2009). In addition, the negative regulator Caprice (CPC) was reported to repress anthocyanin accumulation under nitrogen limitation condition. Similarly, CPC represses anthocyanin accumulation in *35S* overexpressors grown under osmotic, salinity or cold stress, however, no difference was observed between wild-type and *cpc-1* mutant plants (Fig. 6 in Zhu *et al*., 2009). Furthermore, LBD37, LBD38, and LBD39, members of the Lateral Organ Boundry Domain (LBD) transcription factor family, have been shown to negatively regulate nitrogen depletion-induced anthocyanin formation in *Arabidopsis*, possibly via repression of *PAP1* and *PAP2* (Rubin *et al*., 2009). Salinity stress is yet another environmental factor known to trigger anthocyanin accumulation in a number of plant species. Eryilmaz (2006) reported that anthocyanin content was increased by nearly 73% in the cotyledons and 51% in the hypocotyls of tomato seedlings treated with 100 mM NaCl, compared to the control. Similarly, anthocyanin content in cotyledons and hypocotyls of salt-treated red cabbage seedlings increased by approximately 70% and 65%, respectively, in relation to the control. Kaliamoorthy and Rao (1994) reported an up to 40% increase in anthocyanin accumulation in maize as a salinity stress response. Salt-induced anthocyanin accumulation was also shown in sugarcane (Wahid and Ghazanfar, 2005). Salinity leads to water deficit and ionic stress resulting in the destabilization of membranes, inhibition of enzymes, and the overproduction of reactive oxygen species (ROS) (Zhu, 2001; Munns, 2002; Miller *et al*., 2010), and the accumulation of anthocyanins has been proposed to contribute to plant tolerance against abiotic stresses (Gould *et al*., 2002; Nagata *et al*., 2003; Gould, 2004; Zeng *et al*., 2010). Salt stress (especially when prolonged) can cause precocious senescence and result in e.g. chlorophyll loss. In conditions, when chlorophyll is being degraded plants become more susceptible to photoinhibition. It can be hypothesized that, as in the case of senescence, anthocyanins protect the photosynthetic apparatus of salt treated plants from damaging effects of high-energy radiation. We treated *Arabidopsis* wild-type seedlings with 100 mM NaCl solution for five days **(Figure 32)**. Plants in medium

containing salt (left panel), turned reddish, whereas control plants in MS medium remained green.

MS+100 mM NaCl   **MS**

Elevated anthocyanin under salt stress
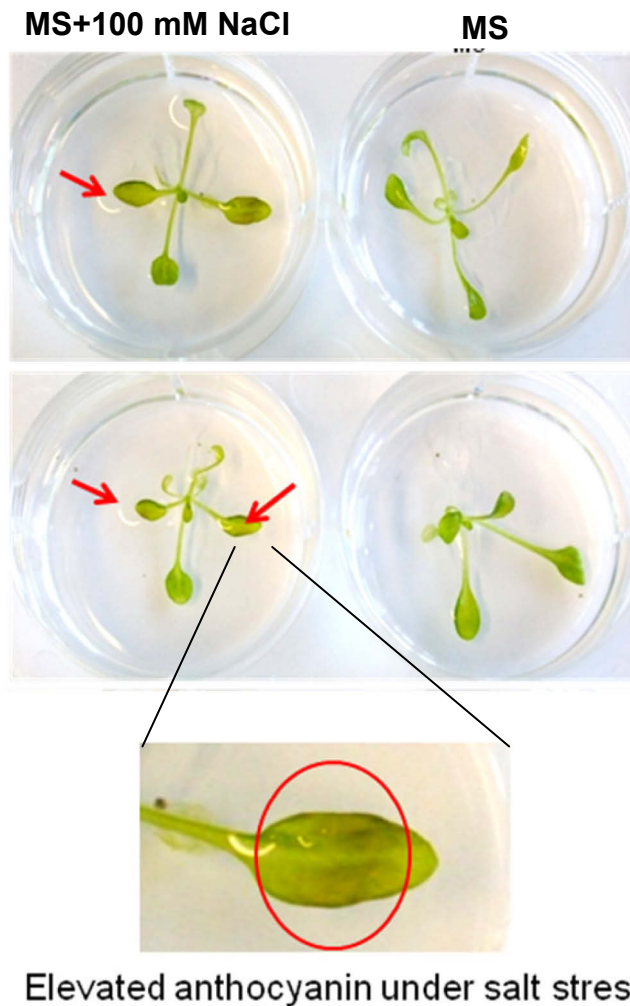
Figure 32. Phenotype of wild-type *Arabidopsis* seedlings under salt stress.

Arabidopsis seedlings were grown on solid MS medium supplemented with 1% sucrose. After two weeks, seedlings were transfered to a liquid MS medium with or without salt (100 mM NaCl). After five days, seedlings treated with salt started to accumulate anthocyanins (arrows and magnified picture)

In contrast to the regulation of anthocyanin biosynthesis under nutrient deprivation, the signaling cascade and involvement of TFs in salt-triggered accumulation of flavonoids/anthocyanins have rarely been investigated so far. Recently, constitutive overexpression of the *Arabidopsis* Shaggy-like Protein Kinase1 (GSK1) in transgenic plants was shown to induce salt stress responses, including the accumulation of

anthocyanins, concomitant with strongly increased *CHS* expression, in the absence of salinity stress (Piao *et al.*, 2001). In the wild type, *CHS* was highly induced by salt stress. These data led to the proposition that GSK1 plays an important role in the signaling cascade(s) that control activation of anthocyanin pathway genes upon exposure of plants to salt stress (Piao *et al.*, 2001). However, nothing is currently known concerning the effect of GSK1 overexpression on the expression of TFs regulating flavonoid/anthocyanin biosynthesis genes. Recently, *MYB44*, a member of subgroup 22 of the R2R3-MYB TF family, was shown to be activated by different abiotic stresses, including dehydration, low temperature and salinity (Jung *et al.*, 2008). After 24 hours of salinity stress, but not under control condition, the expression of *CHS*, *F3H*, *DFR*, *PAP1* and *PAP2* was decreased in transgenic plants overexpressing *MYB44* (Jung *et al.*, 2008). In addition, anthocyanin accumulation was less prominent in *35S*:*MYB44* seedlings than in wild-type plants, particularly following jasmonate treatment (Jung *et al.*, 2010). These data indicate a negative role of MYB44 in stress-induced anthocyanin accumulation. However, a direct regulation of flavonoid/anthocyanin pathway genes by MYB44 has not, as yet, been reported.

4.1. Model of MYB112 Action

We discovered MYB112 as a novel transcriptional regulator of flavonoid biosynthesis in *Arabidopsis thaliana*. Based on our experimental data, we propose a model (**Figure 33**) in which MYB112 acts as a positive regulator of anthocyanin biosynthesis and a negative regulator of flavonol biosynthesis. As we demonstrate, MYB112 activates *PAP1* and *MYB114*, but inhibits *MYB12* and *MYB111*. PAP1 and MYB114 regulate the expression of genes encoding enzymes involved in anthocyanin formation (for example *ANS* and *DFR*) and expression of these genes is increased upon *MYB112* induction. However, it needs to be stressed that only the Landsberg erecta (Ler) *MYB114* allele, and not the Columbia (Col) allele, was functionally characterised. MYB111 and MYB12 control expression of genes involved in flavonol biosynthesis (for example *CHS* and *FLS*) and their transcript levels are decreased in *MYB112-IOE* plants after estradiol treatment. We did not obtain evidence for a direct regulation of either the known anthocyanin or flavonol biosynthesis genes or their regulators. At the current stage of analysis it thus remains

open how the regulation of the flavonoid pathway by MYB112 is achieved. However, one possible scenario is that this regulation occurs through the direct activation of *MYB32* and *MYB7* by MYB112. *MYB32* and *MYB7*, as well as MYB112 early responsive gene *MYB6,* classify to the subgroup 4 of R2R3-MYB factors. Subgroup 4 of R2R3-MYB factors is characterized by the two motifs representing a putative activation domain LlsrGIDPxT/SHRxI/L at the end of the R3 repeat of the DNA binding domain and a putative negative regulatory domain pdLHLD/ELxiG/S in the C-termini (Jin *et al*., 2000). *MYB32* was previously shown to affect expression of flavonoid/phenylpropanoid biosynthesis pathway genes and to affect pollen development. Disruption of *MYB32* by T-DNA insertion leads to the formation of aberrant pollen. A similar phenotype is observed when the closely related *MYB4* gene is mutated or overexpressed. It was speculated that changes in the expression of flavonoid and phenylpropanoid biosynthesis genes influence the flux along these pathways, interfering with pollen development by altering structural components of the pollen wall, such as sporopollenin (Preston *et al*., 2004). Our results reported here indicate that overexpression of *MYB112* also leads to partial pollen sterility. Expression profiling in the *myb112-1* mutant and the *MYB112-IOE* plants treated with estradiol for 5 days revealed significant changes in the expression of a number of phenylpropanoid biosynthesis genes in *MYB112* transgenic plants. *MYB32*, *MYB7* and *MYB4* were recently reported to be direct downstream target genes of MYB46 and MYB83. These two TFs recognize the 7-bp consensus sequence ACC(A/T)A(A/C)(T/C) (Zhong and Ye, 2012; Kim *et al*., 2012), which is highly similar to the MYB112 binding site reported here: (A/T/G)ACC(A/T)(A/G)(A/C)(T/C). MYB46 and MYB83 function redundantly to control the production of all major secondary cell wall components in *Arabidopsis* fibers and vessels, such as lignin, cellulose and xylan (Ko *et al*., 2009; Zhong and Ye, 2012). MYB58 and MYB63 are yet another MYB factors involved in controlling the formation of the secondary cell wall. Contrary to MYB46 and MYB83, they are specifically involved in the regulation of lignin biosynthesis (Zhou *et al*., 2009). Their overexpression was found to induce ectopic deposition of lignin but not cellulose and xylan, whereas their dominant repression resulted in a reduction of secondary wall thickening. In this network, expression of *MYB46/83* and *MYB58/63* is under the control of the Secondary Wall-associated NAC Domain Protein1 (SND1) and its close homologs, NST1, NST2, VND6 and

VND7 (Zhong and Ye, 2009; Zhou *et al*., 2009; Zhong *et al*., 2010). Zhong and Ye (2012) suggest that *MYB32*, *MYB7* and *MYB4* may be involved in fine-tuning the regulation of lignin biosynthesis during secondary wall deposition. Based on microarray experiments, expression of *MYB112* is neither affected by overexpression of the secondary wall NACs (SWNs; Zhong *et al*., 2010) nor *MYB46/83* (Ko *et al*., 2009), and *GUS* promoter activity assays revealed that *MYB112* is mainly expressed in leaves and pollen, while SWNs and *MYB46/83* factors are expressed in vascular tissue. It may, however, be that *MYB112* acts as a SWN-independent regulator of lignin biosynthesis, or of the biosynthesis of other phenylpropanoids, leading to the observed pollen phenotype. Further functional characterization of *MYB7* and *MYB32*, as well as the identification of direct target genes of both TFs will be necessary to refine the *MYB112* regulatory network.

From our studies, we can confirm, that expression of *MYB112* increases during senescence, as well as upon salt and high light stress; conditions in which plants often receive more light energy than can be used for photochemical reactions. Excess light energy leads to photoinhibition and the formation of reactive oxygen species (ROS). Anthocyanins absorb excess quanta, thereby protecting plant tissue from damaging light levels. Accumulation of anthocyanins has been reported to occur under salinity conditions in a number of species including crops and vegetables, such as tomato, maize, sugarcane and many others (see for example Kaliamoorthy and Rao, 1994; Piao *et al*., 2001; Wahid and Ghazanfar, 2006; Keutgen and Pawelzik, 2007; Roychoudhury *et al*., 2008; Matus *et al*., 2010). However, although salinity stress is well known to lead to an accumulation of anthocyanin, the regulatory mechanisms underlying this phenomena have not been studied intensively to date. Herein, we show that *MYB112* expression is induced by salinity stress, whilst its expression is largely unaffected by nitrogen limitation, and sugar levels, in contrast to many of the known transcriptional regulators of flavonoid/anthocyanin biosynthesis (Scheible *et al*., 2004; Misson *et al*., 2005; Lea *et al*., 2007; Morcuende *et al*., 2007; Lillo *et al*., 2008).
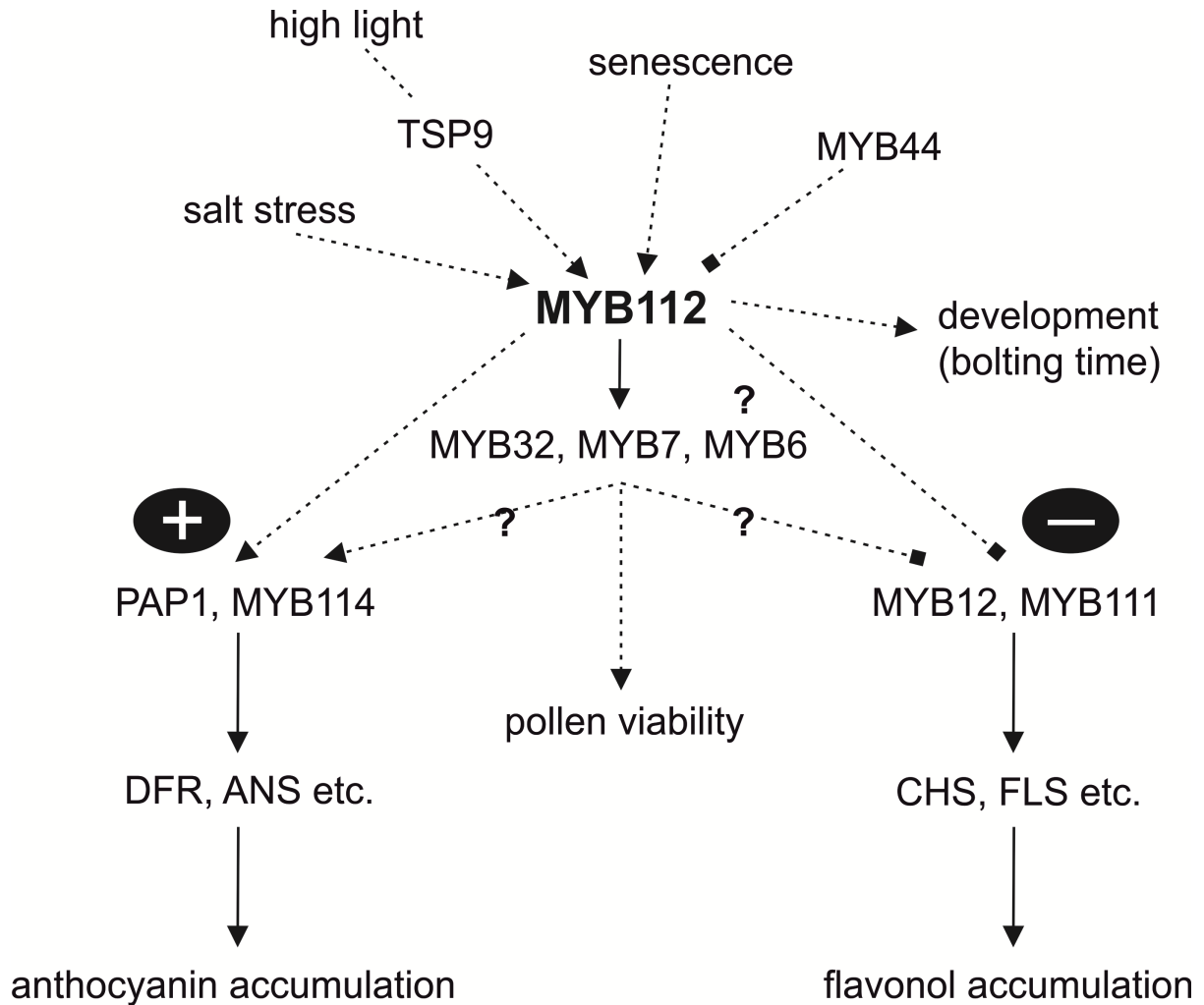
Figure 33. Model of MYB112 action.

MYB112 acts as a positive regulator of *PAP1* and *MYB114*, but inhibits *MYB12* and *MYB111*. PAP1 and MYB114 (in Ler background) regulate the expression of genes encoding enzymes involved in anthocyanin formation (e.g., *ANS* and *DFR*), and MYB111 and MYB12 control expression of genes involved in flavonol biosynthesis (e.g., *CHS* and *FLS*). We propose this regulation to occur through the direct activation of *MYB32* and *MYB7* expression by MYB112. MYB32 was shown to affect expression of flavonoid biosynthesis pathway genes as well as pollen development. Expression of *MYB112* increases during senescence, as well as during salt and high light stress. High light activation of *MYB112* expression can be regulated through TSP9 signaling. In the absence of functional TSP9, high light-induced *MYB112* expression is abolished (Fristedt *et al.*, 2009). Expression of *MYB112* is negatively regulated by MYB44 under conditions of salt stress (Jung *et al.*, 2008). MYB112 also affects bolting time; a similar phenotype is observed for *MYB44* overexpression plants.

We further illustrate that salinity-induced accumulation of anthocyanin is impaired in *myb112* mutants, but stimulated in *35S:MYB112* overexpressors, indicating that MYB112 plays a critical role during salt-induced anthocyanin accumulation. In addition, light quantity and quality have been shown to strongly affect anthocyanin biosynthesis (Mancinelli, 1985; Wade *et al*., 2001; Takos *et al*., 2006; Cominelli *et al*., 2008; Albert *et al*., 2009; Stracke *et al*., 2010; Azuma *et al*., 2012). Here, we report that *myb112-1* mutant accumulates less anthocyanins when subjected to high light stress (500 µmol m^{-2} s^{-1}) for three days, suggesting that *MYB112* is involved in high light-induced anthocyanin accumulation. High light activation of *MYB112* expression may be regulated through TSP9 signaling. TSP9 is a thylakoid-anchored protein, which under high light is phosphorylated and partially released from the membrane. In the absence of functional TSP9, high light-induced *MYB112* expression is abolished (Fristedt *et al*., 2009). Further studies will, however, be required to reveal the details about the signalling pathways that control *MYB112* expression during salinity and high light stress. It would be interesting to investigate the fitness of both *myb112* mutant and *MYB112* overexpression plants under these two stress conditions by monitorning chlorophil and flavonoid/anthocyanin content, SAGs expression, as well as photosynthesis parameters, such as non-photochemical quenching and chlorophyl fluorescence. If anthocyanins protect plants from excessive light, then we should see a difference in photosynthesis parameters when comparing wild-type plants with *myb112* T-DNA mutant, that accumulates less anthocyanin under salinity and high light conditions. Anthocyanins also act as scavengers of ROS. Diaminobenzidine (DAB; Fryer *et al*., 2002) staining staining of *myb112* mutant as well as *35S:MYB112* and *MYB112-IOE* plants treated with estradiol could give an innitial idea about H_2O_2 accumulation in these plants compared to respective controls.

Published literature indicates that the expression of *MYB112* is negatively regulated under conditions of salt stress, by MYB44, a member of subgroup 22 of the R2R3-MYB TF family (Jung *et al*., 2008). Notably, expression of *MYB32* and *MYB7*, the two direct targets of MYB112, was also decreased in *MYB44* overexpression plants upon salt stress (Jung *et al*., 2008). In addition, expression levels of flavonoid/anthocyanin biosynthesis genes, such as *CHS*, *F3H*, *ANS*, *DFR*, *PAP1* and *PAP2*, were

decreased in *35S*:*MYB44* plants under salinity conditions (Jung *et al.*, 2008; E-ATMX-30). Subsequent studies have revealed that *MYB44* overexpressing seedlings accumulate less anthocyanin than wild-type plants, while *myb44* knockout plants show elevated levels of anthocyanin (Jung *et al.*, 2010). Described phenotype of *MYB44* transgenic seedlings is opposite to that of *MYB112* transgenics (see **Figure 19** and **20**). Moreover, bolting time is affected in *35S*:*MYB44* plants. Wild-type plants bolt earlier than *35S*:*MYB44* overexpressors (Jung *et al.*, 2008), what is also evident in *myb112* T-DNA mutant and *MYB112* RNAi plants analysed here (see **Figure 29** and **30**). To verify the model that MYB44 acts as a direct or indirect negative regulator of *MYB112*, we generated estradiol-inducible *MYB44* overexpression (*MYB44-IOE*) plants and treated transgenic seedlings with estradiol in the absence of salt stress, and then induced salt stress (150 mM NaCl) (in presence of estradiol). Using qRT-PCR we detected decreased *MYB112* expression in two out of four tested lines (**Figure 31**), indicating that the regulation of *MYB112* expression by MYB44 may be indirect and may require additional factors, modulating this regulation.

MYB112 also functions as a regulator of plant development and *MYB112*-deficient plants exhibit delayed bolting. It is still unknown which physiological cues determine this phenotype but interestingly a similar phenotype was observed for *MYB44* overexpressing plants (Jung *et al.*, 2008). The bolting phenotype can be related with the fact that certain flavonoids modulate auxin signalling in plants (Jacobs and Rubery, 1988; Kuhn *et al.*, 2011). Flavonoids have been considered natural regulators of cellular auxin efflux and consequent polar auxin transport since Jacobs and Rubery (1988) reported that flavonoid compounds displace the auxin efflux inhibitor 1-naphthylphthalamic acid (NPA) from zucchini (*Cucurbita pepo*) hypocotyl microsomes. Brown *et al.* (2001) observed that plants with a mutation in the gene encoding the first enzyme in flavonoid biosynthesis - *CHS* (*tt4* mutants) display decreased flavonoid accumulation and reduced height in comparison to wild-type plants. The *tt4* phenotype is corelated with enhanced auxin transport from shoot tip to root tip in the absence of flavonoids. Additionally, according to Peer *at al.* (2004) in the presence of excess kaempferol and quercetin in *F3'H* mutant (*tt7*) and *DFR* mutant (*tt3*), basipetal auxin transport is reduced. Later studies have reaffirmed the link between flavonoids and plant architecture by showing that flavonoid-defective

mutants display a wide range of alterations to root and shoot development (Taylor and Grotewold, 2005; Peer and Murphy, 2007; Besseau *et al.*, 2007; Buer and Djordjevic, 2009). Further investigations, including auxin transport measurements, are necessary to clarify if the delayed bolting of *myb112* mutants is caused by an increased basipetal auxin transport.

4.2. Integration of Methods for Functional Characterisation of TFs

The functional characterization of a TF is not a trivial task. Due to the dynamic nature of developmental and environmental responses, transcriptional networks are highly complex. Refinement of the existing methods in combination with emerging approaches will most likely contribute to the progress in our understanding of transcriptional regulation. Commonly used phenotype analysis of gain- and loss-of-function mutants often provides a good biological insight into a TF function but does not allow identifying its downstream targets and gene expression networks controlled by the TF of interest. In order to identify TF-responsive genes we used an inducible overexpression system. Compared to constitutive promoters, inducible promoters offer numerous advantages, namely a transgene can be expressed at a given developmental stage for a specific duration of time. It also gives the opportunity to overexpress a transgene, whose constitutive overexpression is detrimental to the host plant. One of the commonly used inducible systems utilises a fusion between the TF of interest and a steroid-binding domain. In the absence of the inducer, the fusion protein is localised in the cytoplasm and therefore inactive (Lloyd *et al.*, 1994). Upon addition of a steroid, for example dexamethasone (DEX), conformational changes in the steroid-binding domain result in nuclear targeting of the fusion protein and in consequence activation of the TF (Lloyd *et al.*, 1994), whereas the expression level of the chimeric gene itself remains unchanged. One advantage of this system, besides its simplicity, is that direct and indirect effects of TF activity may be separated by using inhibitors of protein synthesis (such as cycloheximide). However, cycloheximide treatment itself causes thousands of expression changes (data from AtGeneExpress Chemical Series by Vinegar and Winter, 2004) and so it is not often used. Therefore, a typical experimental setup involves induction, preferably at the developmental stage that TF is biologically relevant, followed by harvesting and

expression analysis at different times following induction. It is also crucial to use appropriate controls in order to exclude that the changes are caused by application of a steroid (or protein synthesis inhibitor, if used). Other commonly used inducible systems are not restricted to nuclear proteins and rely on transcriptional regulation (Zuo and Chua, 2000; Padidam, 2003). Some of these systems use a chimeric TF, that when induced migrates to the nucleus activating transcription of the gene/TF of interest, whilst others utilise 'stimulus' activated promoters. The inducers range from hormones (estradiol) and chemicals (ethanol) to stress stimuli such as wounding or heat. In our study we used an estradiol (EST)-inducible system. In this system, the gene/TF of interest is cloned downstream of a promoter targeted by the synthetic XVE transcription factor (Zuo *et al.*, 2000). XVE is comprised of the *E. coli lexA* repressor domain fused to the VP16 transactivation domain and the regulatory region of the human estrogen receptor. In the presence of estrogens such as *β*-estradiol or 4-hydroxyl tamoxifen, XVE binds to eight copies of the *lexA* operator fused upstream of the *35S* minimal promoter (O_{lexA}-46) and activates transcription (Zuo *et al.*, 2000). The XVE transcription factor is expressed from the strong synthetic promoter G10-90 that exhibits eightfold higher activity than CaMV *35S* (Ishige *et al.*, 1999). The vector pER8 carries the G10-90::XVE cassette on the same T-DNA as the O_{lexA}-46 promoter.

Short time activation of a TF using an inducible system, followed by genome-wide expression profiling (e.g. microarray ATH1 or RNAseq), facilitates identification of its early responsive genes and is a good starting point towards the identification of direct targets. Microarray results should be further verified using more sensitive qRT-PCR and transactivation assays. In order to fish the direct target genes out of the set of TF early responsive genes a combination of methods is necessary. As TFs exert their function by binding to specific DNA sequences, methods aiming at the identification of the TF binding site (BS) represent a crucial first step towards deciphering direct target genes. The most commonly used BS selection methods are based on SELEX (Systematic Evolution of Ligands by EXponential enrichment), which uses a purified TF protein to enrich short nucleotide sequences that bind tightly to it from a large initial pool of random synthetic DNA fragments (see Chai *et al.*, 2011). After several rounds of selection the nucleotide sequences of the tightly bound DNAs are determined and a consensus DNA recognition sequence is formulated. In our study

we used the CELD method developed by Gang-Ping Xue (CSIRO Plant Industry, Brisbane, Australia). Binding of the TF to the identified consensus DNA sequence may subsequently be confirmed by electrophoretic-mobility shift assay (EMSA). EMSA relies on a difference in the mobility between free and protein bound DNA fragments during gel electrophoresis. The exact sequence requirements for the bound motif can be further investigated by the mutation of individual nucleotides and using these modified sequences to compete for the binding of the TF protein. Besides EMSA, several protocols describe the effective use of an ELISA-based transcription factor binding assay e.g. for the analysis of human NFκB binding to specific DNA sequences. In plants, DNA-Protein Interaction (DPI)-ELISA was established and used for qualitative analyses with HIS-tagged TFs expressed in *E. coli.* Studies confirmed that EMSA and DPI-ELISA result in comparable data, as the binding of *AtbZIP63* to the C-box and *AtWRKY11* to the W2-box could be reproduced and validated by both methods (Brand *et al*., 2010). Recent progress in genome-wide *in vivo* techniques, like DNA adenine methyltransferase identification (DamID), or chromatin immunoprecipitation followed by high-throughput sequencing (ChIP-seq) or DNA microarray analysis (ChIP-chip) enables plant researchers to generate genome-wide, high-resolution DNA-binding maps of transcription factors. ChIP-qPCR on the other hand can be used to confirm that the binding between a TF and an *in vitro* identified BS, occurs also *in vivo*. FAIRE (Formaldehyde Assisted Isolation of Regulatory Elements) is yet another method used to identify transcriptionally active DNA regions, following a stimuli (e. g. TF activation, stress treatment). In the active state, chromatin shows a temporary displacement of nucleosomes, favoring the interaction of DNA-binding proteins with the genomic regulatory elements (Nagy *et al*., 2003; Giresi *et al*., 2007; Giresi and Lieb, 2009). In FAIRE, the total chromatin is crosslinked by formaldehyde and fragmented by sonication followed by phenol:chloroform DNA extraction. In result, the nucleosome depleted fragments of DNA are isolated from the fragments containing high levels of crosslinked proteins. For the genome-wide identification of nucleosome-depleted regions (putative regulatory elements), the DNA fragments present in the FAIRE samples are sequenced by deep sequencing technology.

Whole genome sequencing, the relative ease of transcript profiling by the use of microarrays and qRT-PCR, as well as prompt development of methods leading to

identification of TF binding sites (SELEX, ChIP, etc.) have facilitated the capture of vast amounts of transcript data and gene-to-gene networks.

The metabolome is the final product of a series of gene actions. Hence, metabolomics has a potential to elucidate gene functions, especially when integrated with transcriptomics.

In the present study, we could find gene-to-gene and metabolite-to-gene networks and could identify a new gene function through integrated analysis of metabolomics and transcriptomics.

5. Materials and Methods

General

Standard molecular techniques were performed as described (Sambrook et al., 2001; Skirycz et al., 2008). Primer sequences are given in **Supplementary Table 1**. For gene expression analyses the online tools of Genevestigator (http://www.genevestigator.com; Zimmermann et al., 2004a) and eFP browser (http://www.bar.utoronto.ca/efp/cgi-bin/efpWeb.cgi; Winter et al., 2007) were used.

Plants

Seeds of *Arabidopsis thaliana* (L.) Heynh. ecotype Col-0 were obtained from the *Arabidopsis thaliana* Resource Centre for Genomics (Institut National de la Recherche Agronomique, France; http://dbsgap.versailles.inra.fr/publiclines). *Arabidopsis thaliana* seedlings were grown on selection plates in a climate chamber with a 16-h day length provided by fluorescent light at 30µmol m-2 s-1 and a temperature of 22°C. After two weeks plants were transferred to the soil (Einheitserde GS90; Gebrüder Patzer) and grown under controlled conditions in a greenhouse at 16-h day length (120 µmol m-2 s-1) and a day/night temperature of 21/18°C and relative humidity (RH) 60/75%. The T-DNA insertion lines originated from the SALK collection and GABI-KAT (SALK_098029, GK_093E05).

Constructs

Pro$_{MYB112}$:GUS: A ~1.3-kb fragment upstream of the *MYB112* gene was amplified from genomic *Arabidopsis thaliana* Col-0 DNA by PCR using primers MYB112:GUS-fwd. and MYB112:nested-rev., inserted into plasmid pCR2.1 (Invitrogen, Karlsruhe, Germany) and used as a template for PCR-amplification of the ~1.3-kb region upstream of the translation initiation codon using primers MYB112:GUS-fwd. and MYB112:GUS-rev. The ~1.3-kb promoter was fused via EcoRI and NcoI sites to the β-glucuronidase (*GUS*) reporter gene in pCAMBIA1305.1-Hygromycin (CAMBIA, Canberra, Australia). *35S:MYB112*: MYB112 open reading frame, amplified by PCR from *Arabidopsis* cDNA using primers MYB112-OE-fwd. and MYB112-OE-rev., was inserted into pCR2.1 (Invitrogen) and then cloned via added HindIII sites into a CaMV

35S promoter-containing pGreen0029 vector (Skirycz et al., 2006). *35S:MYB112-GFP*: *MYB112* coding sequence was amplified by PCR from *Arabidopsis* cDNA using primers MYB112-fwd. and MYB112-rev. and inserted into pDONR201 vector (GATEWAY, Invitrogen). Subsequently, the fragment was cloned into the GATEWAY-compatible vector pK7FWG2.0 (Ghent University) using LR reaction. *MYB112-IOE*: *MYB112* coding region was amplified by PCR from *Arabidopsis* leaf cDNA using primers MYB112-IOE-fwd. and MYB112-IOE-rev., inserted into pCR2.1 and then cloned via XhoI and SpeI sites into pER8 vector (Zuo et al., 2000). *Agrobacterium tumefaciens* strain GV3101 (pMP90) was used for *Arabidopsis thaliana* (Col-0) transformations. *MYB44-IOE: MYB44* coding region was amplified by PCR from *Arabidopsis* leaf cDNA using primers MYB44-IOE-fwd. and MYB44-IOE-rev., inserted into pCR2.1 and then cloned via XhoI and SpeI sites into pER8 vector (Zuo et al., 2000). *Agrobacterium tumefaciens* strain GV3101 (pMP90) was used for *Arabidopsis thaliana* (Col-0) transformations. *Pro:fLUC* fusions: ~1.7-kb fragments upstream of the respective gene coding sequences from the genes *MYB6*, *MYB7* and *MYB32* were amplified using PCR from *Arabidopsis* genomic DNA, ligated into the pENTR/D-TOPO vector (Invitrogen) and subsequently recombined into the GATEWAY-compatible vector pGW7 (Licausi et al., 2011) . *Tac:MYB112-CELD-HIS*: *MYB112* coding sequence was amplified using MYB112-CELD-fwd. and MYB112-CELD-rev. and cloned to the pTacLCELD6xHIS (Xue, 2002; Xue; 2005) vector via NheI and BamHI restriction sites.

Isolation of *myb112* T-DNA Insertion and RNAi Lines

T-DNA insertion lines in Col-0 background were obtained from either the SALK (SALK_098029, *myb112-2*) or GABI-Kat (GK_093E05, *myb112-1*) collections. Homozygous plants were identified by PCR using the following primers: for SALK_098029, T-DNA left border primer LB, gene-specific primers SALK_LP and SALK_RP; for GK_093E05, T-DNA left border primer LB, gene-specific primers GK_LP and GK_RP. MYB112 expression in the T-DNA insertion plants was examined by qRT-PCR using gene-specific primers and by end-point PCR using primers annealing to the 5′ and 3′ ends of the *MYB112* coding region. RNAi lines were obtained from AGRIKOLA (http://www.agrikola.org).

Estradiol Induction Experiments

Arabidopsis seedlings transformed with the *MYB112-IOE* construct were grown on solid MS medium supplemented with 1% sucrose and after two weeks were transferred into liquid MS medium supplemented with 10 µM estradiol (EST) for the indicated times. As controls, DMSO-treated *MYB112-IOE* lines or EST-treated empty-vector (EV) plants were used.

RNA Isolation and cDNA Synthesis

Total RNA extraction, cDNA synthesis and qRT-PCR were done as described (Caldana et al., 2007; Balazadeh et al., 2008b; Wu et al., 2012). After grinding plant material in liquid nitrogen, total RNA was isolated with Trizol reagent (Invitrogen) following the manufacturer´s specifications. RNA quality was determined photometrically. RNA integrity was checked on 1% (w ∕ v) agarose formaldehyde gels. 50 µg of total RNA were treated with Turbo DNA-free recombinant DNAse I (Applied Biosystems Applera, Darmstadt, Germany) to remove genomic DNA contamination. RNA integrity was checked again after digestion, and the absence of genomic DNA was verified by real-time PCR using primers for a genomic sequence (*UBQ10*). Two µg of total RNA was used in 20 µL reactions for cDNA synthesis, using RevertAid R-minus cDNA synthesis kit (Fermentas, St. Leon-Rot, Germany). The cDNA was then diluted 1:10 in order to reduce the effect of RNA isolation and cDNA synthesis buffer on the subsequent PCRs.

Expression Profiling by qRT-PCR

Total RNA extraction, cDNA synthesis and qRT-PCR were done as described (Caldana et al., 2007; Balazadeh et al., 2008b; Wu et al., 2012). PCR reactions were run on an ABI PRISM 7900HT sequence detection system (Applied Biosystems Applera, Darmstadt, Germany). Gene expression was analysed using the comparative Ct method. PCR reactions were carried out in technical triplicates using 0.5 µL of diluted cDNA in 5 µL reactions, 2 µL of each 500 nM primer and 2.5 µL of 2x Power SYBR Green PCR Master Mix (Applied Biosystems Applera). Assays were run using the thermal profile: 50 °C for 2 min; 95 °C for 10 min; 40 cycles of 95 °C for 50 s and 60 °C for 1 min. The primers used to test gene expression are shown in

Supplementary Table 3. Experiments were performed using three biological replicates.

Microarray Experiments

Affymetrix ATH1 hybridisations were performed by ATLAS Biolabs (Berlin, Germany). Expression of *MYB112* was induced by 10 µM estradiol in two-week-old seedlings grown on a rotary shaker in liquid MS medium at continuous light, identically treated empty-vector (pER8) transformed seedlings and seedlings treated with DMSO served as controls. Seedlings were harvested after various induction times (1 h, 3 h and 5 h) and RNA extracted from shoots was used for expression profiling.

Reporter Transactivation Assay in Protoplasts

Protoplasts were isolated from *Arabidopsis* (Col-0) plants as described by Yoo et al. (2007) and transformed with *35S:MYB112* effector construct together with *ProMYB32:fLUC*, *ProMYB7:fLUC*, or *ProMYB6:fLUC* and *ProMYB7:fLUC* reporter constructs using 6 µg plasmid DNA each. For normalization of the signal, protoplasts were simultaneously transfected with 6 µg of *35S:rLUC* plasmid. Dual luciferase reporter assays were performed using the kit provided by Promega and luminescence was read using a GloMax 20/20 Luminometer (Promega). Experiments were performed using five biological replicates.

DNA Binding Site Selection

a.   Selection of cellulase-positive clones and purification of MYB112-CELD-HIS fusion protein.

The *Tac:MYB112-CELD-HIS* construct was transformed to *E. coli* XL1-Blue cells. The recombinant *E. coli* cells were screened for cellulase-positive clones by plating transformed cells on Luria Broth (LB)/ampicillin plates containing 0.2% (w/v) carboxymethyl-cellulose (CM-cellulose) substrate. After overnight incubation (12-20h, depending on expression level) at 37°C, the CM-cellulose plates were stained with 0.5% (w/v) Congo Red solution for 10 min at room temperature and destained by washing twice with 1 M NaCl (2 min for the first washing and 10-20 min for the second washing). Afterwards, MYB112-CELD-HIS fusion protein was purified from

cellulase-positive clones. Protein expression was induced using 1mM IPTG and cells were harvested 3 h after induction. Protein purification was performed under native conditions using Ni2+-agarose according to the Qiagen protocol (Qiagen, Hilden, Germany). Protein concentrations were determined by Bradford assay (Promega).

b.   MYB112 binding site selection

This work was performed in collaboration with Dr. G-P. Xue, CSIRO Plant Industry, Brisbane, Australia, according to Xue et al. (2005). Binding site selection was performed using the CELD system (Xue, 2005; Balazadeh et al., 2011) with *Tac:MYB112-CELD-HIS* construct, employing biotin-labeled double-stranded oligonucleotides containing a central 30-nt random sequence. MYB112-selected oligonucleotides were cloned. The cloned oligonucleotides were verified for the presence of MYB112 binding motif by DNA-binding activity assays and sequenced.

Electrophoretic Mobility Shift Assay (EMSA)

MYB112-CELD-HIS fusion protein was purified from *E. coli* expression strain. Cells were sonicated in lysis buffer (50 mM Tris-Cl buffer, pH 7.3, 150 mM NaCl, 1 mM ethylenediaminetetraacetic acid (EDTA), 1 mM dithiothreitol (DTT), 1 mM phenylmethanesulfonyl fluoride (PMSF). Supernatant of centrifuged sample was used for purification using a 1-ml nickel column (GE Healthcare, Munich, Germany) coupled to an Äkta-Purifier FPLC system (GE Healthcare). Aliquots of the flow through fractions were analysed by SDS-PAGE and Coomassie staining. One-ml elution fractions containing the purified MYB112-CELD-HIS fusion protein were pooled and dialyzed against PBS buffer (20 mM Na-phosphate, pH 7.4, 150 mM NaCl). Protein concentration was determined by Bradford assay (Bradford, 1976). 5´-DY682-labeled DNA fragments were obtained from MWG (Ebersberg, Germany). Sequences of labeled DNA fragments and unlabeled competitors are given in **Supplementary Table 1**. Annealing was performed by heating the primers to 100°C followed by slow cooling to room temperature. Binding reaction was performed at room temperature for 20 min as described in the Odyssey Infrared EMSA kit instruction manual. DNA-protein complexes were separated on 6% retardation gel whilst DY682 signal was detected using the Odyssey Infrared Imaging System from LI-COR Biosciences (Bad Hamburg, Germany).

Chromatin Immunoprecipitation coupled to qPCR (ChIP-qPCR)

To investigate *in vivo* binding of MYB112 to its DNA binding site in the promoter of *MYB32*, *MYB7*, *MYB6* and *UGT84A2*, we used ChIP-qPCR, using whole shoots from long day-grown, two-week-old *Arabidopsis* plants expressing GFP-tagged MYB112 protein from the CaMV *35S* promoter (*35S:MYB112-GFP*). Wild-type plants were used as negative control. For the ChIP, we followed a protocol previously described by Kaufmann et al., 2010 employing anti-GFP antibody to immunoprecipitate protein-DNA complexes. The ChIP experiment was run in three independent replications. qPCR was used to test binding of MYB112 to its binding site within the selected promoters; the primers flanked the MYB112 binding site. As a negative control, we used primers annealing to promoter regions of two other *Arabidopsis* genes (At3g18040 and At2g22180) lacking a MYB112 binding site. Primer sequences are given in **Supplementary Table 3**. We analysed ChIP-qPCR data relative to input, as this includes normalization for both background levels and input chromatin going into the ChIP. The amount of genomic DNA coprecipitated by GFP antibody (ChIP signal) was calculated in comparison to the total input DNA used for each immunoprecipitation in the following way: cycle threshold (CT) = CT(ChIP) − CT(Input). To calculate fold enrichment, normalized ChIP signals were compared between *35S:MYB112-GFP* and wild-type plants, where the ChIP signal is given as the fold increase in signal relative to the background signal. Experiments were performed in three biological replicates.

Secondary Metabolite Profiling by LC-MS

Secondary metabolite analysis by LC-MS was performed as described by Tohge and Fernie (2010). All data were processed using Xcalibur 2.1 software (Thermo Fisher Scientific). The obtained data matrix was normalized using an internal standard Isovitexin; CAS 29702-25-8). Metabolites were identified and annotated based on comparisons with data in our previous publications (Tohge et al., 2005, 2007; Hirai et al., 2007; Yonekura-Sakakibara et al., 2008), metabolite databases (reviewed in Tohge and Fernie, 2009), and standard compounds (Yonekura-Sakakibara et al., 2008; Nakabayashi et al., 2009).

Microscopy

We analysed the distribution of MYB112-GFP fusion protein by confocal fluorescence microscopy (Eclipse E600 microscope, Nikon, Düsseldorf, Germany).

Other Methods

Histochemical GUS assays was performed as described by Plesch *et al*. (2001). Pollen viability was analysed using stereomicroscope MZ 12.5 (Leica) after Alexander staining (Alexander, 1969).

Statistical Analyses

Unless otherwise specified, statistical analyses were performed using Student´s t test embedded in the Microsoft Excel software. Only the return of $p < 0.05$ was designated as statistically significant.

References

Abe, H., Urao, T., Ito, T., Seki, M., Shinozaki, K., Yamaguchi-Shinozaki, K. (2003) *Arabidopsis* AtMYC2 (bHLH) and AtMYB2 (MYB) Function as Transcriptional Activators in Abscisic Acid Signaling. Plant Cell **15:** 63-78.

Aharoni, A., De Vos, C.H., Wein, M., Sun, Z., Greco, R., Kroon, A., Mol, J.N.M., O'Connell, A.P. (2001) The strawberry FaMYB1 transcription factor suppresses anthocyanin and flavonol accumulation in transgenic tobacco. Plant J. **28:** 319-332.

Albert, N.W., Lewis, D.H., Zhang, H., Irving, L.J., Jameson, P.E. and Davies, K.M. (2009) Light-induced vegetative anthocyanin pigmentation in *Petunia*. J. Exp. Bot. **60:** 2191-2202.

Alexander, M.P. (1969) Differential staining of aborted and nonaborted pollen. Stain Technol. **44:** 117-122.

Allan, A.C., Hellens, R.P. and Laing, W.A. (2008) MYB transcription factors that colour our fruit. Trends Plant Sci. **13:** 99-102.

Azuma, A., Yakushiji, H., Koshita, Y. and Kobayashi, S. (2012) Flavonoid biosynthesis-related genes in grape skin are differentially regulated by temperature and light conditions. Planta **235:** 1067-1080.

Balazadeh, S., Riaño-Pachón, D.M. and Mueller-Roeber, B. (2008) Transcription factors regulating leaf senescence in *Arabidopsis thaliana*. Plant Biol. (Stuttg.) **10 (suppl. 1):** 63-75.

Balazadeh, S., Wu, A. and Mueller-Roeber, B. (2010a) Salt-triggered expression of the ANAC092-dependent senescence regulon in *Arabidopsis thaliana*. Plant Signal Behav. **5:** 733-735.

Balazadeh, S., Siddiqui, H., Allu, A.D., Matallana-Ramirez, L.P., Caldana, C., Mehrnia, M., Zanor, M.-I., Köhler, B. and Mueller-Roeber B. (2010b) A gene regulatory network controlled by the NAC transcription factor ANAC092/AtNAC2/ORE1 during salt-promoted senescence. Plant J. **62:** 250-264.

Balazadeh, S., Kwasniewski, M., Caldana, C., Mehrnia, M., Zanor, M.-I., Xue, G.-P. and Mueller-Roeber, B. (2011) ORS1, an H2O2-responsive NAC

85

transcription factor, controls senescence in *Arabidopsis thaliana*. Mol. Plant **4:** 346-360.

Baudry A., Heim, M.A., Dubreucq, B., Caboche, M., Weisshaar, B., Lepiniec, L. (2004) T2, TT8, and TTG1 synergistically specify the expression of *BANYULS* and proanthocyanidin biosynthesis in *Arabidopsis thaliana.* Plant J. **39:** 366-380.

Baudry, A., Caboche, M. and Lepiniec, L. (2006) TT8 controls its own expression in a feedback regulation involving TTG1 and homologous MYB and bHLH factors, allowing a strong and cell-specific accumulation of flavonoids in *Arabidopsis thaliana*. Plant J. **46:** 768-779.

Baumann, K., Perez-Rodriguez, M., Bradley, D., Venail, J., Bailey, P., Jin, H., Koes, R., Roberts, K., Martin, C. (2007) Control of cell and petal morphogenesis by R2R3 MYB transcription factors. Development. **134:** 1691-701.

Besseau, S., Hoffmann, L., Geoffroy, P., Lapierre, C., Pollet, B., Legrand, M. (2009) Flavonoid Accumulation in *Arabidopsis* Repressed in Lignin Synthesis Affects Auxin Transport and Plant Growth. Plant Cell **19:** 148-162.

Borevitz, J.O., Xia, Y., Blount, J., Dixon, R.A. and Lamb, C. (2000) Activation tagging identifies a conserved MYB regulator of phenylpropanoid biosynthesis. Plant Cell **12:** 2383-2394.

Bradford, M.M. (1976) A rapid and sensitive method for the quantitation of microgram quantities of protein utilizing the principle of protein-dye binding. Anal. Biochem. **72:** 248-254.

Brand, L.H., Kirchler, T., Hummel, S., Chaban,C., Wanke, D. (2010) DPI-ELISA: a fast and versatile method to specify the binding of plant transcription factors to DNA *in vitro.* Plant Methods. **6:** 25**.**

Breeze, E., et al. (2011) High-resolution temporal profiling of transcripts during *Arabidopsis* leaf senescence reveals a distinct chronology of processes and regulation. Plant Cell **23:** 873-894.

Broun, P. (2005) Transcriptional control of flavonoid biosynthesis: a complex network of conserved regulators involved in multiple aspects of differentiation in *Arabidopsis*. Curr. Opin. Plant Biol. **8:** 272-279.

Brown, D.E.., Rashotte, A.M., Murphy, A.S., Normanly, J., Tague, B.W., Peer, W.A., Taiz, L., Muday, G.K. (2001) Flavonoids Act as Negative Regulators of Auxin Transport *in Vivo* in *Arabidopsis*. Plant Physiol. **126:** 524-535.

Buchanan-Wollaston, V., Page, T., Harrison, E., Breeze, E., Lim, PO., Nam, H.G., Lin, J.F., Wu, S.H., Swidzinski, J., Ishizaki, K., Leaver, C.J. (2005) Comparative transcriptome analysis reveals significant differences in gene expression and signalling pathways between developmental and dark/starvation-induced senescence in *Arabidopsis*. Plant J. **42:** 567-85.

Buer, C.S., Djordjevic, M.A. (2009) Architectural phenotypes in the *transparent testa mutants* of *Arabidopsis thaliana*. J. Exp. Bot. **60:** 751-763.

Butelli, E., Titta, L.,Giorgio, M., Mock, H.P., Matros, A., Peterek, S., Schijlen, E.G., Hall, R.D., Bovy, A.G., Luo, J., Martin, C. (2008) Enrichment of tomato fruit with health-promoting anthocyanins by expression of select transcription factors. Nat. Biotechnol. **26:** 1301-1308.

Caldana, C., Scheible, W.-R., Mueller-Roeber, B. and Ruzicic S. (2007) A quantitative RT-PCR platform for high-throughput expression profiling of 2500 rice transcription factors. Plant Meth. **3:** 1-9.

Candela, H., Martínez-Laborda, A. and Micol, J.L. (1999) Venation pattern formation in *Arabidopsis thaliana* vegetative leaves. Develop. Biol. **205:** 205-216.

Castellarin, S.D., Pfeiffer, A., Sivilotti, P., Degan, M., Peterlunger, E., Dl Gaspero, G. (2007) Transcriptional regulation of anthocyanin biosynthesis in ripening fruits of grapevine under seasonal water deficit. Plant Cell Environ. **30:** 1381-1399.

Chai, C., Xie, Z., Grotewold, E. (2011) SELEX (Systematic Evolution of Ligands by EXponential Enrichment), as a powerful tool for deciphering the protein-DNA interaction space. Methods Mol. Biol. **754:** 249-58.

Chandler, V.L., Radicella, J.P., Robbins, T.P., Chen, J., Turks, D. (1989) Two regulatory genes of the maize anthocyanin pathway are homologous: isolation of *b* utilizing *r* genomic sequences. Plant Cell **1:** 1175-1183.

Chalker-Scott L. (1999) *Environmental Significance of Anthocyanins in Plant Stress Responses.* Photochemistry and Photobiology 70(1): 1-9.

Christie, P.J., Alfenito, M.R. and Walbot, V. (1994) Impact of low-temperature stress on general phenylpropanoid and anthocyanin pathways: Enhancement of transcript abundance and anthocyanin pigmentation in maize seedlings. Planta **194:** 541-549.

Cominelli, E., Gusmaroli, G., Allegra, D., Galbiati, M., Wade, H.K., Jenkins, G.I., Tonelli, C. (2008) Expression analysis of anthocyanin regulatory genes in response to different light qualities in *Arabidopsis thaliana*. J. Plant Physiol. **165:** 886-894.

D'Auria, J.C., Reichelt M., Luck K., Svatoš A., Gershenzon J. (2007) Identification and characterization of the BAHD acyltransferase malonyl CoA: Anthocyanidin 5-O-glucoside-6″-O-malonyltransferase (At5MAT) in *Arabidopsis thaliana*. FEBS Lett. **581:** 872-878.

De Vetten, N., Quattrocchio, F., Mol, J. and Koes, R. (1997) The *an11* locus controlling flower pigmentation in petunia encodes a novel WD-repeat protein conserved in yeast, plants, and animals. Genes Develop. **11:** 1422-1434.

Dixon, R.A. and Paiva, N.L. (1995) Stress-induced phenylpropanoid metabolism. Plant Cell **7:** 1085-1097.

Dubos, C., Le Gourrierec, J., Baudry, A., Huep, G., Lanet, E., Debeaujon, I., Routaboul, J.M., Alboresi, A., Weisshaar, B. and Lepiniec L. (2008) MYBL2 is a new regulator of flavonoid biosynthesis in *Arabidopsis thaliana*. Plant J. **55:** 940-953.

Dubos, C., Stracke, R., Grotewold, E., Weisshaar, B., Martin, C., Lepiniec, L. (2010) MYB transcription factors in *Arabidopsis*. Trends Plant Sci.**15:** 573-81

Eryilmaz, F. (2006) The relationships between salt stress and anthocyanin content in higher plants. Biotechnol and Biotechnol Equipment **20:** 1.

Falcone Ferreyra, M.L., Rius, S.P. and Casati, P. (2012) Flavonoids: biosynthesis, biological functions, and biotechnological applications. Front. Plant. Sci. **3:** 222. doi: 10.3389/fpls.2012.00222.

Feyissa, D.N., Løvdal, T., Olsen, K.M., Slimestad, R., and Lillo, C. (2009) The endogenous *GL3*, but not *EGL3*, gene is necessary for anthocyanin accumulation as induced by nitrogen depletion in *Arabidopsis* rosette stage leaves. Planta **230:** 747-754.

Feild, T.S., Lee, D.W., Holbrook, N.M. (2001) Why Leaves Turn Red in Autumn. The Role of Anthocyanins in Senescing Leaves of Red-Osier Dogwood. Plant Physiol. **127:** 566-574.

Fristedt, R., Carlberg, I., Zygadlo, A., Piippo, M., Nurmi, M., Aro, E.-M., Scheller, H.V. and Vener A.V. (2009) Intrinsically unstructured phosphoprotein TSP9 regulates light harvesting in *Arabidopsis thaliana*. Biochem. **48:** 499-509.

Fryer M.J., Oxborough K., Mullineaux P.M., Baker N.R. (2002). Imaging of photo-oxidative stress responses in leaves. J. Exp. Bot. **53**: 1249–1254.

Gamet-Payrastre, L., Manenti, S., Gratacap, M.-P., Tulliez, J., Chap, H., Payrastre, B. (1999) Flavonoids and the inhibition of PKC and PI 3-kinase. Gen. Pharmacol.: Vasc. Syst. **32:** 279-286.

Gentleman, R.C., Carey, V.J., Bates, D.M., Bolstad, B., Dettling, M., Dudoit, S., Ellis, E., Gautier, L., Ge, Y., Gentry, J., Hornik, K., Hothorn, T., Huber, W., Iacus, S., Irizarry, R., Leisch, F., Li, C., Maechler, M., Rossini, A.J., Sawitzki, G., Smith, C., Smyth, G., Tierney, L., Yang, J.H.Y. and Zhang, J. (2004) Bioconductor: open software development for computational biology and bioinformatics. Genome Biol. **5:** R80.

Giresi, P.G., Kim, J., McDaniell, R.M., Iyer, V.R. and Lieb, J.D. (2007) FAIRE (Formaldehyde Assisted Isolation of Regulatory Elements) isolates active regulatory elements from human chromatin. Genome Res. **17:** 877-885.

Giresi, P.G. and Lieb, J.D. (2009) Isolation of active regulatory elements from eukaryotic chromatin using FAIRE (Formaldehyde Assisted Isolation of Regulatory Elements). Methods (San Diego, Calif) **48:** 233-239.

Gitelson, A.A., Merzlyak, M.N., Chivkunova, O.B. (2001*)* Optical Properties and Nondestructive Estimation of Anthocyanin Content in Plant Leaves. Photochem. and Photobiol. **74:** 38-45.

Goff, S.A., Cone, K.C., Chandler, V.L. (1992) Functional analysis of the transcriptional activator encoded by the maize *B* gene: evidence for a direct functional interaction between two classes of regulatory proteins. Genes and Develop. **6:** 864-875.

Gonzalez, A., Zhao, M., Leavitt, J.M. and Lloyd, A.M. (2008) Regulation of the anthocyanin biosynthetic pathway by the TTG1/bHLH/Myb transcriptional complex in *Arabidopsis* seedlings. Plant J. **53:** 814-827.

Gould, K.S., Neill, S.O. and Vogelmann, T.C. (2002) A unified explanation for anthocyanins in leaves? Adv. Bot. Res. **37:** 167-192.

Gould, K.S. (2004) Nature's Swiss Army Knife: The diverse protective roles of anthocyanins in leaves. J. Biomed. Biotech. **5:** 314-320.

Grotewold, E., Drummond, B.J., Bowen, B., Peterson, T. (1994) The myb-homologous *P* gene controls phlobaphene pigmentation in maize floral organs by directly activating a flavonoid biosynthesis gene subset. Cell **76:** 543-553.

Grunewald, W., De Smet, I., Lewis, D.R., Löfke, C., Jansen, L., Goeminne, G., Vanden Bossche, R., Karimi, M., De Rybel, B., Vanholme, B., Teichmann, T., Boerjan, W., Van Montagu, M.C., Gheysen, G., Muday, G.K., Friml, J., Beeckman, T. (2012) Transcription factor WRKY23 assists auxin distribution patterns during *Arabidopsis* root development through local control on flavonol biosynthesis. Proc. Natl. Acad. Sci. U S A. **5:** 1554-1559.

Guo Y., Gan S. (2011) AtMYB2 regulates whole plant senescence by inhibiting cytokinin-mediated branching at late stages of development in *Arabidopsis*. Plant Physiol. **156:** 1612-1619.

Hansson, M., Dupuis, T., Strömquist, R., Andersson, B., Vener, A.V. and Carlberg, I. (2007) The mobile thylakoid phosphoprotein TSP9 interacts with the light-harvesting complex II and the peripheries of both photosystems. J. Biol. Chem. **282:** 16214-16222.

Hassan, S., Mathesius, U. (2012) The role of flavonoids in root-rhizosphere signalling: opportunities and challenges for improving plant-microbe interactions. J. Exp. Bot. **9:** 3429-3444.

Hichri, I., Barrieu, F., Bogs, J., Kappel, C., Delrot, S. and Lauvergeat, V. (2011) Recent advances in the transcriptional regulation of the flavonoid biosynthetic pathway. J. Exp. Bot. **62:** 2465-2483.

Hoch, W.A., Zeldin, E.L., McCown, B.H. (2001) Physiological significance of anthocyanins during autumnal leaf senescence. Tree Physiol. **21:** 1-8.

Hoch, W.A., Singsaas, E.L., McCown, B.H. (2003) Resorption Protection. Anthocyanins Facilitate Nutrient Recovery in Autumn by Shielding Leaves from Potentially Damaging Light Levels. Plant Physiology **133:** 1296-1305.

Ishige, F., Takaichi, M., Foster, R., Chua, N.-H. and Oeda, K.A. (1999) A G-box motif (GCCACGTGCC) tetramer confers high-level constitutive expression in dicot and monocot plants. Plant J. **18:** 443-448.

Jacobs, M., Rubery, P.H. (1988) Naturally-occurring auxin transport regulators. Science **241:** 346-349.

Jin, H., Martin, C. (1999) Multifunctionality and diversity within the plant MYB-gene family. Plant Mol. Biol. **41:** 577-585.

Jin, H., Cominelli, E., Bailey, P., Parr, A., Mehrtens, F., Jones, J., Tonelli, C., Weisshaar, B. and Martin, C. (2000) Transcriptional repression by AtMYB4 controls production of UV protecting sunscreens in *Arabidopsis*. EMBO J. **19:** 6150-6161.

Jung, C., Seo, J.S., Han, S.W., Koo, Y.J., Kim, C.H., Song, S.I., Nahm, B.H., Choi, Y.D. and Cheong, J.J. (2008) Overexpression of *AtMYB44* enhances stomatal closure to confer abiotic stress tolerance in transgenic *Arabidopsis*. Plant Physiol. **146:** 623-635.

Jung, C., Shim, J.S., Seo, J.S., Lee, H.Y., Kim, C.H., Choi, Y.D., Cheong, J.-J. (2010) Non-specific phytohormonal induction of *AtMYB44* and suppression of jasmonate-responsive gene activation in *Arabidopsis thaliana*. Molecules and Cells **29:** 71-76.

Kaliamoorthy, S. and Rao, A.S. (1994) Effect of salinity on anthocyanin accumulation in the root of maize. Ind. J. Plant Physiol. **37:** 169-170.

Katiyar, A., Smita, S., Lenka, S.K., Rajwanshi, R., Chinnusamy, V., Bansal, K.C. (2012) Genome-wide classification and expression analysis of MYB transcription factor families in rice and *Arabidopsis*. BMC Genomics **13:** 544. doi:10.1186/1471-2164-13-544.

Keutgen, A.J. and Pawelzik, E. (2007) Modifications of strawberry fruit antioxidant pools and fruit quality under NaCl stress. J. Agric. Food Chem. **55:** 4066-4072.

Kuhn, B.H., Geisler, M., Bigler, L., Ringli, C. (2011) Flavonols accumulate asymmetrically and affect auxin transport in *Arabidopsis*. Plant Physiol. **156:** 585-595.

Kim, W.-C., Ko, J.-H. and Han, K.-H. (2012) Identification of a cis-acting regulatory motif recognized by MYB46, a master transcriptional regulator of secondary wall biosynthesis, Plant Mol. Biol. **78:** 489-501.

Kitamura, S., Shikazono, N. and Tanaka, A. (2004) TRANSPARENT TESTA19 is involved in the accumulation of both anthocyanins and proanthocyanidins in *Arabidopsis*. Plant J. **37:** 104-114.

Ko, J.-H., Kim, W.-C. and Han, K.-H. (2009) Ectopic expression of *MYB46* identifies transcriptional regulatory genes involved in secondary wall biosynthesis in *Arabidopsis*. Plant J. **60:** 649-665.

Koes, R.E., Quattrocchio, F., Mol, J.M.N. (1994) The flavonoid biosynthetic pathway in plants: Function and evolution. BioEssays **16:** 123-132.

Koes, R., Verweij, W. and Quattrocchio, F. (2005) Flavonoids: a colorful model for the regulation and evolution of biochemical pathways. Trends Plant Sci. **10:** 236-242.

Koornneef, M. (1990) Mutations Affecting the Testa Color in *Arabidopsis.* Arabidopsis Inf. Service**:** 1-4.

Kranz, H.D., Denekamp, M., Greco, R., Jin, H., Leyva, A., Meissner, R.C., Petroni, K., Urzainqui, A., Bevan, M., Martin, C., Smeekens, S., Tonelli, C., Paz-Ares, J., Weisshaar, B. (1998) Towards functional characterisation of the members of the R2R3-MYB gene family from *Arabidopsis thaliana.* Plant J. **16:** 263-276.

Kar, M., Streb, P., Hertwig, B., Feierabend, J. (1993) Sensitivity to photodamage increases during senescence in excised leaves. J. of Plant Physiol. **141:** 538-544.

Lea, U.S., Slimestad, R., Smedvig, P. and Lillo, C. (2007) Nitrogen deficiency enhances expression of specific MYB and bHLH transcription factors and accumulation of end products in the flavonoid pathway. Planta **225:** 1245-1253.

Levine, M., Tjian, R. (2003) Transcription regulation and animal diversity. Nature **424:** 147-51.

Lepiniec, L.C., Debeaujon, I., Routaboul, J.M., Baudry, A., Pourcel, L., Nesi, N. and Caboche, M. (2006) Genetics and biochemistry of seed flavonoids. Ann. Rev. Plant Biol. **57:** 405-430.

Licausi, F., Weits, D.A., Pant, B.D., Scheible, W.-R., Geigenberger, P. and van Dongen J.T. (2011) Hypoxia responsive gene expression is mediated by various subsets of transcription factors and miRNAs that are determined by the actual oxygen availability. New Phytol. **190:** 442-456.

Lillo, C., Lea, U.S. and Ruoff, P. (2008) Nutrient depletion as a key factor for manipulating gene expression and product formation in different branches of the flavonoid pathway. Plant Cell Environ. **31:** 587-601.

Ludwig, S.R., Habera, L.F., Dellaporta, S.L., Wessler, S.R. (1989) *Lc,* a member of the maize *r* gene family responsible for tissue-specific anthocyanin production, encodes a protein similar to transcriptional activators and contains the myc-homology region. Proc. Natl. Acad. Sci. USA **86:** 7092-7096.

Long, S.P., Humphries, S., Falkowsk, P.G. (1994) Photoinhibition of Photosynthesis in Nature. Annu. Rev. Plant Mol. Biol. **45:** 633-662.

Ma, J., Wei, H., Song, M., Pang, C., Liu, J., Wang, L., Zhang, J., Fan, S., Yu, S. (2012) Transcriptome profiling analysis reveals that flavonoid and ascorbate-glutathione cycle are important during anther development in Upland cotton. PLoS One. doi: 10.1371/journal.pone.0049244.

Mancinelli, A. L. (1985) Light-dependent anthocyanin synthesis: a model system for the study of plant photomorphogenesis. Bot. Rev. **51:** 107-157.

Mandaokar, A., Thines, B., Shin, B., Lange, B.M., Choi, G., Koo, Y.J., Yoo, Y.J., Choi, Y.D., Choi, G., Browse, J. (2006) Transcriptional regulators of stamen development in *Arabidopsis* identified by transcriptional profiling. Plant J. **46:** 984-1008.

Martin, C., Paz-Ares, J. (1997) MYB transcription factors in plants. Trends Genet. **13:** 67-73.

Matus, J.T., Poupin, M.J., Cañón, P., Bordeu, E., Alcalde, J.A. and Arce-Johnson, P. (2010) Isolation of WDR and bHLH genes related to flavonoid synthesis in grapevine (Vitis vinifera L.). Plant Mol. Biol. **72:** 607-620.

Matsui, K., Umemura, Y. and Ohme-Takagi, M. (2008) AtMYBL2, a protein with a single MYB domain, acts as a negative regulator of anthocyanin biosynthesis in *Arabidopsis*. Plant J. **55:** 954-967.

Mehrtens, F., Kranz, H., Bednarek, P. and Weisshaar, B. (2005) The *Arabidopsis* transcription factor MYB12 is a flavonol-specific regulator of phenylpropanoid biosynthesis. Plant Physiol. **138:** 1083-1096.

Miller, G., Suzuki, N., Ciftci-Yilmaz, S. and Mittler, R. (2010) Reactive oxygen species homeostasis and signalling during drought and salinity stresses. Plant Cell Environ. **33:** 453-467.

Misson, J., Raghothama, K.G., Jain, A., Jouhet, J., Block, M.A., Bligny, R., Ortet, P., Creff, A., Somerville, S., Rolland, N., Doumas, P., Nacry, P., Herrerra-Estrella, L., Nussaume, L. and Thibaud, M.C. (2005) A genome-wide transcriptional analysis using *Arabidopsis thaliana* Affymetrix gene chips determined plant responses to phosphate deprivation. Proc. Natl. Acad. Sci. USA **102:** 11934-11939.

Mol, J., Jenkins, G., Schäfer, E., Weiss, D., Walbot, V. (1996) Signal perception, transduction, and gene expression involved in anthocyanin biosynthesis. CRC Crit. Rev. Plant Sci. **15**: 525-557

Morcuende, R., Bari, R., Gibon, Y., Zheng, W., Pant, B.D., Bläsing, O., Usadel, B., Czechowski, T., Udvardi, M.K., Stitt, M. and Scheible, W.R. (2007) Genome-wide reprogramming of metabolism and regulatory networks of *Arabidopsis* in response to phosphorus. Plant Cell Environ. **30:** 85-112.

Moyano, E., Martinez-Garcia, J.F., Martin, C. (1996) Apparent Redundancy in myb Gene Function Provides Gearing for the Control of Flavonoid Biosynthesis in *Antirrhinum* Flowers. Plant Cell **8:** 1519-1532.

Munns, R. (2002). Comparative physiology of salt and water stress. Plant Cell Environ. **25:** 239-250.

Nagata, T., Todoriki, S., Masumizu, T., Suda, I., Furuta, S., Du, Z. and Kikuchi, S. (2003) Levels of active oxygen species are controlled by ascorbic acid and anthocyanin in *Arabidopsis*. J. Agr. Food Chem. **51:** 2992-2999.

Nagy, P.L., Cleary, M.L., Brown, P.O. and Lieb, J.D. (2003) Genomewide demarcation of RNA polymerase II transcription units revealed by physical fractionation of chromatin. Proc. Natl. Acad. Sci. USA **100:** 6364-6369.

Naoumkina, M., Dixon, R.A. (2008) Subcellular localization of flavonoid natural products. Plant Sig. Behav. **3:** 573-575.

Nesi, N., Jond, C., Debeaujon, I., Caboche M., Lepiniec, L. (2001) The *Arabidopsis TT2* Gene Encodes an R2R3-MYB Domain Protein That Acts as a Key Determinant for Proanthocyanidin Accumulation in Developing Seed. Plant Cell **13:** 2099-2114.

Neill, S.O., Gould, K.S. (1999) Optical properties of leaves in relation to anthocyanin concentration and distribution. Canadian J. of Bot. **77:** 1777-1782.

Neill, S.O., Gould, K.S. (2003) Anthocyanins in leaves: light attenuators or antioxidants? Funct. Plant Biol. **30:** 865-873.

Noh, Y.-S. and Amasino, R.M. (1999) Identification of a promoter region responsible for the senescence-specific expression of *SAG12*. Plant Mol. Biol. **41:** 181-194.

Ogata, K., Hojo, H., Aimoto, S., Nakai, T., Nakamura, H., Sarai, A., Ishii, S., Nishimura, Y. (1992) Solution structure of a DNA-binding unit of Myb: a helix-turn-helix-related motif with conserved tryptophans forming a hydrophobic core. Proc. Natl. Acad. Sci. USA **89:** 6428-6432.

Omidbakhshfard, M.A., Omranian, N., Ahmadi, F.S., Nikoloski, Z. and Mueller-Roeber, B. (2012) Effect of salt stress on genes encoding translation-associated proteins in *Arabidopsis thaliana*. Plant Sign. Behav. **7:** 1095-1102.

Osuna, D., Usadel, B., Morcuende, R., Gibon, Y., Bläsing, O.E., Höhne, M., Günter, M., Kamlage, B., Trethewey, R., Scheible, W.-R. and Stitt, M. (2007) Temporal responses of transcripts, enzyme activities and metabolites after adding sucrose to carbon-deprived *Arabidopsis* seedlings. Plant J. **49:** 463-491.

Padidam, M. (2003) Chemically regulated gene expression in plants. Curr. Opin. Plant Biol. **6:** 169-177.

Paz-Ares, J., Ghosal, D., Wienand, U., Peterson, P.A., Saedler, H. (1987) The regulatory c1 locus of *Zea mays* encodes a protein with homology to myb proto-oncogene products and with structural similarities to transcriptional activators. EMBO J. **6:** 3553-3558.

Peer, W.A., Bandyopadhyay, A., Blakeslee, J.J., Makam, S.N., Chen, R.J., Masson, P.H., Murphy, A.S. (2004) Variation in Expression and Protein Localization of the PIN Family of Auxin Efflux Facilitator Proteins in Flavonoid Mutants with Altered Auxin Transport in *Arabidopsis thaliana.* Plant Cell **16:** 1898-1911.

Peer, W.A., Murphy, A.S. (2007) Flavonoids and auxin transport: modulators or regulators? Trends Plant Sci. **12:** 556-563.

Petroni, K. and Tonelli, C. (2011) Recent advances on the regulation of anthocyanin synthesis in reproductive organs. Plant Sci. **181:** 219-229.

Piao, H.L., Lim, J.H., Kim, S.J., Cheong, G.W. and Hwang, I. (2001) Constitutive over-expression of *AtGSK1* induces NaCl stress responses in the absence of

NaCl stress and results in enhanced NaCl tolerance in *Arabidopsis*. Plant J. **27:** 305-314.

Plesch, G., Ehrhardt, T., Mueller-Roeber, B. (2001) Involvement of TAAAG elements suggests a role of Dof transcription factors in guard cell-specific gene expression. Plant J. **28:** 455-464.

Pourcel, L., Routaboul, J.M., Cheynier, V., Lepiniec, L. and Debeaujon, I. (2007) Flavonoid oxidation in plants: from biochemical properties to physiological functions. Trends Plant Sci. **12:** 29-36.

Preston, J., Wheeler, J., Heazlewood, J., Li, S.F. and Parish, R.W. (2004) AtMYB32 is required for normal pollen development in *Arabidopsis thaliana*. Plant J. **40:** 979-995.

Quattrocchio, F., Wing, J., van der Woude, K., Souer, E., de Vetten, N., Mol, J., Koes R. (1999) Molecular Analysis of the *anthocyanin2* Gene of *Petunia* and Its Role in the Evolution of Flower Color. Plant Cell **11:** 1433-1444.

Ramsay, N.A. and Glover, B.J. (2005) MYB–bHLH–WD40 protein complex and the evolution of cellular diversity. Trends Plant Sci. **10:** 63-70.

Rice-Evans, C., Miller, N., Paganga, G. (1997) Antioxidant properties of phenolic compounds. Trends Plans Sci **2:** 152-159

Riechmann, J.L., Heard, J., Martin, G., Reuber, L., Jiang, C., Keddie, J., Adam, L., Pineda, O., Ratcliffe, O.J., Samaha, R.R., Creelman, R., Pilgrim, M., Broun, P., Zhang, J.Z., Ghandehari, D., Sherman, B.K., Yu G. (2000) *Arabidopsis* transcription factors: genome-wide comparative analysis among eukaryotes. Science **290:** 2105-2110.

Riechmann, J.L. (2002) Transcriptional Regulation: a Genomic Overview. In C.R. Somerville., E.M. Meyerowitz. eds, The *Arabidopsis Book*. American Society of Plant Biologists, Rockville, MD.

Roychoudhury, A., Basu, S., Sarkar, S.N. and Sengupta, D.N. (2008) Comparative physiological and molecular responses of a common aromatic indica rice cultivar to high salinity with non-aromatic indica rice cultivars. Plant Cell Rep. **27:** 1395-1410.

Rubin, G., Tohge, T., Matsuda, F., Saito, K. and Scheible, W.-R. (2009) Members of the LBD family of transcription factors repress anthocyanin synthesis and affect additional nitrogen responses in *Arabidopsis*. Plant Cell **21:** 3567-3584.

Sablowski, R.W.M., Moyano, E., Culianez-Macia, F.A., Schuch, W., Martin, C., Bevan, M. (1994) A flower-specific Myb protein activates transcription of phenylpropanoid biosynthesis genes. EMBO J. **13:** 128-137.

Salvatierra, A., Pimentel, P., Moya-León, M.A., Herrera, R. (2013) Increased accumulation of anthocyanins in *Fragaria chiloensis* fruits by transient suppression of *FcMYB1* gene. Phytochemistry. doi:10.1016/j.phytochem. 2013.02.016

Sambrook, J. and Russell D.W. (2001) Molecular cloning: a laboratory manual. Cold Spring Habor Laboratory Press.

Saslowsky, D.E., Warek, U., Winkel, B.S.J. (2005) Nuclear localization of flavonoid enzymes in *Arabidopsis*. J. Biol. Chem. **25:** 23735-23740.

Scheible, W.R., Morcuende, R., Czechowski, T., Fritz, C., Osuna, D., Palacios-Rojas, N., Schindelasch, D., Thimm, O., Udvardi, M.K. and Stitt, M. (2004) Genome-wide reprogramming of primary and secondary metabolism, protein synthesis, cellular growth processes, and the regulatory infrastructure of *Arabidopsis* in response to nitrogen. Plant Physiol. **136:** 2483-2499.

Schmidt, R. and Mohr, H. (1981) Time-dependent changes in responsiveness to light of phytochrome-mediated anthocyanin synthesis. Plant Cell Envirion. **4:** 433-437.

Schwinn, K., Venail, J., Shang, Y., Mackay, S., Alm, V., Butelli, E., Oyama, R., Bailey, P., Davies, K., Martin, C. (2006) A Small Family of MYB-Regulatory Genes Controls Floral Pigmentation Intensity and Patterning in the Genus *Antirrhinum*. Plant Cell **18:** 831-851.

Sekine, S., Tagami, S., Yokoyama, S. (2012) Structural basis of transcription by bacterial and eukaryotic RNA polymerases. Curr. Opin. Struct. Biol. **22:** 110-118.

Shin, J., Park, E. and Choi, G. (2007) PIF3 regulates anthocyanin biosynthesis in an HY5-dependent manner with both factors directly binding anthocyanin biosynthesis gene promoters in *Arabidopsis*. Plant J. **49:** 981-994.

Shirley, B.W., Kubasek, W.L., Storz, G., Bruggemann, E., Koornneef, M., Ausubel, F.M., Goodman, H.M. (1995) Analysis of *Arabidopsis* Mutants Deficient in Flavonoid. Biosynthesis. Plant J. **8:** 659-671.

Sinlapadech, T., Stout, J., Ruegger, M.O., Deak, M., Chapple, C. (2007) The hyper-fluorescent trichome phenotype of the *brt1* mutant of *Arabidopsis* is the result of a defect in a sinapic acid: UDPG glucosyltransferase. Plant J. **49:** 655-668.

Skirycz, A., Reichelt, M., Burow, M., Birkemeyer, C., Rolcik, J., Kopka, J., Zanor, M.-I., Gershenzon, J., Strnad, M., Szopa, J., Mueller-Roeber, B. and Witt, I. (2006) DOF transcription factor AtDof1.1 (OBP2) is part of a regulatory network controlling glucosinolate biosynthesis in *Arabidopsis*. Plant J. **47:** 10-24.

Solfanelli, C., Poggi, A., Loreti, E., Alpi, A. and Perata, P. (2006) Sucrose-specific induction of the anthocyanin biosynthetic pathway in *Arabidopsis*. Plant Physiol. **140:** 637-646.

Stracke, R., Favory, J.J., Gruber, H., Bartelniewoehner, L., Bartels, S., Binkert, M., Funk, M., Weisshaar, B. and Ulm R. (2010) The *Arabidopsis* bZIP transcription factor HY5 regulates expression of the *PFG1/MYB12* gene in response to light and ultraviolet-B radiation. Plant Cell Environ. **33:** 88-103.

Stracke, R., Ishihara, H., Huep, G., Barsch, A., Mehrtens, F., Niehaus, K. and Weisshaar, B. (2007) Differential regulation of closely related R2R3-MYB transcription factors controls flavonol accumulation in different parts of the *Arabidopsis thaliana* seedling. Plant J. **50:** 660-677.

Takos, A.M., Jaffé, F.W., Jacob, S.R., Bogs, J., Robinson, S.P. and Walker, A.R. (2006) Light-induced expression of a MYB gene regulates anthocyanin biosynthesis in red apples. Plant Physiol. **142:** 1216-1232.

Tamagnone, L., Merida, A., Parr, A., Mackay, S., Culianez-Macia, F.A., Roberts, K., Martin, C. (1998) The AmMYB308 and AmMYB330 Transcription Factors from *Antirrhinum* Regulate Phenylpropanoid and Lignin Biosynthesis in Transgenic Tobacco. Plant Cell **10:** 135-154.

Tanaka, Y., Brugliera, F., Kalc, G., Senior, M., Dyson, B., Nakamura, N., Katsumoto, Y. and Chandler, S. (2010) Flower color modification by engineering of the flavonoid biosynthetic pathway: practical perspectives. Biosci. Biotechnol. Biochem. **74:** 1760-1769.

Taylor, L.P., Grotewold, E. (2005) Flavonoids as developmental regulators. Curr. Opin. Plant Biol. **8:** 317-323.

Teng, S., Keurentjes, J., Bentsink, L., Koornneef, M. and Smeekens, S. (2005) Sucrose-specific induction of anthocyanin biosynthesis in *Arabidopsis* requires the *MYB75/PAP1* gene. Plant Physiol. **139:** 1840-1852.

Tohge, T., Fernie, A.R. (2010) Combining genetic diversity, informatics and metabolomics to facilitate annotation of plant gene function. Nat. Protoc. **5:** 1210-1227.

Tohge, T., Nishiyama, Y., Hirai, M.Y., Yano, M., Nakajima, J., Awazuhara, M., Inoue, E., Takahashi, H., Goodenowe, D.B., Kitayama, M., Noji, M., Yamazaki, M. and Saito, K. (2005) Functional genomics by integrated analysis of metabolome and transcriptome of *Arabidopsis* plants over-expressing a MYB transcription factor. Plant J. **42:** 218-235.

Tominaga, R., Iwata, M., Okada, K., Wada, T. (2007) Functional Analysis of the Epidermal-Specific MYB Genes *CAPRICE* and *WEREWOLF* in *Arabidopsis*. Plant Cell **19:** 2264-2277.

Wade, H.K., Bibikova, T.N., Valentine, W.J. and Jenkins, G.I. (2001) Interactions within a network of phytochrome, cryptochrome and UV-B phototransduction pathways regulate chalcone synthase gene expression in *Arabidopsis* leaf tissue. Plant J. **25:** 675-685.

Wahid, A. and Ghazanfar, A. (2006) Possible involvement of some secondary metabolites in salt tolerance of sugarcane. J. Plant Physiol. **163:** 723-730.

Walker, A.R., Davison, P.A., Bolognesi-Winfield, A.C., James, C.M., Srinivasan, N., Blundell, T.L., Esch, J.J., Marks, M.D. and Gray, J.C. (1999) The *TRANSPARENT TESTA GLABRA1* locus, which regulates trichome differentiation and anthocyanin biosynthesis in *Arabidopsis*, encodes a WD40 repeat protein. Plant Cell **11:** 1337-1350.

Wang, Y., Chen, S. and Yu, O. (2011) Metabolic engineering of flavonoids in plants and microorganisms. Appl. Microbiol. Biotechnol. **91:** 949-956.

Wang, H., Cao, G., Prior, R.L. (1997) Oxygen Radical Absorbing Capacity of Anthocyanins. J. Agr. Food Chem. **45:** 304-309.

Weston, L.A., Mathesius, U. (2013) Flavonoids: their structure, biosynthesis and role in the rhizosphere, including allelopathy. J. Chem. Ecol. **39:** 283-297.

Wheldale, M. (1916) The anthocyanin pigments of plants. Cambridge University Press, London, pp 126-141.

Winkel-Shirley B. (2001) Flavonoid biosynthesis. A colorful model for genetics, biochemistry, cell biology, and biotechnology. Plant Physiol. **126:** 485-493.

Winkel-Shirley, B. (2002) Biosynthesis of flavonoids and effects of stress. Curr. Opin. Plant Biol. **5:** 218-223.

Wu, A., Allu, A.D., Garapati, P., Siddiqui, H., Dortay, H., Zanor, M.I., Asensi-Fabado, M.A., Munné-Bosch, S., Antonio, C., Tohge, T., Fernie, A.R., Kaufmann, K., Xue, G.P., Mueller-Roeber, B. and Balazadeh, S. (2012) JUNGBRUNNEN1, a reactive oxygen species-responsive NAC transcription factor, regulates longevity in *Arabidopsis*. Plant Cell **24:** 482-506.

Yonekura-Sakakibara, K., Fukushima, A., Nakabayashi, R., Hanada, K., Matsuda, F., Sugawara, S., Inoue, E., Kuromori, T., Ito, I., Shinozaki, K., Wangwattana, B., Yamazaki M. and Saito K. (2012) Two glycosyltransferases involved in anthocyanin modification delineated by transcriptome independent component analysis in *Arabidopsis thaliana*. Plant J. **69:** 154-167.

Xue, G.-P. (2002) Characterisation of the DNA-binding profile of barley HvCBF1 using an enzymatic method for rapid, quantitative and high-throughput analysis of the DNA-binding activity. Nucl. Acids Res. **1:** e77.

Xue, G.-P. (2005) A CELD-fusion method for rapid determination of the DNA-binding sequence specificity of novel plant DNA-binding proteins. Plant J. **41:** 638-649.

Yoo, S.-D., Cho, Y.-H. and Sheen, J. (2007) *Arabidopsis* mesophyll protoplasts: a versatile cell system for transient gene expression analysis. Nat. Prot. **2:** 1565-1572.

Zeng, X.Q., Chow, W.S., Su, L.J., Peng, X.X. and Peng C.L. (2010) Protective effect of supplemental anthocyanins on *Arabidopsis* leaves under high light. Physiol. Plant. **138:** 215-225.

Zimmermann, P., Hirsch-Hoffmann, M., Hennig, L., Gruissem, W. (2004a) GENEVESTIGATOR. Arabidopsis Microarray Database and Analysis Toolbox. Plant Physiol. **136:** 2621-2632.

Zimmermann, I.M., Heim, M.A., Weisshaar, B., Uhrig, J.F. (2004b) Comprehensive identification of *Arabidopsis thaliana* MYB transcription factors interacting with R/B-like BHLH proteins. Plant J. **40:** 22-34.

Zhang, F., Gonzalez, A., Zhao, M., Payne, C.T. and Lloyd, A. (2003) A network of redundant bHLH proteins functions in all TTG1-dependent pathways of *Arabidopsis*. Development **130:** 4859-4869.

Zhang, C.H., Shangguan, L.F., Ma, R.J., Sun, X., Tao, R., Guo, L., Korir, N.K., Yu, M.L. (2012) Genome-wide analysis of the AP2/ERF superfamily in peach (*Prunus persica*). Genet. Mol. Res. **11:** 4789-4809.

Zhong, R. and Ye, Z.-H. (2009) Transcriptional regulation of lignin biosynthesis. Plant Sign. Behav. **4:** 1028-1034.

Zhong, R., Lee, C. and Ye, Z.-H. (2010) Global analysis of direct targets of secondary wall NAC master switches in *Arabidopsis*. Mol. Plant **3:** 1087-1103.

Zhong, R. and Ye, Z.-H. (2012) MYB46 and MYB83 bind to the SMRE sites and directly activate a suite of transcription factors and secondary wall biosynthesis genes. Plant Cell Physiol. **53:** 368-380.

Zhou, J., Lee, C., Zhong, R. and Ye, Z.-H. (2009) MYB58 and MYB63 are transcriptional activators of the lignin biosynthetic pathway during secondary cell wall formation in *Arabidopsis*. Plant Cell **21:** 248-266.

Zhu, J.K. (2001). Plant salt tolerance. Trends Plant Sci. **6:** 66-71.

Zhu, H.F., Fitzsimmons, K., Khandelwal, A. and Kranz, R.G. (2009) CPC, a single-repeat R3-MYB, is a negative regulator of anthocyanin biosynthesis in Arabidopsis. Mol. Plant. **2:** 790-802.

Zuo, J., Niu, Q.-W. and Chua, N.-H. (2000) An estrogen receptor-based transactivator XVE mediates highly inducible gene expression in transgenic plants. Plant J. **24:** 265-273.

Zuo J., Chua, N.-H. (2000) Chemical-inducible systems for regulated expression of plant genes. Curr. Opin. Plant Biol. **11:** 146-151.

Supplementary materials

Supplementary Table 1. Expression of 50 Hypoxia-responsive Genes in *MYB112-IOE* Seedlings Induced with Estradiol for 5 h in Comparison to DMSO-treated Plants.

| AGI | Annotation | MYB112-IOE (Est-Mock) | | | |
		log2 1st replicate	STDV	log2 2nd replicate	STDV
AT3G02550	LBD41	-2,54	0,66	-2,47	0,14
AT5G10040	unknown protein	-2,08	0,81	-1,40	0,88
AT1G33055	unknown protein	-1,84	0,66	-1,53	0,83
AT4G10270	wound-responsive family protein	-1,74	0,28	-1,11	0,56
AT2G34390	NIP2;1	-1,71	0,46	-2,84	0,97
AT3G10040	transcription factor	-1,65	0,21	-1,39	0,78
AT5G62520	SRO5	-1,47	0,04	-1,85	0,37
AT4G27450	unknown protein	-1,22	1,15	-0,30	0,14
AT5G23990	FRO5	-1,18	0,82	Undetermined	Undetermined
AT2G16060	AHB1	-1,17	0,29	-0,64	0,50
AT2G15880	leucine-rich family protein	-1,07	0,71	Undetermined	Undetermined
AT4G33070	pyruvate decarboxylase	-1,05	0,09	-1,76	0,32
AT5G15120	unknown protein	-1,02	0,34	-1,75	0,06
AT5G39890	unknown protein	-0,96	0,16	-1,29	0,53
AT4G24110	unknown protein	-0,94	0,27	-1,71	0,07
AT4G33560	similar to wound-responsive protein	-0,92	0,65	-1,12	0,20
AT5G42200	zinc finger family protein	-0,92	0,64	-0,41	0,27
AT5G66985	unknown protein	-0,91	0,17	-1,86	0,03
AT2G17850	unknown protein	-0,83	0,04	-1,27	0,38
AT5G20830	SUS1	-0,81	0,56	-2,12	0,62
AT5G39580	peroxidase	-0,79	1,39	0,07	0,36
AT3G29970	germination protein	-0,76	0,34	-0,39	0,01
AT5G37260	myb family transcription factor	-0,67	1,66	-0,27	0,63
AT5G47910	RBOHD	-0,64	0,33	-2,93	0,37
AT4G26270	phosphofructokinase family protein	-0,64	0,84	Undetermined	Undetermined
AT5G45960	GDSL-motif lipase/hydrolase protein	-0,55	0,04	-0,79	0,04
AT2G26400	ARD3	-0,48	1,20	-0,19	0,37
AT4G17260	L-lactate dehydrogenase	-0,46	0,61	0,10	0,43
AT1G43800	acyl-(acyl-carrier-protein) desaturase	-0,41	0,80	-6,04	0,51
AT3G27220	kelch repeat-containinG protein	-0,40	0,35	-2,16	0,90
AT1G19530	unknown protein	0,26	0,26	0,06	0,13
AT4G14980	DC1 domain-containing protein	-0,24	0,01	Undetermined	Undetermined
AT1G77120	ADH1	-0,18	0,60	-0,85	0,03
AT3G47720	SRO4	-0,13	0,54	-2,37	0,55
AT5G44730	haloacid dehalogenase-like hydrolase protein	-0,04	0,37	0,76	0,45
AT3G43190	SUS4	-0,01	0,48	Undetermined	Undetermined
AT4G17670	senescence-associated protein	0,03	0,65	-0,36	0,72

AGI	Annotation				
AT1G72360	ethylene-responsive element-binding protein	0,05	0,66	0,48	0,32
AT5G54490	PBP1	0,12	0,93	-1,19	0,97
AT2G26150	HSFA2	0,16	1,18	-0,60	0,30
AT3G03270	ENOD18 family protein	0,21	1,22	-0,56	0,37
AT2G19590	ACO1	0,25	0,39	-0,31	0,34
AT1G76650	calcium-bindinf EF hand family protein	0,29	0,22	-1,52	0,41
AT3G09940	monodehydroascorbate reductase	0,35	0,66	Undetermined	Undetermined
AT4G32840	phosphofructokinase family protein	0,50	0,96	0,26	0,16
AT5G19550	ASP2	0,53	0,62	-0,17	0,26
AT1G35140	PHI-1	0,65	0,06	-0,20	0,58
AT2G32020	GNAT protein	1,00	0,17	-0,86	0,00
AT2G47520	transcription factor	1,04	0,03	0,43	1,15
AT2G14210	ANR1	Undetermined	Undet.	0,25	0,70

Supplementary Table 2. Expression of 94 sSecondary metabolite-associated genes in *MYB112-IOE* seedlings induced with estradiol for 5 days in comparison to mock-treated plants and *myb112-1* in cComparison to wild-type Plants.

AGI	Annotation	log2 (*MYB112-IOE*_MOCK)	STDV	log2 (*myb112-1*_WT)	STDV
AT1G03495	HXXXD-type acyl-transferase family protein	1,3275345	0,6643544	-1,3573165	0,037558
AT1G22410	Class-II DAHP synthetase family protein	1,2483825	0,0170179	-0,506014	0,079657
AT1G56650	ATMYB75_MYB75_PAP1_SIAA1__production of anthocyanin pigment 1	1,325925	0,1383511	-2,7423085	0,9898738
AT1G74100	ATSOT16_ATST5A_CORI-7_SOT16__sulfotransferase 16	-0,1306075	0,0323226	0,055873	0,0812635
AT2G27820	ADT3_PD1__prephenate dehydratase 1	-0,259751	0,5511261	-2,008763	1,603021
AT3G06350	EMB3004_MEE32__dehydroquinate dehydratase, putative / shikimate dehydrogenase, putative	0,493344	0,1117851	-0,9388085	0,0169458
AT3G50740	UGT72E1__UDP-glucosyl transferase 72E1	-0,1659045	0,1886059	0,401159	0,120252
AT4G13770	CYP83A1_REF2__cytochrome P450, family 83, subfamily A, polypeptide 1	-0,3107005	0,1004396	-0,447995	0,0105769
AT4G36220	CYP84A1_FAH1__ferulic acid 5-hydroxylase 1	1,9179615	0,0394219	-0,546504	0,1091872
AT5G08640	ATFLS1_FLS_FLS1__flavonol synthase 1	-1,942995	0,2275286	-2,0190805	0,2070161
AT5G23010	IMS3_MAM1__methylthioalkylmalate synthase 1	-0,7511095	0,5276014	-1,812874	0,0671087
AT5G49330	ATMYB111_MYB111_PFG3__myb domain protein 111	-2,443585	0,2412309	-0,515396	0,4968118
AT1G03940	HXXXD-type acyl-transferase family protein	0,426377	0,0881522	-0,2566165	0,1989905
AT1G24000	Polyketide cyclase/dehydrase and lipid transport superfamily protein	0,3824415	0,4972	0,72985	1,5436198
AT1G61720	BAN__NAD(P)-binding Rossmann-fold superfamily protein	1,387239	0,1046221	-1,2001245	1,0657648
AT1G74710	ATICS1_EDS16_ICS1_SID2__ADC synthase superfamily protein	-0,3305525	0,232414	-2,7057295	0,3471675
AT2G30490	ATC4H_C4H_CYP73A5_REF3__cinnamate-4-hydroxylase	0,530918	0,0347543	-0,1984765	0,0071071
AT3G19450	ATCAD4_CAD_CAD-C_CAD4__GroES-like zinc-binding alcohol dehydrogenase family protein	0,223909	0,0223361	-1,529141	0,0076269
AT3G53260	ATPAL2_PAL2__phenylalanine ammonia-lyase 2	0,16583	0,1633035	-0,8118105	0,070239
AT4G14090	UDP-Glycosyltransferase superfamily protein	1,1127005	0,2246514	-1,509703	0,066741
AT4G38620	ATMYB4_MYB4__myb domain protein 4	0,3707325	0,2036446	-0,012547	0,1598924
AT5G09640	SCPL19_SNG2__serine carboxypeptidase-like 19	4,422162	0,4451859	Undetermined	Undetermined
AT5G23020	IMS2_MAM-L_MAM3__2-isopropylmalate synthase 2	-0,2195775	0,115781	0,1433235	0,3627012
AT5G54060	UF3GT__UDP-glucose:flavonoid 3-o-glucosyltransferase	1,731333	0,0239073	-2,2567105	0,1498211

AT1G06000	UDP-Glycosyltransferase superfamily protein	-1,10588	0,0634529	-0,6159965	0,1302314
AT1G24100	UGT74B1__UDP-glucosyl transferase 74B1	-0,8091635	0,305823	-0,246813	0,0985367
AT1G65060	4CL3__4-coumarate:CoA ligase 3	-0,9533215	0,2217777	-0,9341755	0,0747447
AT1G78570	ATRHM1_RHM1_ROL1__rhamnose biosynthesis 1	-0,398716	0,0941796	-0,1136455	0,003375
AT2G35500	SKL2__shikimate kinase like 2	-1,126275	0,1366272	-0,3158115	0,0208915
AT3G21240	4CL2_AT4CL2__4-coumarate:CoA ligase 2	0,568726	0,1249571	-1,5621325	0,2854696
AT3G55120	A11_CFI_TT5__chalcone-flavanone isomerase family protein	-1,6539915	0,2100326	-0,044971	0,1753483
AT4G22880	ANS_LDOX_TDS4_TT18__leucoanthocyanidin dioxygenase	1,478491	0,2836234	-4,5279835	0,9815469
AT4G39540	ATSK2_SK2__shikimate kinase 2	-0,264259	0,1434776	-0,763739	0,0705509
AT5G10870	ATCM2_CM2__chorismate mutase 2	0,062958	0,0849334	-1,955037	0,1669083
AT5G23260	ABS_AGL32_TT16__K-box region and MADS-box transcription factor family protein	2,101927	0,3732491	Undetermined	Undetermined
AT5G54160	ATOMT1_OMT1__O-methyltransferase 1	0,761927	0,1522627	-1,7631125	0,2953691
AT1G15950	ATCCR1_CCR1_IRX4__cinnamoyl coa reductase 1	0,202727	0,2377873	-0,570704	0,0775145
AT1G30530	UGT78D1__UDP-glucosyl transferase 78D1	-1,5876055	0,02765	-0,4058135	0,0134159
AT1G66370	AtMYB113_MYB113__myb domain protein 113	0,146818	0,6103109	Undetermined	Undetermined
AT2G16720	ATMYB7_ATY49_MYB7__myb domain protein 7	0,170662	0,1154493	-0,799979	0,1750358
AT2G37040	ATPAL1_PAL1__PHE ammonia lyase 1	0,239998	0,0875059	-0,390686	0,0103931
AT3G21560	UGT84A2__UDP-Glycosyltransferase superfamily protein	1,543588	0,000775	-0,393516	0,0058761
AT3G59030	ATTT12_TT12__MATE efflux family protein	-0,8387565	1,5013496	-0,77467	1,5843435
AT4G31500	ATR4_CYP83B1_RED1_RNT1_SUR2__cytochrome P450, family 83, subfamily B, polypeptide 1	-0,1869605	0,206722	-0,9808825	0,222465
AT5G04230	ATPAL3_PAL3__phenyl alanine ammonia-lyase 3	-0,3192075	0,0314655	-0,53828	0,039079
AT5G11260	HY5_TED 5__basic-leucine zipper (bZIP) transcription factor family protein	0,1050375	0,0363304	-0,4170275	0,0314259
AT5G24520	ATTTG1_TTG_TTG1_URM23__transducin/WD40 repeat-like superfamily protein	-0,215958	0,0788891	-1,674156	0,1366413
AT5G60890	ATMYB34_ATR1_MYB34__myb domain protein 34	-1,474633	0,1854996	-0,977852	0,0779444
AT1G16400	CYP79F2__cytochrome P450, family 79, subfamily F, polypeptide 2	-0,5958585	0,0618188	0,1335445	0,0087872
AT1G34790	TT1__transparent testa 1	-1,55978	0,7465138	Undetermined	Undetermined
AT1G66380	AtMYB114_MYB114__myb domain protein 114	1,1831775	0,3015987	-1,739948	2,2276239
AT2G20610	ALF1_HLS3_RTY_RTY1_SUR1__tyrosine transaminase family protein	-0,8723515	0,1705492	-0,4137455	0,0039591
AT2G37260	ATWRKY44_DSL1_TTG2_WRKY44__WRKY family transcription factor family protein	-0,428698	0,4504412	-2,2834675	0,3877144
AT3G24503	ALDH1A_ALDH2C4_REF1__aldehyde dehydrogenase 2C4	-0,484211	0,1088266	-0,0664165	0,0798104
AT3G62610	ATMYB11_MYB11_PFG2__myb domain protein 11	-0,046992	0,4040139	-2,690686	2,241339
AT4G33510	DHS2__3-deoxy-d-arabino-heptulosonate 7-phosphate synthase	-0,289109	0,1987564	-0,112749	0,2335376
AT5G05260	CYP79A2__cytochrome p450 79a2	Undetermined	Undetermined	Undetermined	Undetermined
AT5G13930	ATCHS_CHS_TT4__chalcone and stilbene synthase family protein	-1,1421735	0,0299764	-1,9796455	0,3632301
AT5G35550	ATMYB123_ATTT2_MYB123_TT2__duplicated homeodomain-like superfamily protein	-0,553034	0,1147521	0,4520905	0,6040679
AT5G61420	AtMYB28_HAG1_MYB28_PMG1__myb domain protein 28	-0,7289735	0,1611164	-1,564989	0,1406181
AT1G16410	BUS1_CYP79F1_SPS1__cytochrome p450 79f1	-0,641772	0,0480479	-0,457333	0,1029491
AT1G48850	EMB1144__chorismate synthase, putative / 5-enolpyruvylshikimate-3-phosphate phospholyase, putative	0,570436	0,2029792	-0,2397365	0,2647924
AT1G66390	ATMYB90_MYB90_PAP2__myb domain protein 90	-0,966584	0,1041158	-2,6387265	0,6577034
AT2G21940	ATSK1_SK1__shikimate kinase 1	0,478307	0,0979244	-1,382551	0,1784893
AT2G40890	CYP98A3__cytochrome P450, family 98, subfamily A, polypeptide 3	0,263388	0,169584	-1,0085	0,2184621
AT3G26900	ATSKL1_SKL1__shikimate kinase like 1	-1,2379895	0,1252477	-0,9531285	0,0636559
AT4G03050	AOP3__2-oxoglutarate (2OG) and Fe(II)-dependent oxygenase superfamily protein	1,686859	0,1462042	Undetermined	Undetermined
AT4G34050	CCoAOMT1__S-adenosyl-L-methionine-dependent methyltransferases superfamily protein	1,206401	0,3689047	-1,523333	0,2441286
AT5G05270	Chalcone-flavanone isomerase family protein	-1,196448	0,1331496	-1,6741035	0,0089187
AT5G17030	UGT78D3__UDP-glucosyl transferase 78D3	Undetermined	Undetermined	Undetermined	Undetermined
AT5G42800	DFR_M318_TT3__dihydroflavonol 4-reductase	1,612345	0,0706852	-4,6200485	0,3002524

AT5G66120	3-dehydroquinate synthase, putative	-0,0381805	0,256778	-0,283577	0,4857937
AT1G17260	AHA10__autoinhibited H(+)-ATPase isoform 10	0,6662985	0,2145383	-0,8680335	0,6966579
AT1G48860	RNA 3'-terminal phosphate cyclase/enolpyruvate transferase, alpha/beta	-0,1437275	0,3536192	-1,121575	0,0906497
AT1G69370	cm-3_CM3__chorismate mutase 3	-0,069192	0,4653159	-1,9181105	0,2381896
AT2G22990	SCPL8_SNG1__sinapoylglucose 1	-0,2509185	0,0392027	-1,302055	0,014483
AT2G45300	RNA 3'-terminal phosphate cyclase/enolpyruvate transferase, alpha/beta	0,524849	0,1727632	-0,670604	0,1543798
AT3G29200	ATCM1_CM1__chorismate mutase 1	0,2709605	0,0427835	-1,055561	0,2358413
AT4G03060		-1,245189	0,0777139	-0,420127	0,116715
AT4G34230	ATCAD5_CAD-5_CAD5__cinnamyl alcohol dehydrogenase 5	0,7914775	0,0241442	0,168255	0,1252102
AT5G07690	ATMYB29_MYB29_PMG2__myb domain protein 29	-1,6591695	0,0194108	-3,086574	0,3088628
AT5G17050	UGT78D2__UDP-glucosyl transferase 78D2	0,321609	0,2576428	-1,4974655	0,1794432
AT5G48100	ATLAC15_LAC15_TT10__laccase/Diphenol oxidase family protein	0,458842	0,3203095	Undetermined	Undetermined
AT1G18590	ATSOT17_ATST5C_SOT17__sulfotransferase 17	-0,7081665	0,1643097	-0,1842715	0,0804157
AT1G51680	4CL.1_4CL1_AT4CL1__4-coumarate:CoA ligase 1	1,136457	0,0619058	-0,9449495	0,3516053
AT1G74090	ATSOT18_ATST5B_SOT18__desulfo-glucosinolate sulfotransferase 18	-0,756494	0,1384317	-0,2924825	0,1677887
AT2G26170	CYP711A1_MAX1__cytochrome P450, family 711, subfamily A, polypeptide 1	-0,4822415	0,0727493	-1,2956925	0,0794314
AT2G47460	ATMYB12_MYB12_PFG1__myb domain protein 12	-1,3995415	0,2520532	-1,467477	0,3928996
AT3G29590	AT5MAT__HXXXD-type acyl-transferase family protein	1,793516	0,8021066	-2,0392105	0,764765
AT4G09820	BHLH42_TT8__basic helix-loop-helix (bHLH) DNA-binding superfamily protein	0,6177415	0,1617726	-1,429673	0,2766258
AT4G34990	AtMYB32_MYB32__myb domain protein 32	2,5352215	0,0852467	-2,5300705	0,5300861
AT5G07990	CYP75B1_D501_TT7__cytochrome P450 superfamily protein	0,342687	0,0405328	-1,4344255	0,1519933
AT5G17220	ATGSTF12_GST26_GSTF12_TT19__glutathione S-transferase phi 12	1,420883	0,1493791	-3,004634	0,5426748
AT5G48930	HCT__hydroxycinnamoyl-CoA shikimate/quinate hydroxycinnamoyl	Undetermined	Undetermined	Undetermined	Undetermined

Supplementary Table 3. Sequences of primers and oligonucleotides.

myb112 T-DNA insertion lines	
SALK_LP	5'-GCAAGAGTCGGTTTTAACAAAAAC
SALK_RP	5'-TTAGATGAGAGGGCCAAATCC
GK_LP	5'-AACGTCTCAATTTCACATGGG
GK_RP	5'-GGAGTTCCATCTTCCTTCACC
LB	5´-GCGTGGACCGCTTGCTGCAACT
***MYB112*-IOE**	
MYB112-IOE-fwd.	5'-**TCGAG**ATGAATATAAGTAGAACAGAATTCGCA
MYB112-IOE-rev.	5'-**ACTAGT**CTACTGTATGAGCCACTTGTTGA
***MYB44*-IOE**	
MYB44-IOE-fwd.	5'-AGTCG**CTCGAG**ATGGCTGATAGGATCAAAGG
MYB44-IOE-rev.	5'-TCATC**ACTAGT**CTACTCGATTCTCCCAACTC
***ProMYB112*:GUS**	
MYB112:GUS-fwd.	5'-**GAATTC**GAATAGGGGGAGTATTATTTTTGAA
MYB112:GUS-rev.	5'-**CCATGG**GCTTTGAGATTCTTAGAAACTTGTG
MYB112:nested-rev.	5'-TCCATGGACCTCTCCTTATTTCT

MYB112 CELD	
MYB112-CELD-fwd.	5'-GTATAA**GCTAGC**AATATAAGTAGAACAGAATTCGC
MYB112-CELD-rev.	5'-CATGTC**GGATCC**CTGTATGAGCCACTTGTTGAG
MYB112 GST	
MYB112-GST-fwd.P1	5'-TCA**CCATGG**ATGAATATAAGTAGAACAGAATTCGC
MYB112-GST-rev.P2	5'-CACAGTCCA**C**GGACCTCTCC
MYB112-GST-fwd.P3	5'-GGAGAGGTCC**G**TGGACTGTG
MYB112-GST-rev.P4	5'- GTCC**C**TGGGGATCCGGCTGCTAATGA**CTCGAG**AGTAAC
Pro:Fluc	
MYB32:LUC-fwd.	5'-**CACC**CTTATTTCAAAATATCCCC
MYB32:LUC-rev.	5'-CTTTCTTCTTCTGATTCTTGTG
MYB7:LUC-fwd.	5'-**CACC**GCGTGTGCATCAACTAT
MYB7:LUC-rev.	5'-AATCAAAGTTAAGGTGTATATTGG
MYB6:LUC-fwd.	5'-**CACC**CACTTGGATTTCCTCTC
MYB6:LUC-rev.	5'-GTGAATGAAGAAGATGGTGTAAG
ChIP-qPCR	
At3g18040-fwd. (neg. 1)	5´-CTATCTTCCGCATCCTTCGGA
At3g18040-rev. (neg. 1)	5´-TCTCAGGTATGGCGTGCTTCTC
AT2G22180-fwd. (neg. 2)	5´-GTTGCGTATGAAGATGACGTGG
AT2G22180-rev. (neg. 2)	5´-GCCGAGTTAACGACGTGCTTAT
MYB6_1-fwd.	5'-AGGAGAAAAAGTAAAGAGACAAGAAAA
MYB6_1-rev.	5'-TGGAGATAAAGTGAGGCTGTGC
MYB6_2-fwd.	5'-CACAACACAGCAAAGCACAGCC
MYB6_2-rev.	5'-CCCATGGTGAATGAAGAAGATGGTG
MYB7-fwd.	5'-TCAAAATAATTGCAAAAGATGCCCA
MYB7-rev.	5'-TAACCAGACCCGGCCCAACATA
MYB32_1-fwd.	5'-TGGAAGGTCACGAACCACTCCC
MYB32_1-rev.	5'-ACACAAACAAGGTTGGTTTTGAGGG
MYB32_2-fwd.	5'-ACTTAATTTGGTCATTTGGATGCCC
MYB32_2-rev.	5'-TGGATGGTTTCGTACTGCAACG
UGT84A2-fwd.	5'-TTGCGCAATGAACATAAACA
UGT84A2-rev.	5'-GGTTGAGAGCTACACCTCAACTTT
EMSA probes	
Labeled probes	
MYB6_1-fwd.	5'-AGGTTACTTACT**TACCTACCTAAT**CTCCATTACCCCAC
MYB6_1-rev.	5'-GTGGGTAATGGAG**ATTAGGTAGGT**AAGTAAGTAACCT
MYB7-fwd.	5'-TGCCCAAAAAAAGTTT**TACCTAAC**AAAAGGTCCAAAAAAA
MYB7-rev.	5'-TTTTTTTGGACCTTTT**GTTAGGTA**AAACTTTTTTTGGGCA
MYB32_1-fwd.	5'-TGCAGCCAAATCTAC**ACCAAAC**CGTACCCAAAAATGAAAT
MYB32_1-rev.	5'-ATTTCATTTTTGGGTACG**GTTTGGT**GTAGATTTGGCTGCA

MYB32_2-fwd.	5'-CCTTTACAACCTCCT**TACCAAAC**TCACTATGGCAAATATA
MYB32_2-rev.	5'-TATATTTGCCATAGTGA**GTTTGGTA**AGGAGGTTGTAAAGG
Unlabeled probes	
MYB6_1-fwd.	5'-AGGTTACTTACT**TACCTACCTAAT**CTCCATTACCCCAC
MYB6_1-rev.	5'-GTGGGTAATGGAG**ATTAGGTAGGT**AAGTAAGTAACCT
MYB7-fwd.	5'-TGCCCAAAAAAAGTTT**TACCTAAC**AAAAGGTCCAAAAAAA
MYB7-rev.	5'-TTTTTTTGGACCTTTT**GTTAGGTA**AAACTTTTTTTGGGCA
MYB32_1-fwd.	5'-TGCAGCCAAATCTAC**ACCAAAC**CGTACCCAAAAATGAAAT
MYB32_1-rev.	5'-ATTTCATTTTTGGGTACG**GTTTGGT**GTAGATTTGGCTGCA
MYB32_2-fwd.	5'-CCTTTACAACCTCCT**TACCAAAC**TCACTATGGCAAATATA
MYB32_2-rev.	5'-TATATTTGCCATAGTGA**GTTTGGTA**AGGAGGTTGTAAAGG
Imap	
MYB32-300-fwd.	5'-**CGGATCCCTCGAGCTGCAGC**GTTTGAAAAAACCATAAAAGCC
MYB32-300-rev.	5'-CTTTCTTCTTCTGATTCTTGTG
MYB32-600-fwd.	5'-**CGGATCCCTCGAGCTGCAGC**TCAAACAAATTTATTATTTGCGATA
MYB32-600-rev.	5'-CTGAGTCTAGTTGTCTACTTA
MYB32-900-fwd.	5'-**CGGATCCCTCGAGCTGCAGC**GATTAACCAAAAAAATTATCAAAC
MYB32-900-rev.	5'-GCTAGGGTTGTAAAAACAAAAG
IRD adapter	5'-CGGATCCCTCGAGCTGCAGC

AGI	Annotation	PrimerFwdSequence (5´-3´)	PrimerRevSequence (5´-3´)
AT3G48000	*MYB112*	GCCACCGCAATCTGCAACTTTTC	AACTCCCTCTCTCGTTCTGCTGGA
AT2G16720	*MYB7*	TGGCTGGATCAATCCCTTTGCTC	GGCAACAAGTGGTCTTTGATTGCG
AT4G34990	*MYB32*	GCCTTCTCGGTAACAAGTGGTC	TCTCGTTGATAGGTCGATGAGTCG
AT4G09460	*MYB6*	ACTCTTGGGTTTGGATCCTGGTC	TCGCACCACGGTTTAGAATCAGC
AT5G67300	*MYB44*	TTCAAGCCTGTGCCTAGACCTGGT	AGACGACGTTTCGATAGGAAGCGG

Flavonoid platform primers:

AGI	PrimerFwdSequence (5´-3´)	PrimerRevSequence (5´-3´)
AT1G03495.1	ACGTGGATTGCAGGAATCGTCTC	TGCATCTGAAGCAGCCATGACG
AT1G03940.1	TGGTGACTCTAGCTTTCATTTGGG	GTCTTCCTCGTTGGCCTTTGTTTC
AT1G06000.1	TTCTTGAGCATCGAGCCGTTGG	TCCGACCATTCCTTCCAGAACC
AT1G15950.1	ACGTTATCTCCTAGCCGAGAGTGC	GGGTTCTTCTCGTCCTTGCACTTG
AT1G16400.1	AGCGCTCATTATGTCCCACCTC	ACATGAATGTGGCTACCTTTGGG
AT1G16410.1	CATTATGTCCCTTCCCATCTTGCG	ACATGAATGTGGCTACCTTTGGG
AT1G17260.1	TGCCTTCATTCTTGCTCAACTTGC	AGCAAAGCTGATGTTGGCATACAC
AT1G18590.1	AGGACACGTTTGTGTCGATGTGG	TGCTAACCACTGGTCCTTGTTGTG
AT1G22410.1	ATCAGAGAAGTGCGACGTGCTG	AAGAAAGCTCTCACTTCAGCCAAG
AT1G24000.1	TTTCGTTGAGGACACGAATCGC	ACAGCCTCGATTTCCGTCTTGC
AT1G24100.1	ACGTTGGAAGGGGTTGAGTTTGGG	TCTGATCACTCCACTGAGGCACAC
AT1G30530.1	TCCTCATGGCTGCTTTGCTTGG	ACGGTGCCGAAGCTAATGTACG
AT1G34790.1	CGCTACAACAATCTTCAGATGCAC	CACCCTTCAACGCAGCAGTAAC

107

AT1G48850.1	TCCTTGTGTTGTTCCACGAGCTG	ACAAATGGCATTGTGCGTATTGCG
AT1G48860.1	GGTGGCAACGCAAGTTATGTCC	ACGAACAGGAGGGCAGTTAGTG
AT1G51680.1	AGGCTTTGCTCATCGGTCATCC	CCAGCTGCTTCTTCTTTCATTGCG
AT1G56650.1	TCCTGTAAGAGCTGGGCTAAACC	CCCTAGAAGCCTATGAAGGCGAAG
AT1G61720.1	TCCATGTCGCAACTCCGATCAAC	GCCGGCTTGATCATGTCTTTCTC
AT1G65060.1	CGCGGTCAACAGATCATGAAAGAG	TGTGTGAAGCCAACCTTCTTCGTC
AT1G66370.1	GCGAATCACCCAAAGGGTTGAG	TTTCGGCACCGATTGAGACCAG
AT1G66380.1	GTCCTTGATTGCTGGTCGATTACC	ACACGGTTCATGCTTCTTACTCAG
AT1G66390.1	AGGGTTCGTCCAAAGGGTTGAG	TGCATCGATTTAGCCCAGCTCTC
AT1G69370.1	ACGAGCTCAGTATCGCTACAACG	GACTCTTGTACCTGTCCACCTTTG
AT1G74090.1	TCAAGCACGACCCAGTGACTTC	TTTGAGCCAAGTGGTGCCTGTC
AT1G74100.1	ACCCACTCCTCAAACGAAACCC	AAACGCGAAGTCGATCTCAACG
AT1G74710.1	GCTTGGCTAGCACAGTTACAGC	CACTGCAGACACCTAATTGAGTCC
AT1G78570.1	AACCAAAGCCATGGTCGAGGAG	TTGCGCGGGTTGTTTAGATCCG
AT2G16720.1	CTCCTAGGCAACAAGTGGTCTTTG	AGTGGCTGGATCAATCCCTTTGC
AT2G20610.1	CCGGCAAAGGCAATTCTTACGG	TCATATAATCAGCAACGGCTCGTC
AT2G21940.1	TGTCCAAAGTGCTCGGTTATACG	GCTTCTTAAGCGCATCGGTCTC
AT2G22990.1	CAAATCGCTGGATACACGAGAGC	CCGTGTGTCCACCTCCTTTGATAG
AT2G26170.1	GCAGAGCTTTGCAGAGAAGTTGG	AGACCATCTCTTGTCCCTGGTG
AT2G27820.1	CGTCACGCGCTTTGTGATGTTG	TCGTCTTAAACGGCCGATCAGTTC
AT2G30490.1	AATGTCGCCGCGATTGAGAC	TCAGGATGGTTCACTAGCTCTGC
AT2G35500.1	TTCTTGCAGAAGGGCCGGATTC	AACAGTACGCACATGGCTGCTC
AT2G37040.1	GCAGTGCTACCGAAAGAAGTGG	TGTTCGGGATAGCCGATGTTCC
AT2G37260.1	CCGTCTCTGCATTGGCTAATATGC	ACCTGCTCGATGTGTACCTTGG
AT2G40890.1	ACAGCATTTCGTTGATGCGTTGC	CCCTGCCGTGATCATATCCCATAG
AT2G45300.1	GCTTCCTGGCTCCAAGTCTCTATC	TGTCCACTACAGTTGTTCCCTCAG
AT2G47460.1	GCATTCCACTTTGGGAAACAGGTG	CGGAGACGTCTTGAGAGATGGATG
AT3G06350.1	ATGAGAGACGGGATGTGCTTCG	TTTGATGAACTCACTTGCCACCTG
AT3G19450.1	TCTCGACCCTTACTTGGCTTGTC	TTCCTCCCAAGAATGACGAGAGG
AT3G21240.1	TGATCTGAGCTCGGTTAGGATGG	TTCTGTCATCCCATAGCCCTGAC
AT3G21560.1	ACGATGGAAGCTGTGTCTTCCG	TGTAAACGGCGTCCGTGACTTG
AT3G24503.1	ACGACGCTGATATTGACAAAGCC	CGCCACGCAAATTTCACCCTTG
AT3G26900.1	TGTGTCTGCTCAAGCTTTGAAGG	AGCTGCTTCAGCACTTCAGTCTC
AT3G29200.1	TGTGACGCTATCTGCCTTCAGTG	TGATGGCGGACTCGTATGCTTC
AT3G29590.1	TGCATGGTGAAGATGCGTGGAG	ACCGTGACCGAAAGTCTGATGC
AT3G50740.1	TGAAAGAGACCGCTGCCGAATC	ACAACGATTCATGCGCCACTCC
AT3G53260.1	ACGTACCCGTTGATGCAGAGAC	AGTCTCACCGTTGGACAAAGCG
AT3G55120.1	ACGCCGTTCCTTCTCTATCTGTC	ACGCACCGGTGACTATTTCACG
AT3G59030.1	TGGTCTAAGTGCAGCAATCAGTG	CGGAACACAAGCACGATGACAC
AT3G62610.1	GCATTCCACTTTGGGAACCAGGTG	TCGACGGTATTGGCGACAGTTG
AT4G03050.1	TTGCGGGAGATGCTCTATGTGC	TACTCGGTGATACGGTGAAGGG
AT4G03060.1	TTGCCGGAGATTCCCTATGTGC	TTGCTGCTGTGTATCTTGTCCTC
AT4G09820.1	AAGACGGCGGTTCAATCTGTGG	ACACCAAGACCCGTTGTTGAGG
AT4G13770.1	AAGAGAGTCAAGCCCGAAACCG	GTTCCCGCCACTACAATATCCAAG
AT4G14090.1	GTTGCGTTTCCGCAGTTTGCTG	TCCAATCCTCCACGTATCCTCCAC
AT4G22880.1	TTGGCTAACAACGCGAGTGGAC	GCGTACTCACTCGTTGCTTCTATG
AT4G31500.1	TGGATATTGTTGTGCCGGGAACTG	ACACTCCTCACTTCGTCTTGAGC

AT4G33510.1	TGGGTGTTGTTCTCATGTTCGG	ACCAGCCATTCTTCCCACCTTG
AT4G34050.1	CTTGATGAAATCGTTGCTGACGAG	GTGTTGTCGTAGCCAATCACTCC
AT4G34230.1	TCACTCCTCTGCTTATGCTTGGG	GCATCTCCTCTGTCTCCTTCATGC
AT4G34990.1	GCCTTCTCGGTAACAAGTGGTC	TCTCGTTGATAGGTCGATGAGTCG
AT4G36220.1	GGTCTCTTGTAACGTTGGTAAGCC	ACGCTGCCCGGTAAGTTATGTTG
AT4G38620.1	AAACTTCACCGAGGAAGAAGACG	CCCGGCAATAAGCGACCATTTG
AT4G39540.1	GCGGCTTTAAACCGTCTTTCAACG	TTGCGCTGGCTTTAGTGTATGC
AT5G04230.1	AGCTTTAGCTGAACCGGAAGGC	AATTTCAGCTCGGCCTCGAACG
AT5G05260.1	AGATCAAAGCACAAGTGACGGAAC	TGCCGCGTTAGACGGATTATCAAC
AT5G05270.1	ACTGAGCTCGAGAAGGTCGTTG	ACCTTCCGTCTCAAACCCGATCTC
AT5G07690.1	AGTTGTAGATTGCGATGGGCTAAC	TGTCTCGCTATGACTGACCACTTG
AT5G07990.1	TGTCTTTGCACCTTACGGACACC	AGCGTTCCAACCTCTTCCTGTC
AT5G08640.1	CACCTGAATACAGGGAGGTGAATG	TCAACGCATCACGCTTTAACCC
AT5G09640.1	TGCCACCTCCTAGCTGCTTTAC	TTTGGCTGTTGCATCGGTTCC
AT5G10870.1	GTGATCTCGCCTGTTTACAAGCTC	ACGTCAACAGCTTCATCAAAGCC
AT5G11260.1	AGAACAAGCGGCTGAAGAGGTTG	TCCTCTCTCTTGCTTGCTGAGCTG
AT5G13930.1	TTCCGCATCACCAACAGTGAAC	CGCACATGCGCTTGAACTTCTC
AT5G17030.1	TCGTGGGTTGCGTACTATGGAG	CGCTCACCTACTTCTTTGACACC
AT5G17050.1	TCTTCTGGTTCGCGGCTGATATG	CGCTCACCTACTTCTTTGACACC
AT5G17220.1	ACAGGTAACAGCAGCTTGTCCAC	CTGGAACTTGACCAAATGGCTGAC
AT5G23010.1	AAGTGGCAATGCGTCGCTTGAG	AGCCCGTGTACTCTTGAACCATC
AT5G23020.1	TGCTACCGCCAACACAATATCCG	ACATTTCAAAGCCATCACGACCTC
AT5G23260.1	CTGCTCCGAACAGAACAGGATG	TCAGGAAGTCGCAATCCGTTGG
AT5G24520.1	AGCTCCTTAGAGTTTGAGGTGCAG	GCGCAAACCAAACCTACTTACGC
AT5G35550.1	ACTCTCCCTAACCAAGCTGGTCTC	CCCGGTCTTAGGTAGTTCTTCCAC
AT5G42800.1	AGGAAGGAAGCTACGATGATGCC	TGTCGGCTTTATCACTTCGTTCTC
AT5G48100.1	TGCATTGGCATGGTGTAGAGCAG	CGGGCATTGTGTGATGTATTCAGG
AT5G48930.1	AGGCGAAATCCAAGGAGGATGG	ACACATGCCCTGCCAACATCTC
AT5G49330.1	GCATTCCCTTCTCGGCAACAGATG	ATCTCCGGAAACGGCAGTGAAG
AT5G54060.1	TGGAGGTTGGATTCAGCAACCG	ACCCAAACCCGCAATGGCTAAC
AT5G54160.1	TGGTGGCATTGGTGCTACACTC	CTCCTCCAACATGCTCAATACCAG
AT5G60890.1	AGACCCGACATTAAGAGAGGAGAG	ATTGCGGCCCACTTGTTACC
AT5G61420.1	AGACTGCGATGGACCAACTACC	TCTCGCTATGACCGACCACTTG
AT5G66120.1	TGGGTCATACCTTTGGCCATGC	TCCATGGAGCCACTCTCCATAACC

Hypoxia platform primers:

AGI	PrimerFwdSequence (5´-3´)	PrimerRevSequence (5´-3´)
AT1G19530.1	AGGTGCAAGTCGCTCACAAGAG	TGGCTTTGTGCACCTTCCTGAG
AT1G33055.1	TGATGAAGGAGTACACGGTGGTTC	AAGGAAGAAGAAGAGGGAGAGAGG
AT1G35140.1	CTACGCGGTTAACGTCGTGTTG	TGTGACCCGCATCTGTTCATGC
AT1G43800.1	ACCAATGTTGGCAACCCGCTTC	TTTCCCTCAGCTCACGAACCTG
AT1G72360.1	AGCCAAGGCTAAGACTGTGCAAC	AGCTTACCACCGCCACATCAAG
AT1G76650.1	AAGAGGGAAGATTCAGCCGGAGAG	CTCTGTTCTTGTCCTCACCATTGC
AT1G77120.1	GCATTTGAATGTGTCCACGATGGC	GAAGGCATCGTCTTTGCTTGGC
AT2G14210.1	AAGAGGAGCAGCATCAACTTCTG	TCCTCTCCCACTAGTTTCCTGTG
AT2G15880.1	TTGTTCCAACACTCACCGATGC	AACGTCAAGAGCTGTCGCTGTG

AT2G16060.1	AGAGACTTGGAGCCAGCCATTC	ACAATGCATACTTGGCCACCTC
AT2G17850.1	AACCAAACCGATCATCTCATCCTG	TACAGTCTTGAAGCCGGAAGAAAC
AT2G19590.1	ACCAGTCAGAGATGGTCAAGGC	TCATCCATCGTCTTGCTGAGTTCC
AT2G26150.1	GCAGCGTTGGATGTGAAAGTGG	TTGGCTGTCCCAATCCAAAGGC
AT2G26400.1	GGACTCGGACAACTATATGAAGGC	TAAGCAGTCCACACTGGTCCAC
AT2G32020.1	ATCGTGTCCTGACACACCCTTG	CGATTGGACGGTCGTCTTCTAAGC
AT2G34390.1	CGTCACAACCACCAAGAGAACTAC	AGTGCAGGTCCTATGCTTCTGG
AT2G47520.1	AGAAGCGTAAACCCGTCTCAGTG	AGCCAGACACGTACACCTTTGC
AT3G02550.1	GAAGCGCAAGCTAACGCAACTG	ATCCCAGGACGAAGGTGATTGG
AT3G03270.1	ATCTCCTTGAAGACGGCGACAC	CCTCCAAAGGAATTAGCGGTGAAC
AT3G09940.1	TTGAGCGTCCTGAACTAACCAAGG	TTGCAAGGGTCGGATTGACTTCG
AT3G10040.1	CATGACCAACAACCACCGCAAC	TTCTGCTGCTGACTCGGAATCG
AT3G27220.1	TATGTGGTTTCAGGGCAGCTTGG	TGAGTCGCAGGAGCATACCTTG
AT3G29970.1	ACCCTCTTCTTGGAGCAATGGG	TCTGCAGTCAGGGTTTAAGAATGC
AT3G43190.1	AGAGCGTTTGGATGCAACTCTTG	TTTGCCTTTGGCTTCAACCCTTG
AT3G47720.1	TCGTTTCCGGTCTTAATCAACTCG	ACACCGCGAGATTCTCCTATCTTG
AT4G10270.1	ATGGACAGTGGCAGTGAGCATC	GTTCCACCGACAAAGACCTAGTTG
AT4G14980.1	GCTATCGGCTGCACAAAGACTG	TGAGGTGATTTGTTGGGCATGGAG
AT4G17260.1	TCCACCCGGTTACTGTTCTTGC	AAGCAAAGCCGGAAGACTGAGG
AT4G17670.1	TCTTGGACTCTTGCTTCCTCTGC	CACTACAGAACGGTGTGTCTCCTC
AT4G24110.1	AGCTGCTTTCGAGCTTGATGGG	TCTGTGAAGCGTCACGAAAGCTG
AT4G26270.1	GAGGTGGTCACGATACCACAAAG	CAGGCCACGTCTTCTAATTTCCTC
AT4G27450.1	CATGTCTTTCGGACAAGCTGCTG	ACAACCTCTGGTGGATGGAGAAG
AT4G32840.1	GCACACCTACATTCCCTTTAACCG	ACATTCGCGCCCACATTCTATCTG
AT4G33070.1	CAATTGCTGGACTGCAAAGGTG	AGCAACTCTTTGCTCGTATCATCC
AT4G33560.1	TGTCCACCACACCCTTTGAGAC	TGGGACCAAAGCAGCTAAGACC
AT5G10040.1	AGTCACGTTTGAACCTCATGCTG	TGCCCTCTGGTGATTAGAGAAGC
AT5G15120.1	ATTGGGTGGTTGATGCTCCAATG	ATGCATGTTCCCGCCATCTTCC
AT5G19550.1	TGTTGGTGCCCTTAGCATTGTCTG	AAGCTTCACCTGGCTCTCAACC
AT5G20830.1	ACAAACCCGGAAGAAACTTGAAGG	GTGGCAACACAATTGCTTCCTGAG
AT5G23990.1	AGCAACCCTCCCAAACTCAAAGAG	TCAACTCTGTGGCTGTCACTATCC
AT5G37260.1	TGCAACCATGGCTATGCAGGAAC	ACTTCTCATGCTCTGCTTCTGTCC
AT5G39580.1	GCGATCTCGTCACTCTTGTTGGAG	TAAACCCACATGCAGCTGTTCCG
AT5G39890.1	GCAAATCTGGTACCGTCCCTTC	ACATCCTCAGGCTTGATTTCATCC
AT5G42200.1	ACGGAATGTGCTGTTTGCCTTG	TTGCAACCGGGAACTAGACGAG
AT5G44730.1	CTTCCTTCGGTTTGAGCAAGGC	GGCGCAATATTATTCCCGGCTCTC
AT5G47910.1	ATGATCAAGGTGGCTGTTTACCC	ATCCTTGTGGCTTCGTCATGTG
AT5G54490.1	GCAAAGGGTTCGAGCTTCTTATGG	CGTCGATGCGTTTCTTCGTAAGC
AT5G54960.1	ACGGATCAATTGGCTGGTCAGTG	ATGACACGCCTGTTTGGCATGG
AT5G62520.1	AAGAGGCGGTGCAGATGAAACAC	TTTCGAAACAGAGCACCAACCG
AT5G66985.1	TGCGACTTCGAAAGGAGAGGAG	TCAGGTGTAGCTGCTTGGACAC

Supplementary Data 1. Sequences of promoter fragments of *MYB6*, *MYB7* and *MYB32* (-1kb) and UGT84A2

```
>MYB6 promoter fragment
TCCTTCATACGACGTCGTTCTTTTGTTAATTTTAAATTTAATTAATGGGAAAAATGTCATTAAAATCT
TCAACTCATTGCAAACATTGATTTAAATCCTCAACTCTCGACGAAACAAAATAAATATTTGACTTTCT
AAATAAATATCTAATTTTTGTTGACCTGGCGATATTAGACACACTGTTAAGTAAATTACTAGATCCCG
TTAACGGAGTTAATTTTTTTGTTAACAGAGGCCCATTAATGCAAACGTTATTGTTTCCAACAACAGA
GTGACGTCGTTTTGTAATAATGACTGAACTAAATTCCCAAATTCAATCTAAGATCTCTAAATCAAGCA
AAATTCCTATCTCTAAATCCCCATATGATTTGAAACTGGAGATTTAATTGAGCCGTTATGACAAAAAC
```

GATGACGTTTTATTGTTAGAGTAAACGTTGTCGTTTTCAATCAACGAGTATGTTAACACACTAAACGT
TCAAGGTCTATTAACCTACTGAACATCATGCCTAATATAGTCATGTCAACAAAAGTTTGATATTTATT
TGAAAAGTCAAGAAGTTTTGGTATTTATTTGGAAAGTAACATAAGTTTGATATTTGTTTCGTTCGCCG
AGAGTTCAAGATTTAAATCAAAGTTTTCAATAAGTTGAGAATTTTAATGACATTTTTTTCCAAAAGAT
AACATGTTTGATAAATATTATTTTTGCATTGTATTTTTCTTAACTACCAACTAAATTATAAGAACAGT
GAGAGAAAGAAAAAAACAAAAACCAAAATCTAAGGAGAAAAAGTAAAGAGACAAGAAAAAAAGAGAAA
AGAAGGTTACTTACTTACCTACCTAATCTCCATTACCCCACACACAACACAGCAAAGCACAGCCTCAC
TTTATCTCCACATAGTCACATGTACATATACCAAACTTAGTCAAAGTCTCCTCCTTTTTATATAACCC
ACAAATTGATCTCTTCTCTCTTCTCTTACACCATCTTCTTCATTCACC*ATGGG*AAGATCTCCTTGTTG
CODING SEQUENCE INDICATED WITH ITALICS

>*MYB7* promoter fragment
GATTATTAATACAAACCTGTACAAGTTTTTGAACGAGTAAAAAATCATAAGTAATTCAATAATAGTTA
AAAACAGTATAAAATAGGGGTATGAGTCACGAAAAAAATTCGAATGGTGACCGAATCGCACATTAATA
AAATTCTCTGCATATATATATATATATATTTGTTATTATTTGAACTGCACCGCACTTTATCCGCAGTT
GAACTGCATGTTTCCATTAAGACTCTGAGAGTAATATATATGATAAAGCTTTTATTTATTATAATCAG
GCTCGACTCATTAGGGTGGAGCGAAAGTGCGACGGTCCAAACCTTATGCCTATTTAAAAAAATTTACA
TAAGAAAAAGTTTTTTATTTTTTGGAAAAAAAGTTGTCAAAATATAATTGATAAAATCCCCAAATTT
CTTTAAAATATATATTAAAAGGCCCTGATTTTATTTCTAAATGACTTTTATATACCAAAGAGCCAATA
TTTTTGTAAAATGTTAAAACACTCAAGATATACTTCAAAATAATTGCAAAAGATGCCCAAAAAAAGTT
TTACCTAACAAAAGGTCCAAAAAAAAGCAAACATTTACCCTAAGACTCAAATTTATGTTGGGCCGGGT
CTGGTTATTATTAAAACGATCAAAGCTAGTGTTTTGTTAAACCGCAATTTTGTAGCATTTCATATGTT
AAGATTTGATGGTTGAAAGGAAAACAAAAATTGTGAATAATAATGGTTATGAGATCTAAAACATCAAA
GGAAAATCAAGAAGAGAAAGGTATAAAATATTGAATAAATAATATGAATGTGGCAGTTATAGTTTGAT
GTAGAATAAAGATTAAACAAAAATCAAGAGCCCCACCAGCCACTCCTTCAAACGTGTCCTACCAACT
CTCTTCTAGAAGCAATTAGGCTCACCTTCCACCTCCAACACCTCTCTCCCCTTCTCTCTCCATAAAAC
CCTCAACAACAGAATCAAAAGCATCATCATCATCAGAAGAAGAGAGTC

>*MYB32* promoter fragment
tatacgaaacgatttgttgagatatgttttaacacttcttaaaggaagtaggataaagtggaaggtca
cgaaccactccccatattGCAGCCAAATCTACACCAAACCGTACCCAAAAATGAAATTAACTTTCCCT
CAAAACCAACCTTGTTTGTGTCTTCTAGATTAATCCTCCAAACTTTTTGATTAACCAAAAAAATTATCA
AACTAACATGTTCTCCTTTTTTCTTTAGAAATTCTAACGAATTTATCTTTATACTGATTTGAATATAC
TTAATTTGGTCATTTGGATGCCCTTTACAACCTCCTTACCAAACTCACTATGGCAAATATATACTATT
TTCCATTGTAACATAAATGTCCATAATTTGAATTAAATTCGTTGCAGTACGAAACCATCCAACTTTGT
CCAAAAACAAAATCCTTATAACTATTTACTTTAATGTAAATATATCCTCTACTTTTGTTTTTACAACC
CTAGCTCAAACAAATTTATTATTTGCGATATAAAATCATATCGAACAAACTCGATGATTTTTTTTTTC
TTACGTTATTAATGAAACTAAAATATAGAAAAAAACAAGATGAACCAAATTTTCACCTATCTAACTAC
TTAAATATAATATGATTAAATTTGGTAAAGTTTGAAAAGTTTCTTTAGGAAATGTGAAATATTGATCA
CAGTTTCTATTGCTAAAATCACCAACAAAACGCATGTCGCCATTCATAATTATGGTTTCACACCTACA
ACTAGGCTAATAAGTAAATAAGTAGACAACTAGACTCAGGTTTGAAAAAACCATAAAAGCCATATAGC
GTTTTCTCATTGAAACTGCGAACACGATCGTGTGAATGTTGCAGTTTCTAGTTTTGATACAAACAAAC
AAAAACACAATTTAATCTTAGATTAAAAGAAAAAAGAGAACGGAGCCCACTAGCCACTCCTTCAAAC
GTGTCTTACCAACTCTCTTCTAGAAACAAATTAGGCTTCACCTTCCTCTTCCAACCTCTCTCTCTCTC
TCTCTTTCTCAAACCGTCTCTCCATAAAGCCCTAATTTCTTCATCACAAGAATCAGAAGAAGAAAG
promoter upstream of -1kb indicated with small latters
PRIMERS USED FOR Imap ARE INDICATED WITH COLORS (MYB32-300: blue, MYB32-600:
orange, MYB32-900:green)

> UGT84A2 promoter fragment (MYB112 BS at the position -1639 kb)
TAGTCAAAGTGTATTGCGCAATGAACATAAACACAACAATATAACAGACCTTTTTAGTGGTAAGAATA
CCCTTTTGGATATTGATATGAGTTTCAAGTTCAAAATCTTCGGTTGAAAAAAAGGAATAAATAATGTC
TTATAATGGTTTGTTACCTAACTAAATAATTAAAGTTGAGGTGTAGCTCTCAACCAATACATTTTTTT
ATAATATTGTTTCAATAATTTAAAGTAGTTAATTATATTCAATAGTATTTATTATCACTTAGTTTTTT
TTATTTATAAATTTTATCGATTAATCTGGTTAGTTTTAGTAGAAACGTATCAAAATGTTTTTACAGTGG
ATTTTTCCCCGAAAAACCATCACAATGTCGGTCCT(...)

111

MYB112 BSs indicated in yellow
sequences used for EMSA assay underlined
sequences of primers used for ChIP-qPCR indicated in various colour

Deutsche Zusammenfassung

Transkriptionsfaktoren (TFs) sind ubiquitäre Regulatoren der Genexpression und spielen eine essentielle Rolle in nahezu allen biologischen Prozessen. Diese Doktorarbeit hat vor allem die funktionelle Charakterisierung von *MYB112* zum Thema, einem Mitglied der R2R3-MYB-TF-Familie aus der Modellpflanze *Arabidopsis thaliana*. Ausgesucht wurde das Gen aufgrund seiner erhöhten Expression in seneszenten Blättern, basierend auf vorangegangenen qRT-PCR Expressionsprofilierungsexperimenten für 1880 TFs in *Arabidopsis* Blättern. *MYB112*-Promotor-GUS-Fusionslinien wurden generiert, um das Expressionsmuster von *MYB112* detailliert zu untersuchen. Unter Zuhilfenahme transgener Ansätze in Kombination mit *Metabolomics* und *Transcriptomics* können wir zeigen, dass *MYB112* eine wichtige Rolle in der Regulation des pflanzlichen Flavonoid-Metabolismus spielt. In *MYB112* Überexpressoren und *MYB112*-defizienten Mutanten kommt es zu erhöhter bzw. verminderter Anthocyanin-Akkumulation. Expressions-*Profiling* zeigt, dass MYB112 einerseits als ein positiver Regulator des Transkriptionsfaktors *PAP1* fungiert, was zu einer erhöhten Anthocyanin-Biosynthese führt, andererseits als negativer Regulator von *MYB12* und *MYB111* auftritt, welche beide die Flavonol-Biosynthese kontrollieren. Wir haben früh auf MYB112 reagierende Gene durch eine Kombination verschiedener Ansätze identifiziert. Diese umfassen Genexpressionsprofilierungs- (Affymetrix ATH1 Microarrays und qRT-PCR) und Transaktivierungs-Experimente in Mesophyll-Protoplasten aus Blättern. Wir zeigen, dass MYB112 an ein 8-bp DNA-Fragment, welches die Kernsequenz (A/T/G)(A/C)CC(A/T)(A/G/T)(A/C)(T/C) aufweist, bindet. Mit Hilfe von *Electrophoretic Mobility Shift Assay* (EMSA) und Chromatin-Immunopräzipitation gekoppelt mit qPCR (ChIP-qPCR) zeigen wir, dass MYB112 *in vitro* und *in vivo* an die Promotoren von MYB7 und MYB32 bindet, was sie damit als direkte Zielgene von MYB112 identifiziert. Es wurde bereits gezeigt, dass MYB TFs eine wichtige Rolle bei der Kontrolle der Flavonoid-Biosynthese in Pflanzen haben. Viele Faktoren, die oberhalb des Anthocyanin-Biosyntheseweges agieren, werden bei Stickstofflimitierung oder erhöhter Saccharose-Konzentration auch verstärkt exprimiert. Außer den erwähnten Bedingungen können auch andere Umweltparameter, wie z. B. erhöhter Salzgehalt

und Starklicht, zu erhöhter Expression führen. Im Gegensatz jedoch zu einigen anderen MYB TFs, die einen Einfluss auf Gene des Anthocyanin-Biosyntheseweges ausüben, ist die Expression von *MYB112* nicht durch Stickstofflimitierung oder Kohlenstoffüberfluss kontrolliert, sondern wird durch erhöhten Salzgehalt sowie Starklicht stimuliert. Somit ist MYB112 ein neuer Regulator, der eine Anthocyanin-Akkumulation unter abiotischen Stressbedingungen kontrolliert.

The pages xiii-xiv (Curriculum vitae) contain private data, therefore are not part of the online publication.